PSTAR — Primary and Secondary Terms Analysis and Renormalization

A Unified Approach to Building Energy Simulations and Short-Term Monitoring

K. Subbarao

September 1988

NOTICE

PREFACE

In keeping with the national energy policy goal of fostering an adequate supply of energy at a reasonable cost, the United States Department of Energy (DOE) supports a variety of programs to promote a balanced and mixed energy resource system. The mission of the DOE Solar Buildings Research and Development Program is to support this goal by providing for the development of solar technology alternatives for the buildings sector. It is the goal of the program to establish a proven technology base to allow industry to develop solar products and designs for buildings that are economically competitive and can contribute significantly to the nation's building energy supplies. Toward this end, the program sponsors research activities related to increasing the efficiency, reducing the cost, and improving the long-term durability of passive and active solar systems for building water and space heating, cooling, and daylighting applications. These activities are conducted in four major areas: Advanced Passive Solar Materials Research, Collector Technology Research, Cooling Systems Research, and Systems Analysis and Applications Research.

Advanced Passive Solar Materials Research - This activity area includes work on new aperture materials for controlling solar heat gains, and for enhancing the use of daylight for building interior lighting purposes. It also encompasses work on low-cost thermal storage materials that have high thermal storage capacity and can be integrated with conventional building elements, and work on materials and methods to transport thermal energy efficiently between any building exterior surface and the building interior by nonmechanical means.

Collector Technology Research - This activity area encompasses work on advanced low- to medium-temperature (up to 180°F useful operating temperature) flat-plate collectors for water and space heating applications, and medium- to high-temperature (up to 400°F useful operating temperature) evacuated tube/concentrating collectors for space heating and cooling applications. The focus is on design innovations using new materials and fabrication techniques.
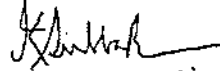
Cooling Systems Research - This activity area involves research on high-performance dehumidifiers and chillers that can operate efficiently with the variable thermal outputs and delivery temperatures associated with solar collectors. It also includes work on advanced passive cooling techniques.

Systems Analysis and Applications Research - This activity area encompasses experimental testing, analysis, and evaluation of solar heating, cooling, and daylighting systems for residential and nonresidential buildings. This involves system integration studies, the development of design and analysis tools, and the establishment of overall cost, performance, and durability targets for various technology or system options.

The research described in this report was supported by the Office of Solar Heat Technologies. It was performed as part of the Short-Term Energy Monitoring (STEM) project. The goal of the project is to develop, field test, and transfer to industry a technique for assessing the energy performance of a residential building through short-term tests. Extensions to nonresidential

buildings, especially for control and diagnostics of heating, ventilation, and air-conditioning systems are planned for the future.

_____
Kris Subbarao, Senior Physicist

Approved for

SOLAR ENERGY RESEARCH INSTITUTE

_____
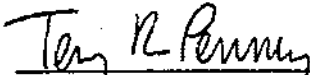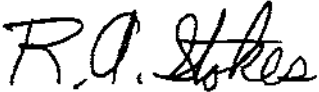Terry R. Penney, Manager
Buildings Research Branch

_____
Robert A. Stokes, Acting Director
Solar Heat Research Division

ABSTRACT

We present a unified method of hourly simulations of a building and analysis of performance data. The method is called Primary and Secondary Terms Analysis and Renormalization (PSTAR). PSTAR allows extraction of building characteristics from short-term tests on a small number of data channels. These can then be used for long-term performance prediction ("ratings"), diagnostics and control of heating, ventilating, and air conditioning (HVAC) systems, comparison of design versus actual performance, etc.

PSTAR is not a new simulator competing with existing simulators although, for a certain class of problems, it does provide a self-contained simulator. It plays an essential role when one is dealing with real building data. It is, in a sense, a way of organizing heat flows that can be obtained from existing or future microdynamic simulators (a microdynamic simulator is one that simulates each component; DOE-2, SERIRES are examples). However, many of the heat flow terms are best obtained through macrodynamics, a calculation that deals with whole building characteristics (such as the loss coefficient). The macrodynamic calculation can be done in a number of ways; a method is developed through fitting building response at selected frequencies.

In predicting building performance given the building description, the above decomposition of heat flows has intuitive value giving quantitative information on the role of various driving forces on the building performance; it has some computational value, too. In determining building characteristics given performance data, the above decomposition plays a critical role. Suppose short-term monitoring has given dynamic data on a few channels (typically, inside and outside temperatures, solar radiation, internal gains, and wind speed). We wish to extract suitable building parameters from the data. The common approach is to view the building as a "black box" and fit the performance data to model parameters. This approach has generally resulted in a dilemma: to keep the number of parameters small the model must be simple, but to be realistic the model must be complex.

The above dilemma is resolved by treating the building not as a black box but as a "gray box"--starting with an audit description of the building obtained by a site visit, the various heat flow terms are calculated. The (known) audit description being different from the (unknown) as-built description, the energy balance equation is not satisfied by the heat flow terms obtained for the audit building with the measured driving functions.

Each heat flow term calculated (i.e., not directly measured) can now be classified as primary or secondary depending on its overall magnitude. Renormalization parameters are introduced for the primary terms such that the renormalized energy balance equation is best satisfied in the least squares sense; hence, the name PSTAR. This involves a simple linear least squares fit. The renormalized energy balance equation is used for the intended application such as long-term extrapolation, control and diagnostics of HVAC systems, building commissioning, etc.

The need for a proper test protocol to elicit the renormalization parameters is emphasized. The renormalized energy balance equation guides one to a suitable protocol. Coheating (the introduction of electrical heat to maintain a constant indoor temperature) and cool-down tests are typically adequate.

Accurate determination of admittance at a specific frequency is possible through sinusoidal heat input.

Additional parameters are introduced for special situations. The above methodology is extended to multizone buildings.

PSTAR is rather comprehensive and, for that reason, rather complex. We believe this is necessary in dealing with real buildings (even if idealized computer-generated data can often be analyzed with simpler models).

One highlighted application is long-term performance prediction from short-term monitoring. A project, Short-Term Energy Monitoring (STEM), is under way with that objective. PSTAR provides the theoretical framework for building parameters, test protocol, and data analysis. Applications to real buildings will be given in subsequent publications.

A number of applications are identified. When combined with modern data acquisition and control systems (such as energy management systems in commercial buildings, power line carrier based data acquisition, etc.) PSTAR provides a powerful tool for a wide range of applications.

PSTAR achieves a synergism among macrodynamics, microdynamics, and performance to give an intuitive as well as quantitative model of building performance. The frequency fitting procedures as well as parameter estimation procedures involve only systems of linear equations and are, therefore, simple and reliable.

TABLE OF CONTENTS

LIST OF FIGURES

LIST OF TABLES

1.0 INTRODUCTION

Although there have been considerable efforts in developing large numerical simulation models for building energy calculations on one hand and in obtaining performance data by monitoring actual buildings on the other, the interplay between theory and experiment has not been as definitive as expected. We believe there are two principal difficulties. The first occurs when, in the absence of extraordinarily detailed measurements, the inputs to the simulation models are mismatched with the outputs that are being compared with experiments. The inputs are material properties and estimates such as solar distribution on various surfaces (not all of which are always measured). The output is system performance. It is, in general, difficult to feed back the outputs for any systematic modification of the large number of inputs. The second difficulty arises because a first-principles calculation of heat transfer processes in real buildings inevitably entails uncontrolled approximations.

Introducing certain definitions is useful. The process of starting from a building description and determining building performance is referred to as the forward process. The process of starting from performance data and determining thermal characteristics of a building is referred to as the inverse process. A simulation that simulates each component (e.g., each wall) or subcomponent (wall layer) and thereby simulates the building is referred to as microdynamic. A simulation that aggregates component characteristics into whole building (or zone) parameters that are subsequently used in the simulation is referred to as macrodynamic. Figure 1-1a schematically illustrates a microdynamic simulation, and Figure I-Ib depicts a macrodynamic simulation. DOE-2 (DOE 1980), BLAST (Hittle 1977), and SERIRES (Palmiter and Wheeling 1980) are familiar examples of microdynamic simulations. In this article, a new simulation called the Primary and Secondary Terms Analysis and Renormalization (PSTAR) is introduced. In its simplest form, PSTAR is a macrodynamic simulation. A fuller version consists of a disaggregation of zone heat flows into several consistuents, obtained by macrolevel calculations with a perturbative formulation of microdynamics.

Typically, microdynamic simulations are designed for the forward process. Macrodynamic simulations for the forward process offer the macroparameters (such as the building loss coefficient, and others) as intermediate quantities. These quantities, which form inputs to the simulation, have important physical significance and provide valuable intuition in analyzing cause and effect relationships. Macrodynamics, by avoiding simulation of each component, results in computational efficiency.

The previously listed features of macrodynamics, while desirable, are not critical for the forward process. For the inverse process, macrodynamics has some critically essential features. Typically, a small number of data channels (air temperatures, power input, solar flux) is measured in monitoring a building; material properties, temperatures, heat flows, etc., of individual components are generally not measured. Even a perfectly accurate microdynamic simulation is of limited use in this situation because the inputs are not sufficiently accurate, and the macrolevel measurements do not allow a systematic modification (or calibration) of the inputs. On the other hand, short-term monitored data can be viewed as giving measured values of the

SERI ◉
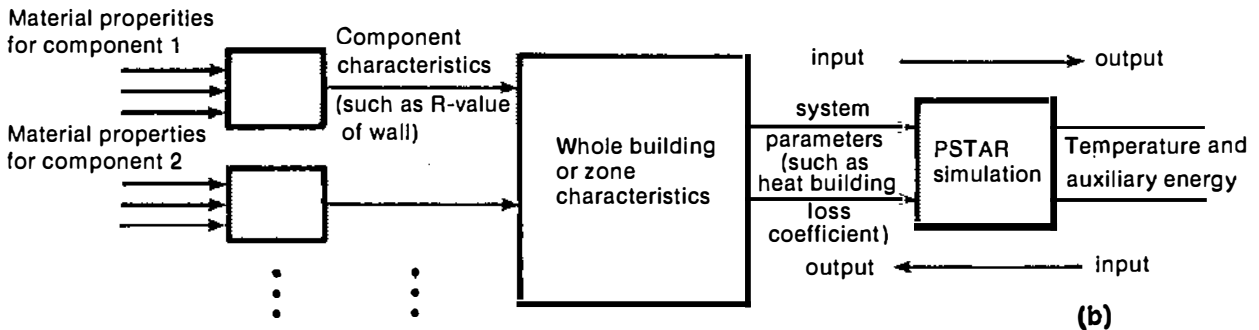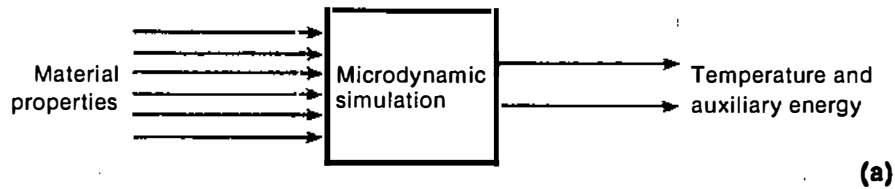
Figure 1-1. Schematic comparison between (a) a microdynamic simulation
and (b) a macrodynamic simulation

macroparameters, which are inputs to the macrodynamic simulation. Macro-
dynamics is, therefore, well suited for such applications as extrapolation of
long-term performance from short-term tests and building as a dynamic
calorimeter.

Macrodynamics should really be viewed as an approximation to the full dynam-
ics. Certain processes, such as heat transfer in phase change materials
(PCMs), are beyond the scope of macrodynamics as formulated in this article,
even though the heat flow renormalization formulated in this article may be
applicable; we will not discuss PCMs further. The full dynamics may entail
variable film conductances, etc. not present in macrodynamics. The full
dynamics can, of course, be studied using microdynamics. Schematically we can
write the equation:

(Full dynamics) = (Macrodynamics) + (Full dynamics - Macrodynamics)

The last term is usually small but often not negligible. Its signal in build-
ing performance data is typically too small to be picked up. It can only be
included in either the forward or the inverse process through a microdynamic
calculation. This article also presents the mathematical framework for the
calculation. Thus, a skillful combination of micro and macrodynamics is
necessary to achieve a complete picture of the energy performance of a build-
ing through the forward or the inverse process. This is the program emphasized
in this article.

This report meticulously details the PSTAR method. In summary, for the for-
ward process it consists of (1) calculation of whole building (or zone)

2

admittances, (2) conversion of these into transfer function coefficients, (3) calculation of solar gains, (4) selection of airflow (infiltration as well as interzone flow) models, (5) calculation of small heat flows through perturbation theory, and (6) simulation through the time series. For the inverse process, there is an additional step involving renormalization of the transfer functions (to fit performance data) that are to be used in subsequent simulations. A suitable monitoring protocol is necessary to elicit all the important building responses. For residential buildings, where introduction of electrical heat of any desired profile is usually possible, a signal enhancement principle ensures accurate determination of certain admittances.

There is extensive literature on the use of frequency response for the forward process. The admittance method (IHVE 1970) is based on the work of, among others, E. Danter, M. G. Davies, J. Harrington, A. G. Louden, and N. O. Milbank. With the response factor method of Stephenson and Mitalas (1967), time-domain simulations were developed. A recent study of room transfer functions was performed by Seem (1987). The Commonwealth Scientific and Industrial Research Organization (Australia) research with contributions from, among others, R. W. Muncey, P. Chandra, C. L. Gupta, K. R. Rao, J. W. Spencer, and P. J. Walsh, was reviewed in Muncey (1979). Niles (1978), Green and Ulge (1979), Hittle and Pedersen (1981), Winn (1982), and Balcomb and Yamaguchi (1983) have, among others, used the frequency response method to analyze design problems—either directly or through response factors, or through network reduction. A recent introduction is given by Palmiter (1986).

Given a resistor capacitor (RC) network of arbitrary complexity with convection to air, radiation exchange among surfaces, etc. (with constant Rs and Cs), the output, say, the indoor air temperature, can be related to the inputs (ambient temperature, solar radiation on different surfaces, etc.) through transfer functions. The different frequency-response-based methods differ primarily in the simplifying assumptions as well as in solution procedures. Response factor formulation readily permits variable infiltration and airflow, imposition of thermostatic and HVAC plant size constraints, etc. One special feature of the PSTAR approach for the forward process includes: interaction factor formulation that provides for the treatment of convective and radiative heat exchange (Subbarao and Anderson, 1983). In a simulation with thermostatic constraints, the inside temperature is sometimes predicted, at other times the auxiliary energy is predicted. Therefore, the roles of the numerator and the denominator in the transfer functions are exchanged. The passage from frequency response to time series is done with this in mind (Sections 3.0 and 4.0).

Direct time-domain simulations (without going through the intermediary of frequency responses) are far more popular. The reasons are apparent. When solar gains from multiple orientations, shading, etc. are involved, and one wishes to include small effects such as sky radiation, nonlinear film coefficients, etc., the frequency-response method becomes unwieldy, if not inapplicable. The PSTAR method is intended to combine the best features of the frequency-response formulation and time-domain formulation.

For the inverse process, simplified electrical circuits apparently were the most popular approach (Kusuda, Tsuchiya, and Powell, 1971; Sonderegger, 1978; Deberg, 1979; Pryor, Burns, and Winn, 1980; Hammersten, 1984; Nielsen and Nielsen, 1984; Norford, Rabl, Socolow, and Persily, 1985; Hammersten, van

Hattem, Bloehm, and Colombo 1986; Duffy and Saunders 1987). Duffy and Saunders have combined coheating tests and cool-down tests with a sequential and iterative analysis to estimate the loss coefficient and effective heat capacitance (Sonderegger, Condon, and Modera 1980). A monthly correlation method or a simple electrical circuit provides long-term extrapolation. This work is described in detail in their report. Estimation of the coefficients of response factor time series was done by Subbarao (1985). Parameterization of the transfer functions and estimation of the parameters was done by Subbarao (1984). A recent review of parameter estimation in buildings is given by Rabl (1988). In this article, we have developed a method to resolve the fundamental dilemma that performance data allow only a small number of parameters to be reasonably estimated, whereas a proper thermal description of a building requires considerably more parameters. The method is applicable to multizone buildings. The method incorporates a perturbation treatment of small effects such as sky radiation, nonlinear aspects of convection, etc.

The relationship between the PSTAR formulation and the Building Energy Vector Analysis (BEVA) formulation (Subbarao 1984), from which PSTAR emerged, is given in Appendix C. The BEVA method was tested in test-cells (Jeon et al., 1987), augmented with the signal enhancement principle, and applied to residential buildings (Subbarao, Burch, Hancock, and Jeon, 1985). Application to nonresidential buildings is performed in Norford, Rabl, Socolow, and Persily (1985). Building-as-a-calorimeter application, especially important for HVAC diagnosis and control in nonresidential buildings, was demonstrated for a residential building in Subbarao, Burch, and Jeon (1986). A general discussion of macrodynamics is given in Subbarao, Burch, and Christensen (1985).

A summary of the new formulation presented in detail in this report is given in a companion article (Subbarao, 1988). We strongly urge that the summary be read first before delving into this detailed report. Application to a real building is given in Subbarao, Burch, Hancock, Lekov, and Balcomb (1988). This discusses a number of practical aspects of applying the method to real buildings. PSTAR has been refined through monitoring and analysis of several residential buildings and is suitable for field applications.

2.0 DISAGGREGATION OF HEAT FLOWS

As the introduction states, the PSTAR approach combines macrodynamics with microdynamics to disaggregate the heat flows into a number of useful constituents. While multizone buildings are considered later, we will outline the disaggregation scheme for a one-zone building with a slab-on-grade floor. The energy balance for the building can be written, under certain mild assumptions, in the following form (we use the heating season terminology; modifications for cooling season are easily achieved):

$$Q_{int}(t) = L[T_{in}(t) - T_{out}(t)] + Q^{in}_{storage}(t) + Q^{out}_{storage}(t)$$

$$- Q_{sun}(t) + Q_{vent}(t) - Q_{aux}(t) + Q_{ground}(t) + Q_{sky}(t) , \quad (2-1)$$

where

Q_{int} = internal gains

L = skin loss coefficient; the first term on the right side denotes the heat loss in the absence of storage effects. T_{in} represents the inside temperature, and T_{out} the ambient temperature

$Q^{in}_{storage}$ = net heat that goes to charging (or, if the term is negative, discharging) the masses caused by inside temperature variations only

$Q^{out}_{storage}$ = net heat that goes to charging (or, if the term is negative, discharging) the masses caused by outside temperature variations only

Q_{sun} = net heat gain by the indoor air node caused by the combined action of sun and solar-radiation-coupled capacitances

Q_{vent} = heat loss caused by infiltration and ventilation

Q_{aux} = heat supplied by the heating system

Q_{ground} = heat flow to the ground

Q_{sky} = heat loss caused by sky temperature depression.

This decomposition of heat flows is extremely useful. Physically, a heat flux meter mounted on a wall would measure the net effect of all the driving functions (T_{in}, T_{out}, sun, etc.) on that particular wall.

The main assumption made in arriving at the decomposition (Eq. 2-1) is that the heat transfer properties are independent of temperature. This assumption is commonly made in many building simulations (DOE-2, for example). If one is interested in relaxing this assumption, for example, to study temperature-dependent film conductances, it is still possible to proceed with a decomposition, such as in Eq. 2-1, by including a correction term that is the difference between the exact heat flow Q_{exact} and the approximate heat flow Q_{approx} given at the right side of Eq. 2-1:

$$Q_{int}(t) = Q_{approx}(t) + [Q_{exact}(t) - Q_{approx}(t)] . \quad (2-2)$$

This decomposition, while trivial, provides an essential framework for the analysis of performance data through the renormalization process discussed in this report. The correction term can be handled through a perturbation formulation given in Section 10.0.

The report gives a mathematical justification with underlying assumptions for this decomposition. The calculation of $Q_{storage}^{in}$, $Q_{storage}^{out}$, and Q_{sun} form a significant part of this report. This calculation involves matching building response at any number of selected frequencies. This decomposition provides a simple linear least squares fit approach to the inverse problem through a renormalization process.

3.0 TRANSFER FUNCTION REPRESENTATION OF BUILDING RESPONSE

In Section 2.0 the heat flows were decomposed into a number of terms without making any approximations. A formulation suitable for calculating the various terms of Eq. 2-1 is the subject of this section. Consider first a single-zone building. (Multizone buildings are reviewed in Section 13.0.) We will initially limit ourselves to a case where solar gains occur essentially only from one face of the building and where there are no shading devices. For definiteness, assume there are no nonsouth windows, but that the south face has any combination of direct gain, Trombe wall, and insulated walls. This restriction will be removed in Section 8.0. Complications such as sky radiation, wind effects, ground losses will all be incorporated later. These simplifying assumptions will help fix the ideas before additional features are considered.

A heat balance at time t, considering all gains to and losses from indoor air, can be represented in the form of a convolution integral, as follows:

$$\int_{-\infty}^{t} dt' \left[\hat{V}(t - t') \cdot \hat{T}_{in}(t') - \hat{W}(t - t') \hat{T}_{out}(t') - \hat{S}(t-t') \hat{I}_{sun}(t') \right]$$

$$= \hat{Q}_{int}(t) + \hat{Q}_{aux}(t) . \qquad (3-1)$$

$\hat{T}_{in}$ and $\hat{T}_{out}$, respectively, represent indoor and outdoor temperatures, and $\hat{Q}_{int}$ and $\hat{Q}_{aux}$ represent the internal gains and auxiliary energy (both are assumed to be instantaneous heat gains by indoor air, if not, the necessary modifications are straightforward). $\hat{I}_{sun}(t')$ is the solar radiation incident on the south face per unit area. The transfer function $\hat{V}$ describes the response of the heat flow from indoor air because of changes in indoor temperature. Similarly, $\hat{W}$ describes the response of the heat flow from indoor air because of changes in outdoor temperature, and $\hat{S}$ that is caused by solar radiation. All heat transfer mechanisms were linearized in writing Eq. 3-1. This linearization is the same as that done in the DOE-2 simulation (DOE, 1980). Simple modifications allow consideration of variable infiltration rates as well as movable insulation. Variable infiltration (based on measurements or from models fitted to one-time measurements, or from pure modeling) can be easily incorporated by calculating infiltration conductance times the inside-outside temperature difference and absorbing this term in internal gains. More generally, any heat flow deemed sufficiently well-determined by a model/measurement can be absorbed into internal gains.

Equation 3-1 is the basis for all the response/weighting factor techniques such as those in DOE 2.1 (DOE 1980). A general discussion of convolution integrals, such as the ones in Eq. 3-1, applied to buildings can be found in Muncey (1979). Considering the temperature or solar radiation time series as a sum of triangular pulses, Eq. 3-1 reduces to response factor series as discussed in Stephenson and Mitalas (1967), DOE 2.1 (1980), and in Kimura (1977). A detailed discussion of component responses and the building response as a sum of component response including component interactions caused by radiation exchange is given by Subbarao and Anderson (1983).

The convolution integrals in Eq. 3-1 are greatly simplified into algebraic expressions upon taking Fourier or Laplace transforms. Fourier transforms are

much better suited for our purposes. We will denote Fourier transform of a function by dropping the ^. Equation 3-1 reduces in the frequency domain to:

$$V(\omega) \, T_{in}(\omega) - W(\omega) \, T_{out}(\omega) - S(\omega) \, Q_{sun}(\omega) = Q_{int}(\omega) + Q_{aux}(\omega) \, . \quad (3\text{-}2)$$

Equations 3-1 and 3-2 are equivalent. We will combine the best features of the time and frequency domains approach to arrive at a hybrid approach for hourly simulations. How this is done is the subject of the next several sections. An important part of that process is the calculation of the frequency domain transfer functions V, W, and S. The calculations are detailed in Subbarao and Anderson (1983). Briefly, at any given frequency the individual component Vs, Ws, and S's are obtained first and (being complex quantities) can be represented by two-dimensional vectors. The addition of these vectors (analogous to UA additions) gives the whole building vectors. An important feature of this method is the incorporation of convection radiation split at the surfaces through "interaction factors."

Note that the functions V, W, and S refer to the building as a whole. Individual components are not explicitly simulated. Simple modifications allow explicit simulation of any selected components and aggregation of the rest of the building. This results in considerable computational efficiency. This feature, while desirable, is not critical given the power of current computers. However, this feature is critical when we consider the inverse process—determining building characteristics from performance data. In typical monitoring, it is necessary to restrict the number of data channels and only whole building variables such as air temperature, internal gains, auxiliary power, etc., are measured. Thus, a whole building formulation turns out to be well-matched with such data.

A note on terminology. With some approximations, a discrete version of Eq. 3-1, in the case when Q_{int} is the output and, say, T_{in} is the only input, can be written in the form,

$$Q_{int}(n) + a_1 \, Q_{int}(n-1) + \ldots + a_r \, Q_{int}(n-r)$$

$$= b_0 \, T_{in}(n-\ell) + b_1 \, T_{in}(n-\ell-1) + \ldots + b_s \, T_{in}(n-\ell-s)$$

Essentially, following Box and Jenkins (1976), this will be referred to as "discrete transfer function model of order (r,s,ℓ)." The relationship between the discrete model and the continuous model is simple in some limiting cases (Box and Jenkins 1976). For typical buildings applications, where the quantities such as T_{in}, Q_{in}, ... are sampled approximately every 15 sec and averaged over an hour or so, the relationship is somewhat complex, especially when considering relatively high frequency response. The most commonly encountered situation is for l=0 and r=s, with several inputs. We simply refer to this as discrete transfer function model of order r.

4.0 TIME SERIES FROM FREQUENCY RESPONSES

Given a detailed building description, one can calculate the frequency response functions V, W, and S at any frequency. Section 5.0 presents how this can be turned into a time series in a form convenient for time-domain simulations of a building with some discrete time interval Δ. In this section we consider a simpler but still experimentally relevant problem involving only one component and only one transfer function (instead of the three transfer functions V, W, and S). Consider a calibrated hot-box experiment (ASTM 1985). A steady-state measurement gives the U-value of a component. The dynamics of the component may be studied by one of two extensions: (1) keeping the inside temperature fixed, the outside temperature may be varied in some desired fashion (sinusoidal, pseudo-random binary sequence, sol-air temperature, etc.) and the heat flow from the inside face of the component is measured; (1) keeping the outside temperature fixed, the inside temperature may be varied in some desired fashion and the heat flow from the inside face of the component is measured. The two measurements give different information about the component: (1) gives information on the W-transfer function, and (2) gives information on the V-transfer function. Experimentally, (2) is a more difficult measurement than (1). Dynamic hot-box measurements of type (1) were carried out (Burch, et al. 1987, Larson and Van Geem 1987). Analysis of such measurements can be done following the method described in this section. Measurements of type (2) give information on the V-admittance that is important in analyzing passive buildings, night setback, precooling of a building, etc. For this reason, we will carry out examples in this section primarily on the V-admittance; we are, therefore, considering hot-box measurements of type (2) or a hypothetical building subject to a constant ambient temperature and no solar radiation, but with varying inside temperature.

When the inside temperature is also a constant, the component or building can be represented by a single resistor. Figure 4-1 shows about the simplest but approximate extension to include inside temperature variations. Two questions arise: (1) how does one determine U_{in} and τ_{in} given a component or building description, and, (2) given the steady-state conductance L, as well as U_{in} and τ_{in}, how do we perform a simulation with time step Δ. The second question is easily answered. The relationship between the heat flow $q_{in}(t)$ from the inside air node at time t is related to the temperature $T_{in}(t)$ through the following relation. (For convenience, we will set the constant T_{out} to zero; if not, we need the term $q_{out} = -L\ T_{out}$ and $q_{in} + q_{out} = q_{int}$ is the heat balance equation.)
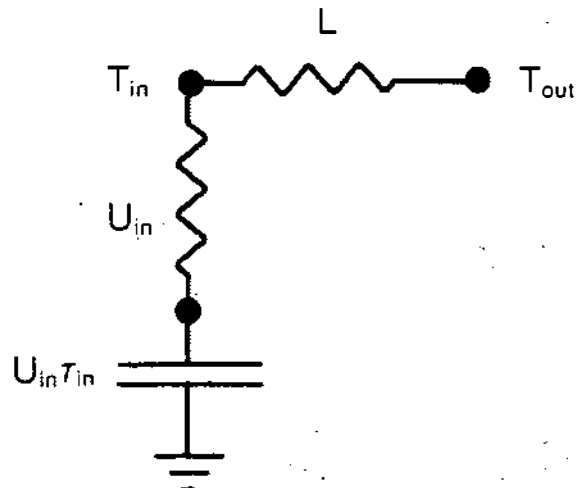
Figure 4-1. A simple dynamical extension of a static model

$$q_{in}(t) = \int_{-\infty}^{t} dt' \; \tilde{V}(t-t') \; T_{in}(t') \; , \qquad (4-1)$$

$$V(t-t') = (L + U_{in}) \; \delta(t-t') - \frac{U_{in}}{\tau_{in}} \exp\left[-(t-t')/\tau_{in}\right] \; , \qquad (4-2)$$

the above relationships can be easily derived from the following differential equation corresponding to Figure 4-1:

$$\dot{q}_{in} + q_{in}/\tau_{in} = (L + U_{in}) \; \dot{T}_{in} + L \; T_{in}/\tau_{in} \; , \qquad (4-3)$$

where

$$q_{in} = U_{in} \; (T_{in} - T) + L \; T_{in} \; , \qquad (4-4)$$

where T is the temperature of the mass. A discrete version with interval Δ can be obtained either from Eq. 4-1 or from Eq. 4-3 and has the form:

$$q_{in}(n) + a_1 \; q_{in}(n-1) = b_0 \; T_{in}(n) + b_1 \; T_{in}(n-1) \; . \qquad (4-5)$$

The precise values of a_1, b_0, and b_1 depend on the discretization scheme as well as on whether instantaneous values or averages within time interval are used.

Let us now take up the first question. Given the component or building description, how does one find L, U_{in}, and τ_{in}? First, we should recognize that Figure 4-1 provides only an approximate description of the component or building (except in the limiting case of an interior water wall, for which it is exact). One can match some response of the component or building with that of Figure 4-1. We chose to match the frequency response. Figure 4-1 allows matching only at one frequency that can be chosen arbitrarily (as long as it is nonzero). Let us call this frequency ω_1. If the component/building admittance is $V(\omega_1) \equiv R_1 + j \; I_1$, then it is easy to show that

$$U_{in} = (R_1 - L) \left[1 + \left(\frac{I_1}{R_1 - L}\right)^2\right] \; , \qquad (4-6)$$

$$C_{in} = \frac{I_1}{\omega_1} \left[1 + \left(\frac{R_1 - L}{I_1}\right)^2\right] \; . \qquad (4-7)$$

For a lightweight frame wall, it can be shown that U_{in} and C_{in} have, as functions of frequency, a rather flat region over the range of frequencies of interest in typical building applications. Figure 4-1 with a fit made at, say, the diurnal frequency, gives a good approximation. For more complex components or buildings, Figure 4-1 is not adequate. One can construct more complicated circuits and proceed to match at multiple frequencies. A circuit-based approach, which is so straightforward for a one-frequency fit, is unwieldy for multiple frequency fit. A simple, systematic approach is developed in this article using transfer functions.

First, we state the following result: If the frequency domain transfer function $V(\omega)$, relating the heat flow q_{in} to the temperature T_{in} through the relationship $q_{in}(\omega) = V_{in}(\omega)T_{in}(\omega)$, can be written in the form:

$$V(\omega) = \frac{b_0 + b_1 e^{-j\omega\Delta}}{1 + a_1 e^{-j\omega\Delta}} \qquad (4-8)$$

then, the following first-order discrete transfer function model holds:

$$q_{in}(n) + a_1 q_{in}(n-1) = b_0 T_{in}(n) + b_1 T_{in}(n-1) . \qquad (4-9)$$

A proof for a more general case is given in Appendix B. Knowing V at zero frequency (L) and one other frequency ω_1 ($V(\omega_1) = R_1 + jI_1$) one can match them with Eq. 4-8 to determine b_0, b_1, and a_1 in terms of L, R_1 and I_1. Appendix B gives the system of linear equations to do this. The result is close, but not identical, to Eqs. 4-5 through 4-7. (In the limit of $\omega \to 0$, the results are identical.) This scheme implies a certain discretization to account for the fact that data are taken with time interval Δ. The relationship between this approach and the network approach can be seen through Eqs. 4-5 and 4-9 and is given in Appendix B.

Multiple frequency fits are performed following the method given in Section 16.0, where the necessary equations are developed in the context of whole-zone admittance. How many and which frequencies are chosen for the fit depends on the component or building. These are, perhaps, best explained through some explicit examples that follow. The method is similar to that of Stephenson and Mitalas (1971). The main difference is that in writing the V-transfer function as N/D, Stephenson and Mitalas determine D by first finding as many roots of the Laplace transform closest to the origin as necessary, and then obtaining N by fitting to the frequency response. Because they deal with a single component, they choose the same denominator for both the V- and W-transfer functions. In contrast, we determine both N and D by fitting to frequency responses and do not require the same denominator for the transfer functions. With a simulation that features thermostatic constraints, T_{in} (= set point) is the input and Q_{aux} is the output during periods of nonzero load, and $Q_{aux}(=0)$ is the input and T_{in} the output during free-float periods. Correspondingly, one of the relevant transfer functions is N/D some times and D/N at other times. We will treat both N and D on the same footing. The reason why we did not require the same denominator for the transfer function is that with interior walls, contributing only to V and not to W, there is no priori reason to require V and W to have a common denominator.

4.1 Example 1: A Frame Wall

Consider the nominal R-11 frame wall of Table 4-1. With combined convection-radiation coefficients at the surfaces, the V-admittance at any frequency can be computed. In particular, V(frequency=0) is the steady-state conductance of 0.06745 Btu/hr°Fft^2. We work with the unit area of the walls in this section. This is represented by point A in Figure 4-2, which is a distance .06745 from the origin along the x-axis. The admittance at $(24 \text{ hr})^{-1}$ is 0.2322 Btu/hr°Fft^2 with a phase angle of 63.54°. The corresponding point is represented by B in Figure 4-2. Starting with zero frequency (point A), as we increase the frequency the representative point traces out the line shown in Figure 4-2. Points at equal frequency intervals of 1/96 hr^{-1} are marked with an *, point B corresponds to the diurnal frequency, and point C, for example, corresponds to the 6-hr cycle.

The polar diagram of Figure 4-2 provides a complete characterization of the response to inside temperature. An approximation should then be designed to reproduce the polar diagram as closely as necessary over the range of

Table 4-1. Description of Two Example Walls

---

a. **Frame Wall:**

Inside film conductance: 1.46 Btu/hr°F ft^2

Layer	Material	Thickness (ft)	Conductivity (Btu/hr·ft·°F)	Density (lbs/ft^3)	Specific Heat (Btu/lb)
1	Drywall	0.0417	0.25	78	0.259
2	Insulation	0.293	0.0265	3.25	0.157
3	Sheathing	0.0417	0.032	10	0.2
4	Wood Siding	0.0833	0.065	27	0.33

Outside film conductance 3.0 Btu/hr °F ft^2

b. **Storage Wall:**

Inside film conductance: 1.46 Btu/hr°F

1	Concrete	0.3	1.0	150	0.2

Outside film conductance: 0.333 Btu/hr°F

---

frequencies of interest. (Alternatively, one can work with Bode diagrams—amplitudes and phases as functions of frequency.) The polar diagram corresponding to the circuit of Figure 4-1 can be readily generated. As noted before, we will work directly with discrete transfer functions, not through circuits.

Fitting Eq. 4-8 to zero and diurnal frequencies we find (with Δ = 1 hour)

$$V(\omega) = \frac{0.7695 - 0.7113\ e^{-j\omega\Delta}}{1 - 0.1365 e^{-j\omega\Delta}} \qquad (4\text{-}10)$$

and, correspondingly,

$$q_{in}(n) - 0.1365\ q_{in}(n-1) = 0.7695\ T_{in}(n) - 0.7113\ T_{in}(n-1)\ . \qquad (4\text{-}11)$$

The polar diagram corresponding to Eq. 4-10 is shown in Figure 4-3 with circles (along with the exact diagram of Figure 4-2 shown with an *). The fit is excellent at low frequencies (up to about 1/16 hr^{-1}) and quite good over a range of higher frequencies, and becomes poor at very high frequencies. For typical building energy analysis applications, this approximation is adequate.

4.2 Example 2: 1-ft Concrete Storage Wall

Consider now the concrete wall of Table 4-1. The outside film conductance of 0.4 Btu/hrft^2°F is supposed to represent double glazing.
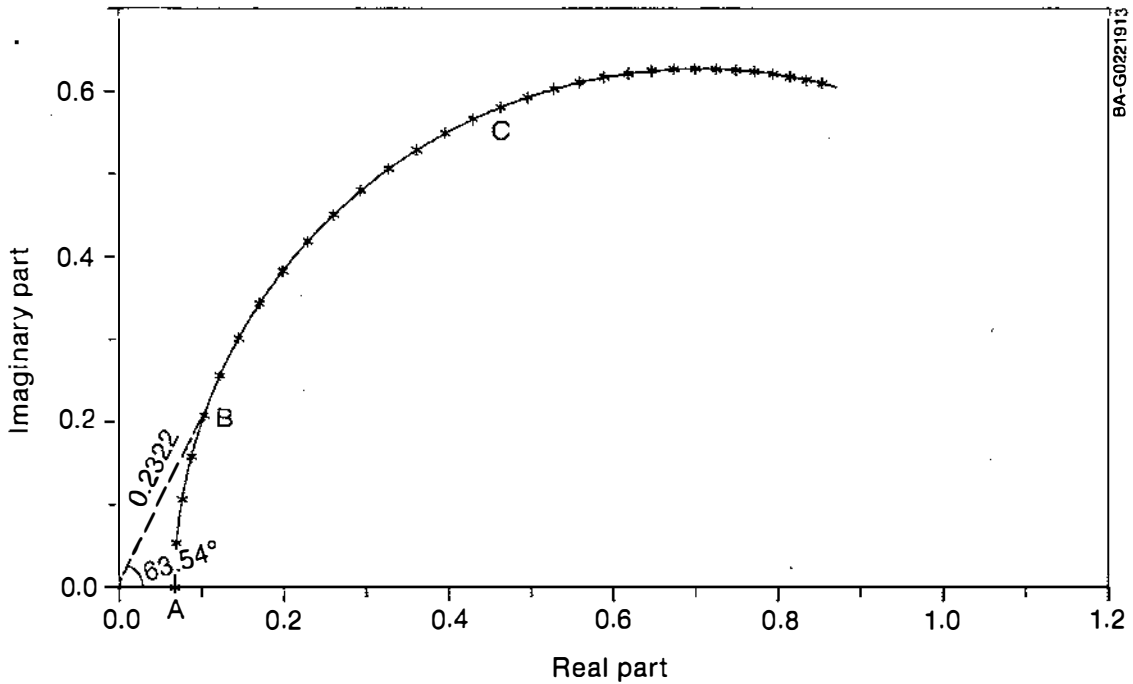
Figure 4-2. Polar diagram representing the V transfer function for a frame wall. The x-axis gives the real part and the y-axis gives the imaginary part of the admittance. The graph was normalized so the admittances were divided by the U-value. The various points above the curve are marked at frequency intervals of $1/96$ hr^{-1}.
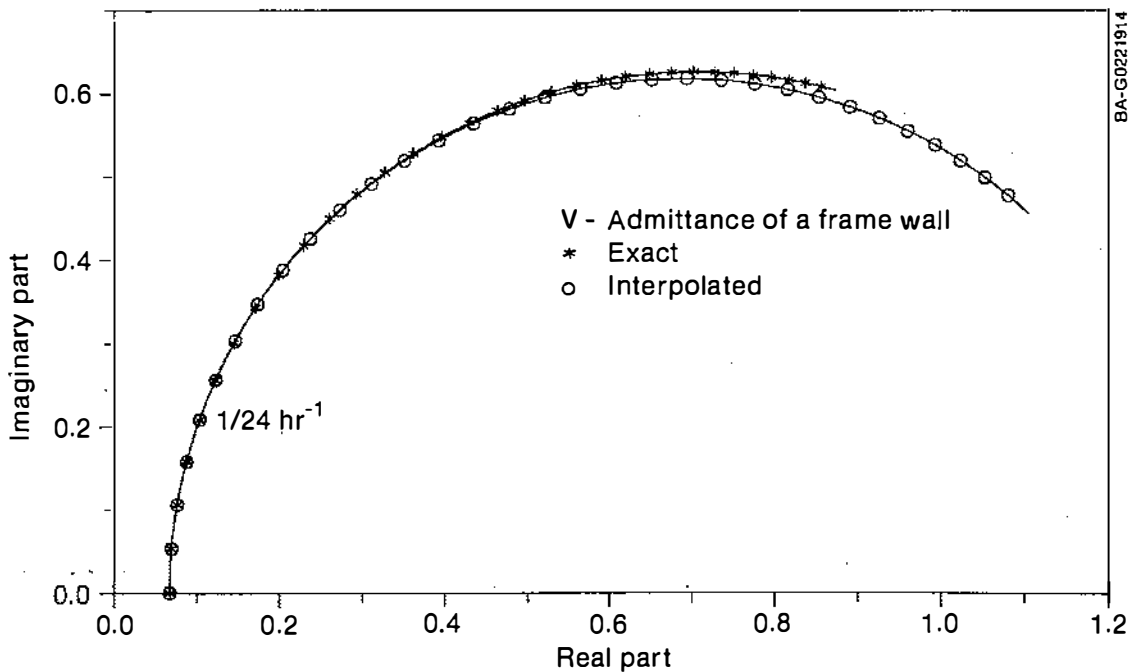
Figure 4-3. Polar diagram of the V-admittance for the frame wall, exact as well as approximate

Figure 4-4 shows the polar diagram of the V-admittance with an *. It is clear that no fit involving only one frequency (in addition to zero) is adequate. A fit at $1/96$ hr^{-1} cycle is also shown in Figure 4-4 with circles. A fit at three frequencies: $1/96$ hr^{-1}, $1/12$ hr^{-1}, and $1/3$ hr^{-1} (see Section 16.0) gives

$$V(\omega) = \frac{1.2307 - 1.1792\ e^{-j\omega\Delta} - 0.6052\ e^{-2j\omega\Delta} + 0.5608\ e^{-3j\omega\Delta}}{1 - 0.7803\ e^{-j\omega\Delta} - 0.6123\ e^{-2j\omega\Delta} + 0.4255\ e^{-3j\omega\Delta}} , \quad (4\text{-}12)$$

and correspondingly

$$q_{in}(n) - 0.7803\ q_{in}(n-1) - 0.6123\ q_{in}(n-2) + 0.4255\ q_{in}(n-3)$$

$$= 1.2307\ T_{in}(n) - 1.1792\ T_{in}(n-1) - 0.6052\ T_{in}(n-2) + 0.5608\ T_{in}(n-3).$$

$$(4\text{-}13)$$

Figure 4-5 shows the resulting excellent fit. If one had no interest in frequencies as high as $1/3$ hr^{-1}, then a fit might be made at, say, $1/96$ hr^{-1}, $1/48$ hr^{-1}, and $1/12$ hr^{-1} to get a seemingly different set of coefficients, or one might be content to fit at only two frequencies: $1/96$ hr^{-1} and $1/12$ hr^{-1}. All those different sets of coefficients produce essentially indistinguishable performance if the inside temperature dominantly contains only the range of frequencies where the polar diagrams corresponding to the different sets are practically indistinguishable. For this reason, it is best to regard the polar diagram as the fundamental object, and the transfer function coefficients as convenient intermediate quantities.
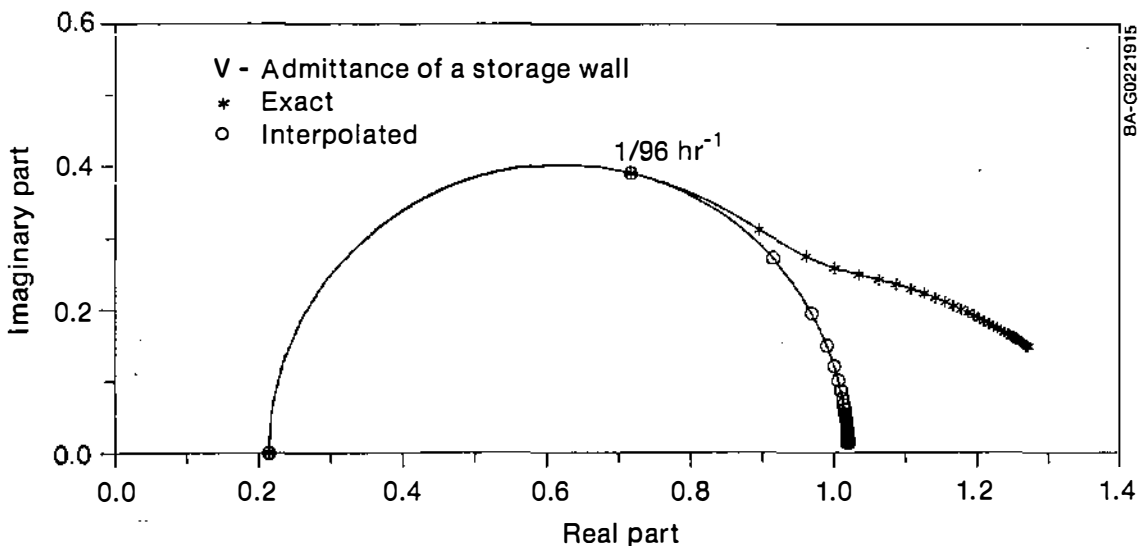
Figure 4-4. Polar diagram for a 12 in. concrete wall: exact (*) and approximate (o) based on matching at the 96-hr cycle
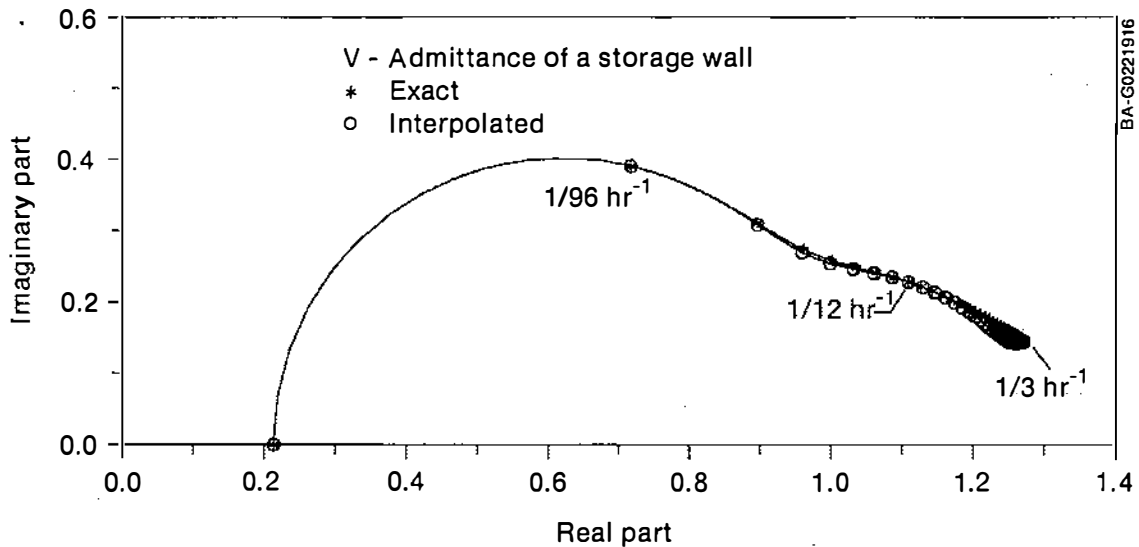
Figure 4-5. Polar diagram for a 12 in. concrete wall: exact (*) and approximate (o) based on matching at 96-hr, 12-hr, and 3-hr cycles

We will briefly mention the stability criterion here and return to it in more detail later. It is necessary to check, in equations such as 4-13, that the polynomials

$$1 - 0.7803 \, z^{-1} - 0.6123 \, z^{-2} + 0.4255 \, z^{-3} \, , \qquad (4\text{-}14)$$

$$1.2307 - 1.1792 \, z^{-1} - 0.6052 \, z^{-2} + 5.608 \, z^{-3} \, , \qquad (4\text{-}15)$$

have zeros with magnitude less than unity. In the language of networks, this amounts to all relevant time constants being positive. If not, predictions of q_{in} (if Eq. 4-14 violates the stability criterion) or of T_{in} (if Eq. 4-15 violates the stability criterion) will be subject to errors. These errors are often large enough to exceed computer limits. The stability criterion may be difficult to satisfy if one attempts to fit the frequency response at an excessive number of frequencies, or at frequencies too close to each other (the determinant in Section 16.0 then becomes nearly singular).

4.3   Example 3:   1-ft Concrete Storage Wall in a Type (a) Hot Box (W-Admittance)

With constant T_{in} and no sun, consider the heat $q_{out}(n)$ from the inside surface, not the outside surface. The subscript out on q_{out} simply reminds us that we are studying the response to outside temperature of the heat flow from the inside surface. It is defined in analogy with Eq. 4-1 and is related to $T_{out}(n)$ through a discrete transfer function. We can introduce an extra degree of freedom, namely, a time delay. The necessary modifications to the equations in Section 17.0 are straightforward. By fitting at zero frequency, $1/96 \, hr^{-1}$ and $1/4 \, hr^{-1}$ with a time delay of 2 hours we get

$$W(\omega) = \frac{e^{-2j\omega\Delta}(0.00141 + 0.00127 \, e^{-j\omega\Delta} + 0.00057 \, e^{-2j\omega\Delta})}{1 - 1.6140 \, e^{-j\omega\Delta} + 0.6293 \, e^{-2j\omega\Delta}} \, , \qquad (4\text{-}16)$$

15

with the corresponding time-series

$$q_{out}(n) - 1.6140\ q_{out}\ (n-1) + 0.6293\ q_{out}\ (n-2)$$

$$= 0.00141\ T_{out}\ (n-2) + 0.00127\ T_{out}\ (n-3) + 0.0057\ T_{out}\ (n-4)\ .$$

$$(4-17)$$

Figure 4-6 gives a comparison of the exact polar diagram for the wall with the approximate one corresponding to Eq. 4-16.

For heat flow through the massive concrete wall, introduction of a time delay as previously done is reasonable. The time delay is simply an additional degree of freedom that can be exercised when necessary to build in some physics beyond just frequency matching. In other words, given a set of frequencies and corresponding admittances, as well as a time delay (or advance), one can find the transfer function coefficients. Different choices of the time delay lead to different transfer function coefficients. The best choice of time delay depends on the component as well as the driving function. When we consider heat flow through a whole building, these are typically light-weight components and introduction of a time delay is unwarranted. Therefore, we set the time delay to zero.

As illustrated by the previous examples, we first draw the polar or Bode diagram for the component or building and, after some experience, decide at a glance how many and which frequencies to choose for matching the transfer functions. It is prudent to choose as few frequencies as necessary for the matching. The question of optimal choice of frequencies, taking into account building response as well as the spectrum of driving functions, needs further study. The stability criterion imposes a stringent constraint. The method described here has generally been adequate for typical buildings applications.

The following will make use of z-transforms. One can, of course, adhere to Fourier transforms (and discrete Fourier transforms for sampled data). It will be convenient to switch between Fourier transforms and z-transforms, as required. A mathematical discussion of these transforms can be found in textbooks (e.g., Eveleigh 1972). An intimate knowledge of z-transforms is not necessary to follow the process; Appendixes A and B contain a brief discussion of the relevant aspects of z-transforms. Refer to Eq. 5-3 of Section 5.0 to see how the time domain simulation is performed.

Assuming sampled data with sampling interval Δ, we can take z-transform of Eq. 3-1 to get

$$V(z)\ T_{in}(z) - W(z)\ T_{out}(z) - S(z)\ I_{sun}(z) = Q_{int}(z) + Q_{aux}(z)\ . \quad (4-18)$$

(We have used the same notation for Fourier or z-transform of functions; the context should make it clear what we are referring to.)

When the transfer function $V(z)$, $W(z)$ and $S(z)$ are ratios of polynominals in z^{-1}, the time-domain simulation is enormously simplified. Appendix B outlines this principle. Let
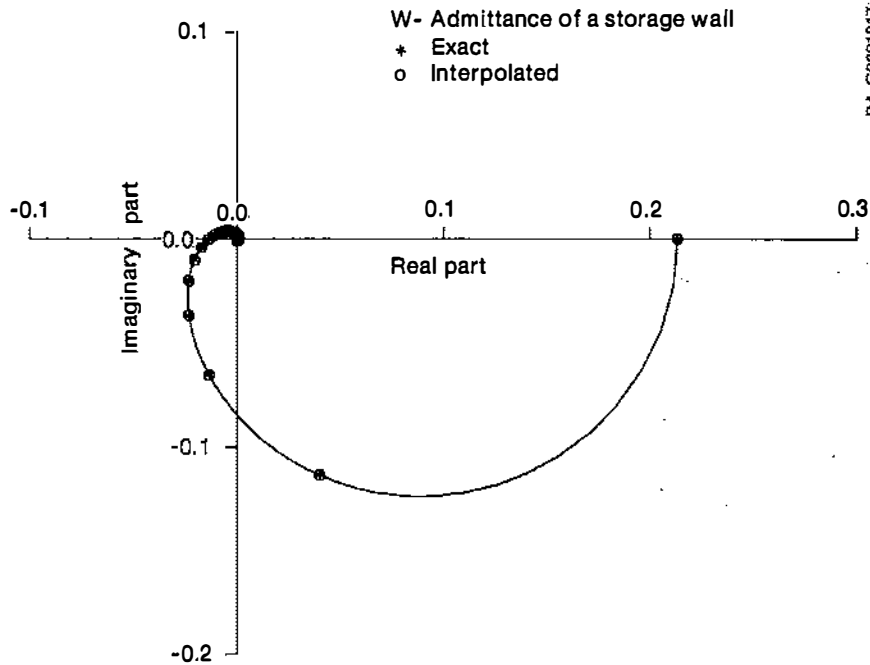
Figure 4-6. Polar diagram of the W-admittance of the 12 in. concrete wall: exact (*) and approximate (o) based on matching at 96-hr and 4-hr cycles with a 2-hr delay

$$V(z) = \frac{P_{num}^{in} (z^{-1})}{P_{den}^{in} (z^{-1})} , \qquad (4-19)$$

$$W(z) = \frac{P_{num}^{out} (z^{-1})}{P_{den}^{out} (z^{-1})} , \qquad (4-20)$$

$$S(z) = \frac{P_{num}^{sun} (z^{-1})}{P_{den}^{sun} (z^{-1})} , \qquad (4-21)$$

where

$$P_{num}^{in} (z^{-1}) = b_0^{in} + b_1^{in} z^{-1} + \ldots + b_{r_{in}}^{in} z^{-r_{in}} , \qquad (4-22)$$

$$P_{den}^{in} (z^{-1}) = 1 + a_1^{in} z^{-1} + \ldots + a_{r_{in}}^{in} z^{-r_{in}} . \qquad (4-23)$$

Although not necessary, it is convenient to make the denominator and numerator polynominals of the same degree; we assume this throughout. Similar expressions hold for the other transfer functions.

5.0 TIME-DOMAIN SIMULATIONS FROM BUILDING DESCRIPTION: THE FORWARD PROBLEM

In the previous section we saw how, from a building description, we first calculated V, W, and S at zero and a selected number of frequencies, and then determined the coefficients of the polynominals (Eqs. 4-19 through 4-23). In this section we discuss how this can be turned into an hourly simulation.

Substituting the expressions contained in Eqs. 4-19 through 4-23 into Eq. 4-18 and rearranging, we get (dropping z's for notational simplicity):

$$P_{den}^{out} \cdot P_{den}^{sun} \cdot P_{num}^{in} \cdot T_{in} - P_{den}^{in} \cdot P_{den}^{sun} \cdot P_{num}^{out} \cdot T_{out} - P_{den}^{in} \cdot P_{den}^{out} \cdot P_{num}^{sun} \cdot I_{sun}$$

$$= P_{den}^{in} \cdot P_{den}^{out} \cdot P_{den}^{sun} \cdot (Q_{int} + Q_{aux}) . \qquad (5\text{-}1)$$

We can multiply out the product of the polynominals to get polynominals of degree $r = r_{in} + r_{out} + r_{sun}$, as follows:

$$P_{den}^{out} \cdot P_{den}^{sun} \cdot P_{num}^{in} = \zeta_0^{in} + \zeta_1^{in} z^{-1} + \ldots + \zeta_r^{in} z^{-r} \qquad (5\text{-}2)$$

and similar expressions for the other polynominals with superscripts "out," "sun," and "int" respectively. As Appendix A outlines, this leads directly to the time-domain equation

$$\zeta_0^{in} T_{in}(n) + \zeta_1^{in} T_{in}(n-1) + \ldots + \zeta_r^{in} T_{in}(n-r)$$

$$- \zeta_0^{out} T_{out}(n) - \zeta_1^{out} T_{out}(n-1) - \ldots - \zeta_r^{out} T_{out}(n-r)$$

$$- \zeta_0^{sun} I_{sun}(n) - \zeta_1^{sun} I_{sun}(n-1) - \ldots - \zeta_r^{sun} I_{sun}(n-r)$$

$$= 1 \cdot (Q_{int}(n)j + Q_{aux}(n)) + \zeta_1^{int} (Q_{int}(n-1) + Q_{aux}(n-1)) + \ldots +$$

$$\zeta_r^{int} (Q_{int}(n-r) + Q_{aux}(n-r)) , \qquad (5\text{-}3)$$

where $T_{in}(n-k)$ denotes the inside temperature at time $(n-k)\Delta$, $k = 0, \ldots, r$, etc.

The simulations are initialized with some assumed values of $T_{in}(n-1)$, ..., $T_{in}(n-r)$ and $Q_{aux}(n-1)$, ..., $Q_{aux}(n-r)$. (T_{out}, I_{sun}, and Q_{int} are, of course, given quantities at all time steps.) Then with $Q_{aux}(n)$ set to zero, $T_{in}(n)$ is calculated from Eq. 5-3. If this violates the thermostatic constraint, then $T_{in}(n)$ is set to a value satisfying the constraint and $Q_{aux}(n)$ is calculated. If this violates the capacity of the HVAC system, $Q_{aux}(n)$ is set to its limiting value and $T_{in}(n)$ is calculated. In any case, $T_{in}(n)$ and $Q_{aux}(n)$ are determined. We can advance to the next time step.

It is important to recognize the fundamental difference between the simulation based on Eq. 5-3, previously described, and a microdynamic simulation. In Eq. 5-3, every one of the coefficients depends (in a complicated, but

calculable manner) on all the components. The component heat flows are not explicitly present. By contrast, a microdynamic simulation first calculates component heat flows and then performs a zone energy balance. The fact that Eq. 5-3 deals with whole building quantities is the key feature that defines the proper parameters that can be obtained from building performance data. This is discussed in the next section.

If one is interested in heat flow from a particular component, we can rewrite the energy balance Eq. 4-18 as follows:

$$V_{rest} \cdot T_{in} - W_{rest} \, T_{out} - S_{rest} \, I_{sun} + Q_{comp} = Q_{int} + Q_{aux} \, , \quad (5\text{-}4)$$

$$Q_{comp} = V_{comp} \, T_{in} - W_{comp} \, T_{out} - S_{comp} \, I_{sun} \, , \quad (5\text{-}5)$$

where the subscript "comp" refers to the component transfer function and the subscript "rest" refers to the rest of the building. By writing all transfer functions as ratios of polynominals and initializing them in the obvious manner, we first calculate $Q_{comp}(n)$ from Eq. 5-5 and then substitute it into Eq. 5-4 and proceed as before. The interpretation of Q_{comp}, as well as the calculation of V_{comp}, W_{comp}, and S_{comp} when taking into account convection to air and radiation to other surfaces, is quite intricate. The interaction factor formulation in Subbarao and Anderson (1983) provides the necessary framework.

Studies such as replacing the component of interest by another component are now quite direct. It is only necessary to change V_{comp}, W_{comp}, S_{comp} suitably (keeping in mind the interaction factors).

It is crucial to note how we started with the frequency response of a building and ended with time-domain simulations. Knowing the response at all frequencies is tantamount to knowing the response to a driving function of any profile. We determined the response at all frequencies by knowing the response at certain selected frequencies and interpolating for all other frequencies. Thus, the response of the building to any ambient weather as well as to internal heat can be studied. Typically in buildings applications, the dominant frequencies in ambient weather and the damping from thermal inertia imply that the response to a small number of frequencies and interpolation is adequate. We gave a method to choose these frequencies based on polar diagrams. The approximations can be systematically improved by including as many frequencies as one wishes. The implication of including a large number of frequencies is that the polynominals are of a high degree and, therefore, the number r of past values one has to keep in Eq. 5-3 is high. This presents no particular problem for the forward process, but can be a problem for the inverse process with short-term data.

6.0 REARRANGEMENT OF HEAT FLOWS

In this section, we break up the various heat flow terms in Eq. 2-1 or Eq. 4-18 into a number of components. This decomposition has an appealing physical significance, and is critical for the inverse process. Consider the first term, the V term. The transfer function V(z) was written in the form of Eq. 4-19 with Eqs. 4-22 and 4-23 by fitting V(z) at r_{in} frequencies (in addition to the zero frequency). It can be rewritten as

$$V(z) = L + (1 - z^{-1}) \sum_{i=1}^{r_{in}} \frac{\beta_i^{in}}{1 - \alpha_i^{in} z^{-1}}$$

(6-1)
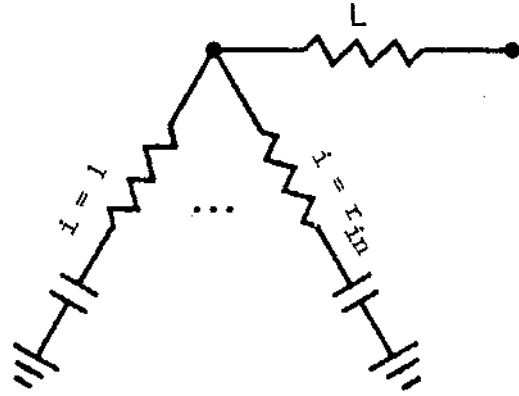
A schematic representation of Eq. 6-1 is shown in Figure 6-1. This is a generalization of the discussion of Figure 4-2. A similar decomposition

Figure 6-1. Schematic diagram representing the different terms in Eq. 6-1

of the W-transfer function will be done; the corresponding circuit representation is rather clumsy. To represent both V and W, the corresponding circuits can be combined. Because transfer functions are our primary objects, we will not pursue the circuits further.

The quantity α_i^{in} is simply related to the time constant C_i/U_i in the ith branch. They are the roots of the polynomial $P_{den}^{in}(z^{-1})$ of Eq. 4-19. The quantity β_i^{in} is proportional to the capacitance C_i in the ith branch (with the constant of proportionally involving the time constant). The precise relationship depends on the discretization scheme. As stated in Section 4.0, stability requires α_i^{in} to be within the unit circle; for buildings applications, they should also be real and positive (although we can relax the positivity constraint, if necessary).

In a view of Eq. 6-1, the term $V(z) \ T_{in}(z)$ of Eq. 4-18 can be decomposed into a number of terms. The term $L \ T_{in}$ is obvious. Consider a term of the form

$$Q_i^{in}(z) = \frac{(1-z^{-1}) \beta_i^{in}}{1-\alpha_i^{in} z^{-1}} T_{in}(z) .$$

(6-2)

In time domain with internal Δ, this can be written as

$$Q_i^{in}(n) - \alpha_i^{in} Q_i^{in}(n-1) = \beta_i^{in}[T_{in}(n) - T_{in}(n-1)] .$$

(6-3)

We can now write

$$Q_i^{in}(n) = q_i^{in}(n) + q_i^{I,in}(n) \ , \tag{6-4}$$

where

$$q_i^{in}(n) = \beta_i^{in}\left[T_{in}(n) - (1-\alpha_i^{in})\sum_{k=1}^{n-1}(\alpha_i^{in})^{k-1}T_{in}(n-k) - (\alpha_i^{in})^{n-1}T_{in}(o)\right] \ , \tag{6-5}$$

$$q_i^{I,in}(n) = (\alpha_i^{in})^n q_i^{I,in}(o) \ . \tag{6-6}$$

Thus, the charge or discharge from an RC element can be written as a sum of two terms as in Eq. 6-4. The term $q_i^{in}(n)$ gives the net charging of the capacitor because of indoor temperature history from the initial time up to the present, and the second term $q_i^{I,in}(n)$ gives the net charging of the capacitor because of indoor temperature history from the remote past to the present. This last term is succinctly contained in the initial heat flow $q_i^{I,in}(o)$ and decays exponentially. It is easy to see that q_{in} of Section 4.0 is equal to $L\ T_{in} + Q_{storage}^{in}$ where $Q_{storage}^{in} = \sum Q_i^{in}$.

With similar decomposition of the other two terms in the left side of Eq. 3-1 we get

$$L\left(T_{in}(n) - T_{out}(n)\right) - S_o I_{sun}(n)$$

$$+ \sum_{i=1}^{r_{in}}[q_i^{in}(n) + q_i^{I,in}(n)] - \sum_{i=1}^{r_{in}}[q_i^{out}(n) + q_i^{I,out}(n)]$$

$$- \sum_{i=1}^{r_{sun}}[q_i^{sun}(n) + q_i^{I,sun}(n)] = Q_{int}(n) + Q_{aux}(n) \ . \tag{6-7}$$

Equation 6-7 gives the decomposition we are seeking. The first term is the effect of the steady-state loss coefficient. This is corrected for the charging and discharging of capacitors by the q^{in} and q^{out} terms. Similarly, $S_o I_{sun}(n)$ is the steady-state solar gains corrected for the storage effects by the q^{sun} terms. The term $\Sigma\ q_i^{in} + q_i^{I,in}$ is the $Q_{storage}^{in}(t)$ term of Eq. 2-1. Identification of other terms is similar.

Equation 6-7 can be easily generalized to include additional terms; inclusion of infiltration heat flow is obvious. Multizone heat flows are included through additional transfer functions as shown later. Ground heat flow, sky temperature depression, etc. give additional terms as we will show later.

7.0 DETERMINATION OF TRANSFER FUNCTIONS FROM SHORT-TERM PERFORMANCE DATA: THE INVERSE PROCESS

In Section 5.0, we showed how the PSTAR simulation is performed starting from a building description, i.e., we addressed the forward problem. In this section we address the inverse problem, namely, determination of transfer functions starting with performance data. The transfer functions must, in principle, be determined at every value of the frequency (or time). In calculating them from a building description, i.e., in solving the forward problem, the calculation is done for any desired value of frequency (or time) and, in general, no special problems arise. In experimentally determining them from performance data, it would be equally straightforward if one can tune the driving functions to any desired frequency and measure the amplitudes and phases of the heat flows. Performance data on real buildings in real weather, however, has all the frequencies and all the driving functions jumbled; it is necessary to disentangle them. One can treat the transfer functions at every frequency as unknown parameters and attempt to estimate them from performance data. This attempt is doomed because it involves far too many parameters to be estimated with reasonable certainty. We are assuming that we only have system (i.e., whole building) performance data. If we have component (for example, wall) performance data with heat flows or temperatures measured at various places through the wall, a larger number of parameters can, in principle, be estimated.

A strict view of the inverse process is that the building is a black box whose characteristics are to be determined from a knowledge of performance data and nothing else. This viewpoint creates a dilemma. A proper thermal' characterization of a building requires a rather large number of parameters. This is why the forward process is so complex. Performance data, especially short-term data, allow meaningful estimation of only a small number of parameters. This is why simple circuits are favored for the inverse process. This force-fitting of a complex system into a simple model of the system generally results in the parameters being nonrepeatable or sensitive to the choice of the model, thereby defeating much of the purpose of the inverse process. This section presents a technique we refer to as "transfer function renormalization" that allows a complex model of the building with only a small number of parameters to be determined from performance data.

We have a more liberal viewpoint of the inverse process. In addition to the performance data, we will use an audit description of the building, namely, a microlevel description with a best estimate (perhaps from a handbook) of the properties. From the performance data and the audit building, we will obtain the macroparameters for the as-built building through transfer function renormalization, which operationally reduces to renormalization of heat flows.

A number of transfer function renormalization schemes can be envisioned. After studying a number of them, we have arrived at the following scheme that results in: (1) a (generalized) linear least squares fit and (2) parameters with simple physical significance. The simplicity of linear least squares fit over a nonlinear fit is tremendous.

The renormalization scheme is simple. First, start with the audit description to determine, through the frequency matching process of Sections 3.0 and 5.0, α's and β's, then using measured values of T_{in}, T_{out} and I_{sun}, determine the time series of

$$L\left(T_{in}(n) - T_{out}(n)\right) , S_o I_{sun}(n) , q_i^{in}(n), q_i^{out}(n) \text{ and } q_i^{sun}(n) .$$

Let us use subscript "audit" to denote these terms. Eq. 6-7 would be satisfied by these audit quantities if the audit building was the same as the as-built building. This, however, is rarely the case and indeed is the reason for testing the building. Introduce a set of parameters to be determined from a linear least squares fit, as follows:

$$p_0 L \left(T_{in}(n) - T_{out}(n)\right) - p_0^{sun} S_o I_{sun}(n)$$

$$+ \sum_{i=1}^{r_{in}} \left[p_i^{in} q_i^{in}(n) + (\alpha_i^{in})^n p_i^{I,in}\right] - \sum_{i=1}^{r_{out}} \left[p_i^{out} q_i^{out}(n) + (\alpha_i^{out})^n p_i^{I,out}\right]$$

$$- \sum_{i=1}^{r_{sun}} \left[p_i^{sun} q_i^{sun}(n) + (\alpha_i^{sun})^n p_i^{I,sun}\right] = Q_{int}(n) + Q_{aux}(n) . \tag{7-1}$$

The parameters to be determined from a least squares fit of Eq. 7-1 to the measured values are p_0, p_0^{sun}, p_i^{in}, p_i^{out}, p_i^{sun}, $p_i^{I,in}$, $p_i^{I,out}$, $p_i^{I,sun}$. There are, thus, $2 + 2(r_{in} + r_{out} + r_{sun})$ parameters.

From Eq. 7-1 it is clear that the audit transfer functions are related to as-built transfer functions, as follows:

$$V^{as\text{-}built}(\omega) = p_0 L + (1-e^{-i\omega\Delta}) \sum_{k=1}^{r_{in}} \frac{\beta_k^{in} p_k^{in}}{1 - \alpha_k^{in} e^{-i\omega\Delta}} \tag{7-2}$$

with similar relations for W and S. Eq. 7-2 can be rearranged in the form of a ratio of polynomials in z^{-1} of degree r_{in}. This allows, following Section 5.0, a simulation of the as-built building for long-term extrapolation, building-as-a-caliorimeter, etc. The as-built loss coefficient is p_0 times the audit value. The capacitances β_k^{in} are renormalized to $p_k^{in} \beta_k^{in}$. The time-constants (α's), however, remain at their audit values. This is the key assumption that allows a linear estimation scheme possible. This assumption is well justifiable, even though it may not be initially apparent. If a circuit has several RC elements, i.e., several time constants ("several" translates, in practice, to two or more), as in Figure 6-1, one can vary the individual α's over a broad range of values, but adjust β's such that the system performance is practically indistinguishable. Thus the β's provide all the degrees of freedom we need.

Not all of the $2(r_{in} + r_{out} + r_{sun}) + 2$ parameters are statistically significant. Sometimes, having too many parameters may even result in violation of

the stability criterion. From Figure 6-1, it is easy to see that the p_i's should all be positive; if not, the stability criterion may be violated. While statistical tests can be performed to determine whether to introduce any of the parameters, we will first build in as much physics as possible. The q^{in} terms, for example, can be arranged in order of increasing α's, aggregated into a small number of groups which share the same p; if $r_{in} = 4$, then $p_1^{in}(q_1^{in} + q_2^{in}) + p_2^{in}(q_3^{in} + q_4^{in})$ would replace the corresponding terms in Eq. 7-1. We can go even further and introduce one parameter p^{in} instead of separate p_i^{in}, and one parameter p^{out} instead of the separate p_i^{out}, and one parameter p^{sun} instead of the separate p_i^{sun}. A glance at the graphs of the heat flows indicates whether any of the flows are so small that introducing renormalization factors for them might be unjustified. The renormalization procedure is general enough that any heat flow (caused by sky temperature depression, infiltration, etc.) can also be renormalized. It is generally unwise to renormalize small heat flows.

Equation 7-2 corresponds to multiplying the conductance L in Figure 6-1 by p_0, and the conductance as well as the capacitance in the kth leg by p_k^{in}. If the original circuit satisfied the stability criterion, the circuit with modified values should continue to do so when p_0 and p_k^{in} are positive. However, because discretization introduces additional assumptions, it is best to check if the renormalized transfer function satisfies the stability criterion.

Consider one of the initial heat flow terms, say, $(\alpha_1^{in})^n p_1^{I,in}$ in Eq. 7-1. This really should have been of the form (see Eq. 6-7) $(\alpha_1^{in})^n q_1^{I,in}(o) p_1^{I,in}$. Because the initial heat flows $q_1^{I,in}$ of the audit building is unknown anyway, we can absorb it in the $p_1^{I,in}$ term that is to be determined by fitting to the data. Now $p_1^{I,in}$ will have dimensions of heat flow.

Consider two of the initial heat flow terms, whether they both belong to the same driving function is irrelevant. For specificity, consider $(\alpha_1^{in})^n p_1^{I,in} + (\alpha_1^{out})^n p_1^{I,out}$. If α_1^{in} and α_1^{out} are equal, only the sum $p_1^{I,in} + p_1^{I,out}$ is well determined; the individual terms $p_1^{I,in}$ and $p_1^{I,out}$ are ill determined. If the two α's are close, the situation is similar. Since all α's are constrained to be between 0 and 1 (or, if we relax positivity, between -1 and 1) it is pointless to have too many α's. Furthermore, the initial heat flows decay exponentially because of the factor α^n. Thus, from a practical point of view, we can (1) choose the fitting period to begin several hours after the start of the data and ignore all initial flow terms, (2) choose some representative α's for initialization, say, only the α_1^{in}'s, or (3) choose a combination of (1) and (2). We favor the option (1) as far as possible.

The role of the initial heat flow terms is perhaps best seen through the example in Section 17.0.

8.0 SOLAR GAINS FROM MULTIPLE ORIENTATIONS AND SHADING

Real buildings have solar gains from multiple orientations and have shading devices. The formulation of the previous section is modified in this section to account for these effects. Previously, we assumed that the only solar gain in the problem is from a single orientation with incident flux I_{sun}. (If we have transmittance depending on incident angle, then transmitted radiation may be more appropriate as the driving function.) This is quite reasonable in the absence of any shading devices. For long-term extrapolation, the seasonal motion of the sun is automatically included in using I_{sun} as the driving function. (If the distribution of radiation over different absorbing surfaces has a seasonal dependence, the above treatment is only approximate.) In this section, we address shading devices as well as gains from multiple orientations.

Note that in the presence of shading devices, I_{sun} is not an appropriate driving function even for a single orientation. For example, consider a direct gain south window with an overhang at a time of the year when the overhang partially blocks direct sun. On a cloudy day the equivalent solar aperture (S_o) will be much higher than on a sunny day if we use I_{sun} as the driving function. It is more appropriate in this case to use as the driving function the total radiation $q^i_{sun}(t)$ incident (or transmitted) on the component labeled i. Thus the term $S \cdot I_{sun}$ in Eq. 4-18 is changed to $S_i q^i_{sun}$.

The physical interpretation of S_i is now quite different. The quantity $S_i(\omega=0)$ now no longer represents the equivalent aperture area, but represents the fraction of total incident radiation that the component transmits under steady conditions. The interpretation of S_i at any other frequency is similarly obtained. In fact, the unit area of S as defined in Section 3.0 is equal to the S of this section (if we assume one-dimensional heat flows through radiation-receiving elements).

If we write S_i (in z-transformed space) as a ratio of polynominals in z^{-1}, we can proceed exactly as before, except that instead of the meteorological quantity I_{sun} as the driving function, we have to use the component-dependent quantity q^i_{sun}. The calculations of $q^i_{sun}(t)$, including shading and incident angle modifiers, are quite tedious. Fortunately, the microdynamic simulations have codes that perform these calculations. It is expedient, therefore, to use the microdynamic simulations for such calculations. However, it is generally difficult to extract $q^i_{sun}(t)$ from a microdynamic simulation through manipulation of inputs and outputs only. We, therefore, modify the calculations so that only input-output manipulations are needed; such a capability is highly desirable because it entails no code modifications. Furthermore, we wish to avoid as much as possible dealing explicitly with individual components and consider summing over the components. These objectives are accomplished as follows: first, model the entire building on a microdynamic simulation. With constant and equal T_{in} and T_{out} and the desired (measured, or typical meteorological year (TMY), etc.) solar radiation, calculate the cooling loads. These loads are equal to the calculated solar gains. Let us call this $Q_{sun}(t)$. The $S \cdot I_{sun}$ term in the heat balance Eq. 4-18 is replaced by $Q_{sun}(t)$. For the forward process, after Q_{sun} has been calculated, there is one fewer transfer function to deal with, and the rest of the calculations are simplified. In fact, we can just add $Q_{sun}(t)$ to the internal gains term.

In Eq. 6-7, where heat flow terms are decomposed, all the terms with a sub or superscript "sun" are replaced by $Q_{sun}(n)$.

At this point, it can be argued that if a microdynamic simulator is needed to obtain Q_{sun}, the entire simulation for the forward process might as well be performed on that simulator. This is quite so, PSTAR, in this case, may have intuitive value through disaggregated heat flows. For the inverse process, PSTAR is essential. Even for the forward process, PSTAR can be used for a stand-alone simulation by simplfying the thermal representation of the wall through the frequency matching process; one can deal with surface transfer functions to ensure that an explicit surface node is present where solar radiation can be absorbed.

For the inverse process we need to renormalize, in a suitable manner, the audit solar gains. While one can envision breaking Q_{sun} into a number of pieces (depending on orientation or radiation-receiving component, etc.). These pieces introduce considerable complications. The simplest scheme is to change the $Q_{sun}(n)$ term into $p^{sun} Q_{sun}(n)$. This is probably adequate in a majority of buildings. In the event that additional renormalization is needed we need a suitable generalization.*

First, note that the above simple renormalization scheme can be viewed as treating Q_{sun} as the solar driving function with a transfer function of 1 for the audit building, and a transfer function of p^{sun} for the as-built building. A generalization is to replace the transfer function p^{sun} for the as-built building by a ratio of polynomials of degree unity. As in Section 6.0, this can be rearranged in the form

$$p^{sun} + \frac{p'_{sun}(1-z^{-1})}{1 - \alpha_{sun} z^{-1}} . \qquad (8\text{-}1)$$

(In the limit $p'_{sun} = 0$, we recover the previous formulation.) The solar parameters to be estimated from a least squares fit are p^{sun}, p'_{sun}, α_{sun}, and $p^{I,sun}$ (for initialization).

For notational simplicity we will drop $p^{I,sun}$. It can be reintroduced easily. Considering the discussion at the end of Section 7.0 we may not even need this term.

Note that negative values of p^{i}_{sun} tend to delay the renormalized solar gains over the audit gains, and positive values of p_{sun} tend to advance them. (We have not performed the necessary numerical studies to determine whether it is safer to bias the audit description to make p'_{sun} negative.)

---

*In using a microsimulation for obtaining Q_{sun}, ensure that the time conventions (whether the hour number represents the hour beginning at that value or ending at that value, etc.) are consistent. Although one can burden the renormalization process to account for any inconsistencies, it is unwise to do so. We assume that time conventions are all consistent.

The estimation of α_{sun} introduces nonlinearities. It is, however, easy to deal with because $0 < \alpha_{sun} < 1$. Perform a linear estimation with α_{sun} varied over a range of values between 0 and 1, and pick the value of α_{sun} that produces the best fit. The solar terms in Eq. 7-1 are then replaced by

$$p^{sun} Q_{sun}(n) + p'_{sun} q_{sun}(n) , \qquad (8-2)$$

with q_{sun} given by (compare Eq. 6-5)

$$q_{sun}(n) = Q_{sun}(n) - (1 - \alpha_{sun}) \sum_{k=1}^{n-1} \alpha_{sun}^{k-1} Q_{sun}(n-k) - \alpha_{sun}^{n-1} Q_{sun}(0) . \qquad (8-3)$$

(An approximation that eliminates the above nonlinear estimation is to fix the value of α_{sun} at, say, 0 and estimate only p^1_{sun}.) Note that working with the transfer functions (as for T_{in} and T_{out} driving functions) is much more desirable than working with heat flows (as for solar gains in this section). The complexity of multiple orientations and shading makes this compromise necessary.

So far, we have assumed that the building has solar gains from only one orientation (but possibly with shading devices). We will now take up gains from multiple orientations (possibly with shading devices). Consider the case when all radiation-receiving surfaces are identical but oriented differently. An example might be an office building with all four faces symmetric (assuming no opaque wall gains or roof gains). Our previous discussion now holds except $q_{sun}(t)$ now represents the total incident on the radiation-receiving components in all orientations. We can proceed as before to determine $Q_{sun}(t)$ and renormalize it in exactly the same manner as before.

We have seen then that in two extreme situations: (1) all solar gains are from a single orientation with no shading devices (complex sun-to-building coupling e.g., mixture of direct gain and Trombe wall, but simple solar) and (2) all radiation-receiving components are identical, but possibly oriented in different directions (complex solar, but simple sun-to-building coupling), we have a formulation based on renormalizing calculated solar gains. In these cases I_{sun} or q_{sun}, respectively, play the same role as an ambient temperature i.e., they provide the proper driving function. The building can be thought of as bathed in I_{sun} or q_{sun} with only the radiation-receiving surfaces responding. In all other cases, additional approximations will have to be made to proceed in a simple manner. We simply use the formulation based on calculating $Q_{sun}(t)$, and renormalizing it as before.

The potential pitfalls of the above approximations must be recognized. If the inputs to the microsimulation, from which Q_{sun} was obtained, turn out to be accurate for one orientation and inaccurate for another, the global renormalization scheme given previously will be oblivious to it. Correctly determined east solar gains may be unnecessarily renormalized to improve the incorrectly determined west gains. Correctly determined roof gains may be unnecessarily renormalized in spring (and summer) to improve the incorrectly determined south gains during the test period in winter. The former can, in principle, be rectified by additional measurements during the short-term testing period. The latter is inherent in the long-term extrapolation process.

Despite these caveats, it is reassuring that the proposed renormalization scheme is applicable in the two limiting cases (simple building but complex solar and complex building but simple solar) as mentioned before. We will, therefore, use the renormalization scheme. Modifications, such as not renormalizing a part of the solar gains deemed accurate and renormalizing the other part, are all possible and straightforward.

From the previous discussion, it follows that one should ensure that during the short-term test period clear weather prevails at least in a representative manner. If cloudy weather prevails throughout the test period, the solar renormalization obtained from the data may not be applicable for clear periods.

APPENDIX TO SECTION 8.0

We give here another approach of methodological interest. Its practical applications have not been explored. Note that every term in the heat balance Eq. 3-1 is of the form: whole building transfer function × driving function. When we have several radiation-receiving components, the resulting equation has explicit terms for each component. We would like to rewrite it in a form without explicit component terms, but with only whole building terms. This can be done, as follows:

To the extent that diffuse radiation is isotropic, it is essentially like an ambient temperature and summing over components is automatic. We are then left to consider beam radiation. Let $I_{dn}(t)$ be the beam flux. Then

$$I_i^{sun}(t) = \frac{I_i^{sun}(t)}{I_{dn}(t)} I_{dn}(t) . \tag{8-1a}$$

The ratio $I_i^{sun}(t)/I_{dn}(t)$ is actually a periodic function with a period of 24 hours that has slow changes over the course of a season. It is independent of cloud cover. We can therefore write it as

$$\frac{I_i^{sun}(t)}{I_{dn}(t)} = \sum_{k=0}^{\infty} f_{i,k}^c \cos(k\omega_D t) + f_{i,k}^s \sin(k\omega_D t) , \tag{8-2a}$$

where ω_D is the diurnal frequency. The terms $f_{i,k}^c$ and $f_{i,k}^s$ are very slowly varying functions of time. We can now write

$$\sum_i \int \hat{S}_i(t-t') I_i^{sun}(t') \, dt' = \sum_k \int \left(\sum_i \hat{S}_i(t-t') f_{i,k}^c\right) I_{dn}(t') \cos(k\omega_D t')$$

$$+ \left(\sum_i \hat{S}_i(t-t') f_{i,k}^s\right) I_{dn}(t') \sin(k\omega_D t') . \tag{8-3a}$$

Thus, we can look upon $I_{dn}(t') \cos k\omega_D t'$ and $I_{dn}(t') \sin k\omega_D t'$, $k = 0,1,2,\ldots$ as a series of driving functions and $\sum_i S_i f_{i,k}^c$ and $\sum_i S_i f_{i,k}^s$ as the corresponding whole building transfer functions. For practical calculations, $k = 0,1,2$ is probably sufficient. We now have several driving functions and can proceed in the same manner as before.

9.0 HEAT FLOW TO GROUND

Heat flow to the ground is a significant path of heat flow that needs careful attention. The fact that this heat flow path has large time constants--larger than the typical short-term test period--creates special problems. We will address these problems in the context of incorporating ground heat flow in the inverse process. We outline only the general principles here.

First, consider a slab-on-grade building. A term $Q_{ground}(t)$ for the heat flow to the ground was included in Eq. 2-1. One can calculate this term for the audit building and renormalize it with a factor to fit performance data. In general, this is unsatisfactory. A calculation that accounts for the response of the slab to hourly variations in T_{in} (and, less important, to hourly variations in T_{out}) as well as to variations on much larger time scales is not readily done. Even if it were, a single renormalization factor for heat flows from disparate time scales is questionable. The following method is, therefore, proposed:

The convolution integral representing $Q_{ground}(t)$ can be written in the frequency domain as

$$Q_{ground}(\omega) = V_{ground}(\omega) \, T_{in}(\omega) - W_{ground}(\omega) \, T_{out}(\omega) \,. \qquad (9\text{-}1)$$

The function $V_{ground}(\omega)$ (and similarly the W) can be decomposed into

$$V_{ground}(\omega) = V_{fast}(\omega) + V_{slow}(\omega) \,. \qquad (9\text{-}2)$$

The term $V_{fast}(\omega)$ accounts for the fast response (that is, to hourly variations of T_{in}) and V_{slow} for the slow response. This decomposition should be done keeping in mind the spectrum of the driving function. Equation 9-2 must be valid at frequencies at which the driving functions have significant spectral content. The heat flow contributed by V_{fast} can be absorbed into the heat flow from the rest of the building. The heat flow from $V_{slow}T_{in} - W_{slow}T_{out}$ will be practically constant over the short-term test period and can be renormalized, as appropriate. The methods of Mitalas (1983) and the Interzone Temperature Profile Estimation (Krarti, Claridge and Kreider 1985) can be used to obtain the slow response.

For a building with an unconditioned basement (or crawl space), the basement can be treated as a separate zone. As far as the living zone is concerned, the basement temperature can be thought of as another driving function.

Equation 7-1 has the following additional terms (subscript or superscript B stands for basement):

$$p_B L_B \big(T_{in}(n) - T_{basement}(n) \big) + \sum p_i^B q_i^B(n) + (\alpha_{in}^B)^n \, p_i^{I,B} \,,$$

because the basement temperature usually changes very little, the term $q_i^B(n)$ is small and it is probably best to fix p_i^B at 1 and $p_i^{I,B}$ at 0. (The floor between the main level and the basement contributes to the V-admittance of the main level in the usual manner.) It is, thus, simple to include the basement in the main level heat balance. This will be illustrated with real-building data in future publications.

We will now consider performing an energy balance for the basement zone; this is where heat flow to the ground enters in an essential manner. The considerations are similar to those for a slab-on-grade building. An excessively detailed calculation is probably unwarranted because the basement temperature tends to stay nearly constant. The heat balance is similar to that for a slab-on-grade building except for the term $p_B L_B (T_{in}(n) - T_B(n))$, and a term $f \cdot Q_{gas}$ where f is the fraction of gas input, Q_{gas}, to a furnace in the basement that ends up as direct heat in the basement. (A more complex model of heat flow to basement from the furnace can, of course, be incorporated.) The renormalization factor p_B is known from living zone heat balance. The quantity f can be obtained as follows: from flue gas measurements, the fraction of gas input that leaves the furnace as heat that can be obtained. From building calorimetry (Subbarao, Burch and Jeon. 1986), the fraction of gas input that ends up as delivered heat in the main level is obtained. The difference gives f. One can proceed in a manner similar to that for the slab-on-grade problem, except that one should expect to determine only one or two renormalization parameters.

The above cursory discussion needs to be refined through numerical studies as well as real-building studies. For certain applications, it is not necessary to perform an energy balance for the basement zone. As far as the performance of the main zone is concerned, the primary reason for performing an energy balance on the basement zone is to predict the basement temperature. If this temperature is available through measurements, or if it can be reasonably estimated through other means, it is not necessary to perform an energy balance for the basement.

10.0 PERTURBATION THEORY OF SMALL EFFECTS

The primary variables, such as the building loss coefficient, have a strong signal in the performance data. A number of effects such as variable film conductances are often too small to be determined from whole building performance data. Yet, they are sufficiently important to merit further consideration. An outline of a perturbation approach is presented here.

Let $\{a\}$ be the set of building inputs such as conductivities of wall materials, etc., and $\{b\}$ the set of heat-transfer characteristics. The distinction between the two sets is not well defined, but it is still useful to have the two sets. For example, an element of the set $\{b\}$ might be a temperature and wind dependent convective heat transfer coefficient. Let the set $\{b_o\}$ make the system linear. $Q(\{a_{actual}\}, \{b\})$ is the actual heat flow we are interested in.

$$Q(\{a_{actual}\}, \{b\}) = Q(\{a_{actual}\}, \{b_o\})$$
$$+ [Q(\{a_{audit}\}, \{b\}) - Q(\{a_{audit}\}, \{b_o\})]$$
$$+ [Q(\{a_{actual}\}, \{b\}) - Q(\{a_{audit}\}, \{b\})$$
$$-Q(\{a_{actual}\}, \{b_o\}) + Q(\{a_{audit}\}, \}b_o\})] . \quad (10\text{-}1)$$

The last term is of order $(b-b_o) \times (a_{actual} - a_{audit})$, and can be thought of as a higher order term and neglected. Then

$$Q(\{a_{actual}\}, \{b\}) \approx Q(\{a_{actual}\}, \{b_o\})$$
$$+ [Q(\{a_{audit}\}, \{b\}) - Q(\{a_{audit}\}, \{b_o\})] . \quad (10\text{-}2)$$

Because the term (the dominant term) $Q(\{a_{actual}\}, \{b_o\})$ is from a linear system, it can be renormalized as before. The quantity

$$Q(\{a_{audit}\}, \{b\}) - Q(\{a_{audit}\}, \{b_o\}) , \quad (10\text{-}3)$$

can now be obtained from running a microsimulation twice--once with $\{b\}$ and once with $\{b_o\}$. This quantity is nothing but the $Q_{exact} - Q_{approx}$ term of Eq. 2-2 for the audit building. The point of this section is that this term, being a secondary term, can be assumed to be the same for the as-built building.

11.0 DATA REQUIREMENTS FOR PARAMETER ESTIMATION

In Section 4.0 we outlined the calculation of the transfer function, and in Sections 7.0 and 8.0 we defined the parameters that renormalize the calculated transfer functions and heat flows to fit the monitored data. In this section we discuss the type of data that are expected to lead to a reliable determination of the renormalization parameters. If these are not sufficiently well determined, the errors propagate in long-term extrapolation and other applications.

Any parameter estimation should address possible errors and their effect. The effect depends on specific applications. It is sufficient to note here that it is desirable, and often critical, to reduce errors of estimation. Although performance data under normal conditions (meaning that no efforts are made to subject the building to special driving functions) sometimes yield surprisingly reliable estimates of the parameters, typically the uncertainties are significantly large. It is easy to see that the building heat capacity will be poorly determined unless the inside temperature varies significantly during the period of analysis. There are similar, more subtle constraints that affect the determination of steady-state properties. If a building is monitored for a long period, we can expect that all important building responses will be contained in the data. However, if the building is to be monitored only for the short term, one should ensure that during this period all important responses are elicited. This usually implies that some form of testing (in contrast to passive monitoring) is necessary.

Subbarao, Burch, Hancock, and Jeon (1985) clearly demonstrate that short-term data taken without regard to a protocol are usually inadequate to determine the parameters reliably. By estimating the building parameters from actual performance data from an unoccupied residential building (the Maplewood residence) in Arvada, Colorado, the report showed that two radically different estimates yield basically the same short-term behavior.

It is clear, then, that a test protocol should be chosen carefully to ensure that all the parameters are estimated to the desired accuracy. Although the optimal test protocol designed to give the required accuracy, with the shortest possible test period and as little intervention as possible in the building operation, is not readily found, some general principles can be established. These are discussed in the next section.

12.0 THEORETICAL FOUNDATIONS FOR THE TEST PROTOCOL

The previous section argued that to estimate the building parameters reliably from short-term performance data, it is necessary to subject the building to suitable tests. The protocol is for such tests and is the main topic of this section.

The test protocol should be devised to yield as much information as possible, with as short a test duration as possible. The energy balance equation should be used as a guide for devising a test protocol. We will outline the theoretical foundation of the specification of the tests.

The outdoor temperature and solar radiation are beyond the control of the experimenter. The inside temperature and electrical heat input, however, can be controlled. In nonresidential buildings, introduction of electrical heat may not be feasible, and existing HVAC systems may have to be used. These should be chosen optimally during the test period. For specificity, let us suppose that we are interested in the four parameters, P_0, P_{in}, P_{sun}, $P_{furnace}$ in the equation ($Q_{storage}^{out}$ is usually too small to warrant a renormalization parameter)

$$Q_{int} = P_0 L(T_{in} - T_{out}) + P_{in} Q_{storage}^{in} + Q_{storage}^{out} + P_{sun} Q_{sun}$$

$$+ P_{furnace} Q_{gas} + Q_{other} , \qquad (12-1)$$

where Q_{gas} is the gas input to the furnace with (constant) heating system efficiency (including duct losses, etc.) $P_{furnace}$. The quantity Q_{other} denotes all other known or small heat flows, such as infiltration, extra radiation caused by sky temperature depression, etc. To minimize the interplay among different parameters, it is necessary that the corresponding heat flows be uncorrelated. The simplest method of ensuring this is to have periods where only one heat flow dominates. The corresponding parameter is then well determined. This can be accomplished for the parameter P_0 through coheating, which maintains a constant inside temperature through electrical heat throughout a night. Toward the end of the coheating period, the term $L(T_{in} - T_{out})$ dominates. By maintaining a constant inside temperature and alternating between electric heating and furnace heating during a night, and taking the difference between the electric heating hour and the furnace heating hour in Eq. 12-1 allows a good determination of $P_{furnace}$. Such tests were proposed and performed by Sonderegger (1978) and Sonderegger, Condon, and Modera (1980). PSTAR allows a systematic correction coming from the residual flows because of other terms. A period of sunshine is necessary for a good determination of P_{sun}. A period of variation in inside temperature (induced by the sun or by nighttime cool down) is necessary for a good determination of P_{in}. The fact that $Q_{storage}^{in}$ and Q_{sun} tend to be uncorrelated over a period of a day is useful. (A period of large ambient temperature fluctuation may provide a means of estimating P_{out}.) A night of constant inside temperature maintained alternately by electric and furnace heating, a sunny daytime period, a warmup or cool-down period are, therefore, necessary. From a plot of the various flows, one can find the appropriate "windows" for estimating the

various parameters. In general, a window should be designed so that either (1) the heat flow associated with one renormalization parameter dominates, or (2) if more than one parameter is to be determined, that the corresponding heat flow terms are uncorrelated. An iteration procedure for improving the estimates from the various windows should be used. The idea of using an iterative method was proposed in the context of a different model by Duffy (Duffy and Saunders 1987).

When there is more than one zone, say, a basement zone in addition to the living zone, two coheating periods are necessary. One can then establish a determinant condition to be satisfied by the temperature differences so that two linearly independent equations for two loss-coefficients can be obtained. We found it difficult to get a good value of L_B (the loss coefficient) from main level to the basement because the heat flow to the basement is generally not large enough.

We will now discuss a test that introduced electrical heat of a sinusoidal profile. This appears to give extraordinarily accurate values of the V-admittance at that particular frequency, thereby providing a clean comparison between the design versus actual admittances. For this reason, sinusoidal tests have a variety of applications, and have been applied to a residential building (Subbarao, Burch, Hancock, and Jeon 1985). From knowing the building loss coefficient, and the admittance with respect to inside temperature at one (or more) frequency obtained from such sinusoidal tests we can, using the qualitative features of the audit description, devise an interpolation of the admittance for all frequencies. This, then, gives the real building admittances to be used in the evaluations of the $Q_{storage}^{in}$ term. Then, the p_{in} term need not be estimated from performance data. This process is detailed for an example building later.

The diurnal frequency is a dominant frequency in the driving functions and is also appropriate from the point of view of the response of typical buildings. (The diurnal frequency is too high for adequate characterization of very massive buildings and too low for ultralight buildings; it is a reasonable choice for most buildings.) However, if the heat input is at the diurnal frequency, there will be confounding effects from natural driving functions. In other words, the frequency of heat input should be chosen to be near, but not too near, the diurnal frequency. We have used 16-hr cycles with success.

The accuracy of the V-admittance determination from sinusoidal tests rests on the following "signal enhancement" principle. If two periods have all the driving functions qualitatively similar except one, then parameters estimated from period 1 (although by themselves subject to significant uncertainty) are quite sufficient for subtracting all of the effects during period 2 except the one driving function. What remains is the building response to this one driving function. This provides a strong signal from which to extract the response to that driving function.

Let us see how this principle applies to V determination. The building is monitored under normal conditions for, say, two days and temporary values of the parameters obtained. Over the next two days, electrical heat will be introduced according to the profile $Q_{prof} = \bar{Q} + \Delta Q \sin[\omega(t-to)]$ with a suitable choice of ω and t_o. (We earlier argued for a period of 16 hours.)

We then use the temporary values of the building parameters to calculate what the inside temperature would have been in the absence of Q_{prof}. The remaining temperature response can be fit to

$$\overline{T}_{in} + \Delta T \sin [\omega(t-t_o')] \ ,$$

then $\Delta Q/\Delta T$ gives the magnitude $|\vec{V}|$ and $(t_o'-t_o)$ gives the phase of $\vec{V}$. Thus, admittance at the 16-hr cycle can be accurately determined. The signal enhancement principle can be easily extended when more than one driving function changes.

We have emphasized sinusoidal profile for the heat input. Other forms, such as step functions and square waves, are perhaps easier from an experiment point of view. While experimental ease is an important consideration, there are distinct theoretical advantages for sine waves:

● For a linear system, if the input is a sine wave, the output must be a sine wave of the same frequency. The goodness of the fit to sine wave of the output is an approximate measure of the validity of the linearity approximation. Thus, sine wave profile provides a self test.

● Sine waves at different frequencies are approximately orthogonal over finite time intervals. Thus, any errors in subtracting the behavior at the other frequencies (especially at the strong diurnal frequency) have only a small effect on the admittance estimates. Therefore, the V admittance at 16 hours is a very robust estimate.

The sine wave heat input and the signal enhancement principle enable us to obtain the V-admittance at the chosen, e.g., 1/(16 hr), frequency. If, instead, we introduce a pseudo-random binary sequence (prbs) of heat input, the signal enhancement principle allows a determination of V-admittance over a broad range of frequencies. Letherman, Palin, and Park (1982b) showed how the prbs method can be used to determine the V-admittance of a simple test enclosure in a laboratory where the outdoor temperature is a constant, solar radiation, and incidental internal gains (because of refrigerator, lights, etc.) are absent. They also studied (1982a) sinusoidal heat input. In real buildings subject to variable outdoor temperature, solar radiation, and individual internal gains, the signal enhancement principle allows us to subtract these effects and reduce them to the problem considered by Letherman, Palin, and Park (1982a).

While a sinusoidal heat profile is desirable, it is by no means necessary. The transfer function renormalization approach is well suited to handle basically any type of data. Rise and decay tests are adequate for the long-term extrapolation problem. If an accurate determination, even at a single frequency, is desired (as for a design versus actual comparison), sine waves are desirable.

So far, we have been primarily concerned with the building characteristics that may involve a heating system of constant efficiency. We will now introduce parameters to characterize the space conditioning system and attempt to estimate them from data. One possible approach is to determine the building parameters first, and then use the building itself as a dynamically calibrated calorimeter to determine complex heat flows, in particular, heat delivered

from a heating system (Subbarao et al. 1986). This is an alternative to the method of switching from electric to furnace heating.

For nonresidential buildings, imposing a heating and cooling profile, other than on-off, can be difficult. It is clear that if one monitors a building long enough, all required parameters ought to be obtained with relevant accuracy. A combination of on-off tests and longer normal operational data should be adequate. There are significant issues relating to HVAC system performance monitoring that need to be addressed.

From the above discussion, the following two protocols emerge for a one-zone residential building:

The first involves (1) a night of coheating that provides a window for p_0, daytime data + a night of cool down + daytime data that provide a wide window for p_{in} and p_{sun}, and (2) a night of furnace operation that provides a window for $p_{furnace}$. The tests last for three nights and two days.

The second scenario involves (1) a night of coheating that provides a window for p_0, and (2) a 16-hr sinusoidal heat input over three cycles that provides a window for obtaining the V-admittance at the 16-hr cycle, and then over all frequencies through interpretation thereby giving $Q_{storage}^{in}$ for the as-built building. This period also allows a determination of p_{sun}, and (3) a night of furnace operation that provides a window for $p_{furnace}$. The tests last for four nights and three days.

Theoretically, the second protocol appears to have some advantages. Numerical as well as experimental work is necessary to evaluate them. Protocol optimization is another area requiring further study, as previously mentioned.

13.0 PSTAR FOR MULTIZONE BUILDINGS

We have discussed the PSTAR simulation based on the energy balance equation, renormalized to fit performance data, for one-zone buildings. Extension to multizone buildings is addressed in this section.

From a thermal point of view, multizone issues fall into the following three categories:

(1) Under certain conditions, a multizone problem can be reduced to an effective one-zone problem with the transfer functions acquiring additional contributions because of the presence of the other zones. The previous one-zone formation essentially remains intact with additional computations involved in transfer function determination. An example of this is the effect of attic zone on the rest of the building zone.

(2) If the zones have marked temperature differences, one should introduce a set of parameters for each of the zones, and additional ones for interzonal couplings and estimate them. An example of this is the living zone and a sunspace in a residential building.

(3) The greatest challenge is when the zones do not have marked temperature differences, as in typical occupied areas of buildings. We can begin by introducing a set of parameters for each of the zones and additional ones for interzone couplings. This presents no difficulty to the forward problem. But as far as the inverse problem is concerned, given the relatively small temperature differences, it is unlikely that all the parameters are well determined. For this case, we will develop a formula that redefines the parameters, and allows those for which a strong signal exists in the performance data to be obtained from regression and those for which a strong signal does not exist to be treated perturbatively. This formula forms an important part of this article.

Each of the three cases is discussed below. The heat balance equations below form the basis of discussions in all the categories. With subscript i, referring to i^{th} zone, the heat balance for zone i has the form (for a single zone this reduces to Eq. 3-1):

$$\int_{-\infty}^{t} dt' \left[\hat{V}_i(t-t') \, \hat{T}_{in,i}(t') - \hat{W}_i(t-t') \, \hat{T}_{out}(t') - \sum_j \hat{W}_{ij}(t-t') \, \hat{T}_{in,j}(t') \right]$$

$$- \hat{Q}_{sun,i}(t) = \hat{Q}_{int,i}(t) + Q_{aux,i}(t) \, . \tag{13-1}$$

W_{ij} refers to the transfer function giving heat flow in zone i caused by temperature fluctuations in zone j. It can be shown that W_{ij} is symmetric: $W_{ij} = W_{ji}$. W_{ij} is essentially like W, except it is calculated only for the common walls between zones i and j. The term $Q_{int,i}$ refers to effective internal gains and, as such, contains not only heat generation caused by people, appliances, and lighting, but also because of infiltration and interzonal air flow. This is analogous to the inclusion, in the one-zone case, of infiltration heat loss in internal gains. In this case, other airflow terms, namely, interzonal airflow terms are included. The airflow is an input to the

model and is obtained from separate measurements and modeling. Airflow measurements and models are given in Balcomb and Yamaguchi (1983), and Burns and Kirkpatrick (1987).

We will develop the multizone methodology for two zones. Generalization to n zones is direct. The z-transform of Eq. 13-1, written explicitly for the two zones, gives

$$V_1 \, T_{in,1} - W_{12} \, T_{in,2} - W_1 \, T_{out} - Q_{sun,1} = Q_{int,1} + Q_{aux,1} \; , \qquad (13\text{-}2)$$

$$V_2 \, T_{in,2} - W_{12} \, T_{in,1} - W_2 \, T_{out} - Q_{sun,2} = Q_{int,2} + Q_{aux,2} \; . \qquad (13\text{-}3)$$

13.1 Equivalent One-zone Case

If we are only interested in the performance of zone 1 then, under certain conditions, we can reduce the problem to an effective one-zone problem. We will describe these conditions and discuss their applicability.

Solving for $T_{in,2}$, from Eq. 13-3, and substituting into Eq. 11-2 gives

$$\left(V_1 - \frac{W_{12}^2}{V_2} \right) T_{in,1} - \left(W_1 + \frac{W_{12} W_2}{V_2} \right) T_{out} - \left(Q_{sun,1} + \frac{W_{12}}{V_2} Q_{sun,2} \right)$$

$$= Q_{int,1} + \frac{W_{12}}{V_2} Q_{int,2} + Q_{aux,1} + \frac{W_{12}}{V_2} Q_{aux,2} \; . \qquad (13\text{-}4)$$

Let us make the additional assumption that $f_{1,aux}$ and $f_{1,int}$ defined below are constants:

$$f_{1,aux} = \frac{\hat{Q}_{1,aux}}{\hat{Q}_{1,aux} + \hat{Q}_{2,aux}} \; , \qquad (13\text{-}5)$$

$$f_{1,int} = \frac{\hat{Q}_{1,int}}{\hat{Q}_{1,int} + \hat{Q}_{2,int}} \; , \qquad (13\text{-}6)$$

i.e., that the fraction delivered to zone 1 of the total auxiliary (and internal gains) input into zone 1 + zone 2 is a constant. We further assume

$$f_{1,int} = f_{1,aux} = f_1 \; . \qquad (13\text{-}7)$$

This assumption is not necessary; if they are unequal, an additional transfer function is needed to relate auxiliary input to space gains. We can then use $Q_{int} \equiv Q_{1,int} + Q_{2,int}$ and $Q_{aux} = Q_{1,aux} + Q_{2,aux}$ as the driving functions and write Eq. 11-4 in the form:

$$V \, T_{in,1} - W \, T_{out} - Q_{sun} = Q_{int} + Q_{aux} \; , \qquad (13\text{-}8)$$

where

$$V = \frac{V_1 - W_{12}^2/V_2}{f_1 + (1-f_1) \, W_{12}/V_2} \; , \qquad (13\text{-}9)$$

with similar relations for W and Q_{sun}.

Equation 13-8 has the same form as the one-zone Eq. 4-18. All the considerations of one zone, therefore, apply. Note that the temperature of zone 2 has been eliminated, and need not be measured. The equivalent loss coefficient can be obtained from the zero frequency behavior of Eq. 13-9.

Let us discuss the validity of Eqs. 13-5 through 13-7. If the building is free floating (i.e., has no auxiliary heating or cooling), or if a single auxiliary source supplies heating and cooling to both zones without separate controls (in particular, if $f_1 = 1$ as it is if zone 2 is an attic), then Eq. 13-5 is valid. The validity of Eqs. 13-6 and 13-7 can be judged in the obvious manner.

The analysis above can be easily extended to any number of zones. As long as auxiliary and internal gains are partitioned in the same constant proportion among the various zones, the thermal behavior of a zone, including influences from all other zones, can be represented by an equivalent one zone.

The above discussion of an equivalent one-zone approximation works well for an area such as an attic. It does not apply to a basement, to buildings with multiple thermostats, or to flow-between zones, etc.

13.2 Multizone Building with Large Temperature Differentials

In the previous section, we saw that if we are interested in the thermal behavior of only one of the two zones then, under certain assumptions, the effect of the second zone can be absorbed into an effective one-zone case. If those assumptions are not satisfied, or if we are interested in the thermal behavior of both zones, we need a different formula. An example of this is a building with a sunspace. In this case, referring back to Eqs. 13-2 and 13-3, we can write every one of the transfer functions V_1, W_1, S_1, V_2, W_2, S_2, and W_{12} as ratios of polynominals in z^{-1} and proceed exactly as for the one-zone problem, except that simultaneous solution for $T_{in,1}$, $T_{in,2}$, $Q_{aux,1}$ and $Q_{aux,2}$ is necessary. For the inverse process, we can introduce renormalization factors for the primary heat flow terms and estimate the parameters as before.

13.3 Multizone Building Without Large Temperature Differentials

In the previous case, when there are large temperature differentials, a strong signal exists for estimating parameters for each zone. When the temperature differentials are not large, the signal is weak. Examples of this case are nonresidential buildings and residential buildings with room thermostats or with direct gain induced temperature differentials. Such multizone buildings present the greatest challenge for multizone analysis. The analysis below shows how to find the right combination of parameters for which a strong signal exists and how to estimate them from performance data. The others are determined by a calculation based on building description.

The mathematical formulation of PSTAR for the previously discussed buildings is given next. First, consider a two-zone building; generalization to more than two zones is given later. The heat balance equations are Eq. 13-2 and 13-3.

The six transfer functions V_1, V_2, W_1, W_2, S_1, S_2 and W_{12} will be regrouped as follows:

$$V = V_1 + V_2 - 2W_{12} \ , \tag{13-10}$$

$$W = W_1 + W_2 \ , \tag{13-11}$$

$$S = S_1 + S_2 \ , \tag{13-12}$$

$$v = V_1 - V_2 \ , \tag{13-13}$$

$$w = W_1 - W_2 \ , \tag{13-14}$$

$$v' = V_1 + V_2 + 2W_{12} \ , \tag{13-15}$$

$$s = S_1 - S_2 \ , \tag{13-16}$$

then

$$V \, T_{in} + v \, \Delta_{12} - W \, T_{out} - S \, I_{sun} = \left(Q_{1,int} + Q_{2int} \right) \ , \tag{13-17}$$

$$v \, T_{in} + v' \, \Delta_{12} - w \, T_{out} - s \cdot I_{sun} = \left(Q_{1,int} - Q_{2,int} \right) \ , \tag{13-18}$$

where

$$T_{in} = \left(T_1 + T_2 \right)/2 \ , \tag{13-19}$$

$$\Delta_{12} = \left(T_1 - T_2 \right)/2 \ . \tag{13-20}$$

Equation 13-17 tells us that using the average inside temperature gives us a one-zone problem except for the term $v \cdot \Delta_{12}$ (note again that in $Q_{1,int} + Q_{2,int}$, the airflow terms cancel out). The term $v \cdot \Delta_{12}$ is small and can be treated perturbatively simply by using the audit values. The rest of the terms are handled routinely. Whether Eq. 13-18, which contains terms with substantial uncertainty, leads to a useful renormalization process awaits further study.

Generalization to n zones is direct:

$$V \, T_{in} + \sum V_i \, \Delta_i - W \, T_{out} - S \, I_{sun} = \sum Q_{int,i} \ , \tag{13-21}$$

where

$$V = \sum_{i,j} V_i - \sum W_{ij} \ , \tag{13-22}$$

$$W = \sum W \ , \tag{13-23}$$

$$S = \sum_i S_i \ , \tag{13-24}$$

$$T_{in} = \sum_i T_i/n \ , \tag{13-25}$$

$$\Delta_i = T_i - T_{in} \ . \tag{13-26}$$

Equation 13-21 is the analog of Eq. 13-17. There will be subsidiary equations analogous to Eq. 13-18. As before, all airflow terms cancel out in $\sum Q_{int,i}$. The transfer functions V, W, and S should have regressible renormalization factors. The rest can have renormalization factors as deemed necessary.

14.0 WHY PSTAR?

The role of PSTAR in the forward and the inverse processes will be discussed in this section.

PSTAR is not a new simulator competing with existing simulators (DOE-2, BLAST, SUNCODE, among others) for the forward process. It is a way of disaggregating heat flows; each of these flows can be obtained by existing or future micro-dynamic simulators. Many of the heat flow terms are best obtained through macrodynamics. In some limiting cases, all heat flow terms can be obtained through macrodynamics. The role of the PSTAR approach for the forward process is (1) to provide a quantitative understanding of the role of different driving functions, (2) to provide a self-contained simulator if certain approximations are allowable, and (3) to provide simplifications for component simulations.

The power of the PSTAR approach comes into play in the inverse process; synergism among microdynamics, macrodynamics, and performance data is achieved. Several equivalent thermal parameter models are described in the literature for the inverse process. A calibrated microsimulation, in which the micro-level inputs are "tweaked" to fit short-term data, has been attempted. In the following section, we compare and contrast PSTAR with other approaches.

For specificity we will compare the following three models: a calibrated microsimulation, the equivalent thermal circuit of Figure 14-1, and PSTAR. The comments on the circuit of Figure 14-1 are generally applicable to other similar circuits.

A microsimulation is designed for the forward process. When the microsimulation is applied to the inverse process, it is calibrated by tweaking the microparameters (conductivities, specific heats, areas, etc.) to fit the macrolevel short-term performance data. We believe this calibration procedure is rather arbitrary and allows little hope of leading to reliable extrapolation to periods outside the calibration period. There is no expectation that the calibrated inputs provide a reliable detailed description of the building. A microsimulation usually takes several days for initialization. This presents a problem for short-term tests with a few days' data. It does not appear that a calibrated microsimulation is a viable approach to the inverse problem with macro-level data.
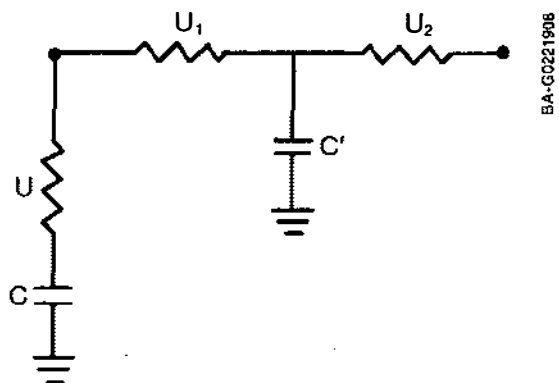

Figure 14-1. A representative simplified network representation of a building

43

The PSTAR method of renormalization or calibration of the transfer functions should be contrasted with the calibration of a microsimulation. The transfer functions that get renormalized are macrolevel (i.e., zone level) quantities. This process does not involve any adjustment of the microlevel properties (such as conductivities, specific heats etc.). The procedure for renormalization is well defined. The renormalized transfer functions are directly used in subsequent simulations.

We consider the following criteria in the comparative evaluation of PSTAR with simple equivalent circuit formulations:

● Consistency: results from a simulation based on the parameters of the model calculated from a detailed building description should agree well with the results from a direct microsimulation.

● Repeatability: parameters estimated from data from different periods should agree with each other within the errors of estimation.

● No cross-talk among parameters: parameters characterizing response to different driving functions should not get mixed up.

● Component characterization: the parameters being macroparameters should be obtainable from component parameters in a relatively simple manner (for example, the building loss coefficient is simply related to component UAs).

The above criteria are not all independent, but it is still useful to consider them separately.

Regarding cross-talk, it is clear that if the V transfer function (relating heat flow to inside temperature), the W transfer function (relating heat flow to outside temperature), and other transfer functions (interzone etc.) are all independently parameterized, the cross-talk is avoided. But circuits that appear simple often suffer from cross-talk. Referring to the circuit of Figure 14-1, it is easy to show that

$$V = U \ \frac{j\omega \ C/U}{1 + j\omega \ C/U} + U_1 \ \frac{j\omega \ C'/(U_1+U_2)}{1 + j\omega \ C'/(U_1+U_2)} + W \ .$$

with

$$W = U_1 \ \frac{1}{1 + j\omega \ C'/(U_1+U_2)} \ .$$

Even if the outside temperature is constant (implying that only W at zero frequency i.e., the heat loss coefficient can be determined) it is clear that, with appropriate inside temperature variations, V is well determined. For that reason, W is also spuriously determined. The seemingly simple circuit parameters mix up different transfer functions. In isolated cases V and W are related. For example, for a homogeneous single layer wall, the surface-to-surface transfer functions are characterized by two parameters: UA of the wall and a time constant. But, in general, interior masses and exterior

masses give enough freedom to design a building with any desired values of V and W and, therefore, they should be deemed independent.

The solution to cross-talk is to introduce separate parameters for V and W (and other transfer functions). The resulting circuits may be complicated in appearance. This was the approach in Subbarao (1984). In this article, we worked within the framework of transfer functions. A circuit has a unique transfer function, but a given transfer function can typically be represented by several circuits. The circuit corresponding to PSTAR depends on the order of the polynomials (in z^{-1}) of the nominator and denominator in the transfer function representation. Rather high-order circuits can be obtained without proliferating the number of parameters to be estimated by the renormalization approach.

The inverse process is sometimes viewed as an attempt to fit the data to an RC-circuit with as few resistors and capacitors as possible. In this view, the calculation of the values of resistors and capacitors is of secondary importance, and is done in an ad hoc manner. As long as such a calculation procedure exists, however ad hoc it is, the parameters can be calculated from a component description. However, if the calculation proceeds through frequency response of the components, as the PSTAR calculation does, the whole zone admittance can be written as a sum of component admittances. The radiation-convection split at surfaces is taken into account through interaction factors. The component admittances can be measured directly from dynamic hot-box tests. Thus, component characteristics can be readily incorporated into the analysis, and the effect of substituting one component for another assessed.

Regarding consistency, it is clear that given an equivalent circuit, one can always think of buildings for which it works well, and those for which it fails. When it fails, one can add additional resistors and capacitors; this might solve the forward problem, but may result in far too many parameters to be useful for the inverse problem. PSTAR, however, provides a systematic way of ensuring high-order models without proliferating the number of parameters to be estimated. By incorporating solar geometry, small heat flows such as those caused by sky temperature depression, etc., PSTAR is, for all practical purposes, as accurate as the front-end microdynamic model.

In regards to repeatability, it must be recognized that because the equivalent circuit elements are estimated by best fit to the data and because the circuit is an approximate (often a poor) representation, an excellent fit is possible, but only for the particular mix of the driving functions. The parameters, therefore, depend on the mix of driving functions. This results in an adverse effect on repeatability. However, PSTAR is designed to use its knowledge of building description to maximize the applicability of the model for any mix of driving functions. It is, of course, possible that the data do not permit an accurate determination of the renormalization parameters; this is an issue for the test protocol, not for the model.

In summary, we believe that viewing the inverse process as a choice of an RC network with as few resistors and capacitors as possible, and then exploring the applicability of different circuits for different situations is fundamentally flawed. This creates the dilemma of either choosing a simple circuit that may lead to a poor representation of the building, but with circuit elements that can be estimated with possibly large biases, or a more complex network providing a good representation of the building with poorly determined parameters.

PSTAR resolves this dilemma by using the audit building description as the starting point to arrive, through renormalization, at a good representation of the building without proliferating the number of parameters to be estimated. PSTAR allows a hierarchy of models without increasing the number of parameters to be estimated. The higher the order of the model (while still satisfying the stability criterion), with properly selected frequencies for matching, the better the transfer functions reproduce the audit building response and, presumably after renormalization, the as-built building response. The expectation then is that the estimated transfer functions as functions of frequency are not sensitive to the order of the model as long as it is sufficiently high.

It is, of course, possible to imagine situations where the PSTAR approach would fail. For example, if we have a building with roughly equal areas of Trombe wall and frame wall, and if the frame wall properties are accurately known and the Trombe wall properties are far off, then the calculated transfer function may have the wrong dependence on frequency that cannot be adequately corrected by a simple renormalization scheme. It is also possible to imagine a situation in which, just before the start of the test, the building is subjected to strange driving functions. Such situations, we believe, are too rare for practical concern. Equivalent circuit approaches probably fail even worse in such cases. In general, the farther the audit building description is from the as-built, the more challenging the renormalization problem. If they are too far apart, it may be impossible to renormalize the audit building into a reasonable as-built one. Whether this is of much practical concern has not been systematically investigated.

Extension to multizone buildings, a systematic approach to solar gains from multiple orientations, and perturbation treatment of small gain are all important features of the PSTAR approach. In the case of multizones, the separation of parameters with a strong signal from those that do not have a strong signal is an important element in arriving at a manageable inverse process.

Note that in the limit when the building is represented by a simple RC circuit, $Q_{storage}^{out} = 0$ and $Q_{storage}^{in} = C(T_{in}(n) - T_{in}(n-1))$. We will then be regressing $Q_{int}(n)$ versus $L[T_{in}(n) - T_{out}(n)]$ and $C[T_{in}(n) - T_{in}(n-1)]$. Actually, audit values of L and C are unnecessary for regression purposes

because they can be absorbed into the regression coefficients. We are then performing a black-box version of the inverse process.

For the determination of $Q_{storage}^{in}$, $Q_{storage}^{out}$, and Q_{sky} we used a transfer function approach with frequency response fitting. Other approaches are possible within the PSTAR framework: for example, a transfer function approach with step function response matching. Frequency response provides, we believe, the best way of combining building response (through polar or Bode diagrams) with weather characteristics (through spectral decomposition) to arrive at an optimal evaluation of the transfer function coefficients. One can even bypass the transfer function approach and obtain $Q_{storage}^{in}$, $Q_{storage}^{out}$, and Q_{sky} from a microsimulation in much the same was as Q_{sun} was. (A simulation with T_{in} = constant and I_{sun} = 0 with desired values of T_{out} leads to a determination of $Q_{storage}^{out}$, for example.) This approach presents problems. The first is that for long-term extrapolation in the presence of a thermostat, it is cumbersome (requiring source code modifications) to incorporate the renormalized energy balance equation. The second problem is that if more than a multiplicative renormalization is necessary for, say, $Q_{storage}^{in}$, the transfer function approach provides a natural decomposition of $Q_{storage}^{in}$ into two (or more) terms that can be separately renormalized. The approach of obtaining $Q_{storage}^{in}$ from a microsimulation becomes cumbersome in this respect also. A minor problem is in the initialization for fitting to test data.

In summary, transfer function formulation with frequency response fitting appears to be the best way to incorporate PSTAR. Even after accepting this, there are many questions about details. The method given in this report has the advantage of requiring only solution of linear equations. It has the disadvantage that sometimes, especially if one is fitting at a relatively large number of frequencies, the roots may have magnitudes larger than one (making the selection or number of frequencies unacceptable), or between -1 and zero (making the selection or number of frequencies undesirable). Note that choosing the Nyquist frequency as one of the frequencies for matching (2-hr cycle for hourly data) forces a root at -1. When the roots are unacceptable, one can choose a different set of frequencies until acceptable roots are obtained. Variations such as least squares fit on T_{in} (by solving equations such as 4-18 for T_{in}), instead of least squares fit on energy balance are possible.

A generalization to exact matching at selected frequencies is to match at additional frequencies in the least squares sense. Suppose a transfer function, say V, is to be represented as a ratio of polynomials of degree n in z^{-1} in the form $P_{num}(z^{-1})/P_{den}(z^{-1})$. Select m frequencies ω_i ..., ω_m such that m is greater than or equal to n. Minimize the sum of squares (with unequal

$$\sum_i |P_{num}(e^{-j\omega_i\Delta})/P_{den}(e^{-j\omega_i\Delta}) - V(\omega_i)|^2$$

(with unequal weights, if necessary) with the constraint that all roots be between -1 and +1. This leads to nonlinear equations. Although it is possible to incorporate such a scheme, we present a simple method in this report that requires solving only linear equations. Suppose we minimize instead

$$\sum \left| P_{num}(e^{-j\omega_i\Delta}) - V(\omega_i) P_{den}(e^{-j\omega_i\Delta}) \right|^2 .$$

This leads to a set of linear equations much like exact matching at n frequencies. The necessary equations can be easily derived (Doebelin, 1980). It is necessary to check if the roots of the polynomials satisfy the stability constraint; if not, one should select different values for the frequencies or a different number of them. The exact matching process corresponds to the special case of m=n.

It is important to obtain a good match of the high frequency response to better represent building performance when the driving functions change rapidly. This may require independent renormalization of the high frequency response.

Extension to include HVAC systems (more complex than a constant efficiency furnace) is, in principle, quite direct. From flow, temperature and power measurements, and manufacturer's data (which provide an audit description), various heat flow terms can be calculated (knowing power input etc.). This can be appropriately divided into primary and secondary terms; the primary terms are renormalized using a linear least squares fit.

Extension to include phenomena such as moisture absorption and desorption is possible. In the energy balance equation, additional terms are needed due to moisture transport as well as the interaction between heat and mass transfer.

It is, sometimes, convenient to use the microdynamic simulator for applications. We cannot, of course, create an as-built microdescription of the building. However, we can create a simple building description with a small number of artificial walls with layers and properties that reproduce the renormalized macrolevel response of the building.

14.1 How Good is PSTAR

Recall that PSTAR is a unified approach for the forward process--to predict building performance given building description. It is also an approach for the inverse process--to determine building characteristics given performance data.

How good is PSTAR for the forward process? In view of the discussion following Eq. 2-4, this question becomes: how good is the time domain simulation based on matching the frequency response at selected frequencies? Comparisons with SUNCODE indicate that for typical buildings with a two- or three-frequency fit (say, at 4-day, 2-day, and 12-hr cycles), the agreement is excellent except when high frequency behavior (in the 2-hr cycle range) is important when the driving functions are changing rapidly (such as during morning heatup after a night setback). When high frequency behavior is important, film coefficients and details of radiative transfer become significant and even detailed microdynamic simulations tend not to agree with each other and with measurements. As noted before, the high frequency response matching and renormalization needs further work.

Inverse process is where PSTAR plays a vital role. How good is it for the inverse process? This question should be addressed through computer-generated data as well as real building data. Nominal studies, over a range of audit descriptions for a range of buildings in a range of climates, need to be per-

formed and various outputs assessed. A preliminary evaluation by Palmiter, Toney, and Brown (1988), based on a large number of simulations of several building types tested at various times of the year in two different climates, indicates that the method "shows considerable promise. In most cases, it gave annual heating and cooling load predictions of high accuracy and repeatability with minimal sensitivity to building prototype and climate. The accuracy attained is impressive in light of the fact that only 54 hours of 'measured' data were used." The study also identified problem areas that are being further investigated. As far as study using real building data is concerned, a test house has been instrumented and short-term tests conducted once every 10 days or so for several months. Repeatability of the building parameters as well as extrapolation to different time periods are being examined and will be reported in future publications.

15.0 APPLICATIONS

Because PSTAR is a systematic approach to the forward as well as the inverse process, there are numerous applications. These were discussed in the context of the earlier BEVA approach (Subbarao and Flowers 1984; Subbarao, Burch, and Christensen 1985). We simply list them here and refer to the cited articles for further details.

● Long-term performance prediction from short-term tests including retrofit benefit determination from before and after tests

● Component contribution to building performance, either through calculations or through dynamic hot-box measurements

● Building-as-a-calorimeter for determining complex heat flows--in particular, heating system efficiency (Subbarao et al. 1986) and HVAC system diagnostics

● Predictive load control of space-conditioning.

Some of these applications were realized and others are being investigated. Initial focus was to develop a short-term test method for residential buildings with a view to extrapolating to long-term performance. PSTAR forms the basis for this Short-Term Energy Monitoring (STEM) project at SERI.

A particularly attractive application to nonresidential buildings is as follows: an energy simulation is often done for building design. This simulation capability can subsequently be used for building commissioning, comparison of design versus actual performance, HVAC control, and diagnostics. The PSTAR method provides a natural framework for such applications.

16.0 STEPS IN APPLICATION

In this section we establish the various steps in the application of the PSTAR technique. As implied by the title of this report, the technique is applicable for the forward as well as the inverse processes. The differences between the two processes are:

- In the inverse process, some of the heat flows calculated from a building description and the measured driving functions are renormalized by a linear least squares fit to measured data.

- In the inverse process, some of the heat flows, such as infiltration, may be based on certain measurements. For the forward process, the calculated heat flows are all we have. In what follows, we will give the steps involved in the inverse process. For the forward process the step involving renormalization is to be skipped; all heat flows are derived from calculations only.

We will first give the steps for a one-zone building in the heating mode:

Step 1: Identify all the relevant terms in the energy balance equation: (Important Note: Despite previous sign conventions in this report, which had pedagogical use, we write the energy balance as a sum of terms equal to zero. A positive value of a term indicates a heat gain and a negative value of a term indicates heat loss from the air mode.)

$$Q_{int}(n)$$

$$+ (-L[T_{in}(n) - T_{out}(n)])$$

$$+ Q_{storage}^{in} (n)$$

$$+ Q_{storage}^{out} (n)$$

$$+ Q_{sun} (n)$$

$$+ Q_{vent} (n)$$

$$+ Q_{ground} (n)$$

$$+ Q_{sky} (n)$$

$$+ Q_{aux} (n) = 0 \ . \tag{16-1}$$

Determine whether each term is:

(a) A primary but unknown flow so that it is obtained first by a calculation from an audit description and subsequent renormalization

(b) A secondary flow so that it is obtained by a calculation from an audit description only

(c) Obtained by direct measurement (with modeling if necessary). An example of this type is Q_{vent} that may be obtained by a model fit to a one-time test.

Q_{int} are the internal gains treated as known. During short-term testing in an unoccupied building, it consists of electrical heat introduced through computer-controlled heaters to follow a specific profile. This flow is a measured term.

L is the steady-state loss coefficient; the second term is therefore the static heat loss caused by a difference between the inside temperature T_{in} and outside temperature T_{out}. This flow is usually a primary term.

$Q_{storage}^{in}$ is the heat discharged from (or, if the term is negative, charged into) the mass in the building. This term is obtained from an audit description and the T_{in} time series only. This term provides a correction to the second term resulting from dynamics. This flow is usually a primary term.

$Q_{storage}^{out}$ is the storage effect caused by mass coupled with T_{out}. This term is obtained from an audit description and the T_{out} time series only. This term provides a correction to the second term resulting from dynamics. This flow is usually a secondary term.

Q_{sun} is the heat gain at the air node because of solar radiation. This term is obtained by performing a simulation of the audit building with $T_{in} = T_{out} = $ constant (and with all other heat flows set to zero). The resulting cooling load gives Q_{sun}. This flow is typically a primary term.

Q_{vent} is the heat loss because of infiltration; this is obtained by a combination of a one-time measurement and modeling. This flow is typically a measured term.

Q_{ground} is the heat flow to the ground. For simplicity we shall consider here a building with a crawl space whose temperature is equal to the ambient temperature. This term can then be set to zero.

Q_{sky} is the heat loss because of sky temperature depression below ambient air temperature. This term is obtained either from an audit description and $T_{out} - T_{sky}$ time series, or through a microdynamic simulation with $-h_{sky}(T_{out} - T_{sky})$ as a negative solar flux on the relevant surfaces (h_{sky} is the radiative conductance to the sky, and T_{sky} the effective sky temperature for the given surface). This flow is typically a secondary term.

Q_{aux} is the heating energy supplied by the heating system. If the system efficiency (assumed constant) of a heating system is being studied, it is a primary term. For the purposes of this section, we set this to zero.

In what follows, the renormalized energy balance equation is taken to be:

$$Q_{int}(n) - p_0 \cdot L\,(T_{in}(n) - T_{out}(n)) + p_{in} \cdot Q_{storage}^{in}(n)$$

$$+ Q_{storage}^{out}(n) + p_{sun} \cdot Q_{sun}(n) + Q_{vent}(n) + Q_{sky}(n) = 0, \qquad (16\text{-}2)$$

where

P_0, P_{in} and P_{sun} are the renormalization parameters associated with the three primary terms. The problem is now reduced to determining these parameters. (More generally, $Q_{storage}^{in}$ can be decomposed into two or more components, each with its own renormalization parameters. Also, Q_{sun} can have more than one parameter associated with it. These were discussed elsewhere in the report and the necessary modifications can easily be worked out.

The identification of whether a term is primary or secondary follows quite unambiguously from an inspection of graphs of the terms for the audit building during typical driving functions. After some experience, one can identify them from a building description. Probably the most common situation is for the three noted terms to be primary. If a primary term is misidentified as secondary, the necessary calibration of the audit values through the measurements will not take place; if a secondary term is misidentified as primary, its corresponding renormalization factor will typically come out to be so far from unity as to be unreasonable. (Recall that a perfect audit description implies renormalization factors of unity.) One should then reset the renormalization factor to writing (which is equivalent to identifying the term as secondary).

Step 2: Obtain the audit information needed to calculate the flows. This need not be detailed, because the renormalization process is designed to provide the necessary corrections to fit to the as-built building.

Step 3: Determine a test protocol to elicit the renormalization parameters.

The test data are needed to determine the renormalization parameters for the three primary heat flows: $L(T_{in}-T_{out})$, $Q_{storage}^{in}$, and Q_{sun}. The data analysis is done sequentially and iteratively to determine the parameters. None of the terms in Eq. 16-2 are neglected at any stage. Different windows in the data will be used where some of the parameters are expected to be well determined. The necessary windows can be obtained from Eq. 16-2. If we choose a period when $Q_{storage}^{in}$ and Q_{sun} are small, P_0 is well determined. Thus, by maintaining a constant indoor temperature for several hours through the night (i.e., by coheating), the terms $Q_{storage}^{in}$ and Q_{sun} can be made small during the last two hours. Thus, a night of coheating should give a good determination of P_0.

Having obtained a preliminary estimate of P_0, a cool-down period at night (when Q_{sun} is small) should give a good determination of P_{in}. Daytime data on a typical sunny day should give a good determination of P_{sun}.

The test protocol consists of a night of coheating, a night of cool down, and daytime data on a relatively sunny day.

Step 4: Obtain the test data

The data channels consist of:

- Indoor air temperature
- Outdoor air temperature

- Wind speed
- Electrical power into the house.

Perform the additional measurements necessary to determine Q_{vent} (tracer gas, blower door, etc.).

Step 5: Calculate the heat flows for the test period. The terms in our simple case are

Q_{int}, which is measured

Q_{vent}, which is measured/modeled

$L(T_{in} - T_{out})$, which is direct once we obtain the loss coefficient from the audit description using standard UA summation

Q_{sun}, which is obtained from a microsimulation as the cooling load with $T_{in} = T_{out}$ = constant

Q_{sky}, which is obtained either by a macrodynamic approach very similar to the calculation of $Q_{storage}^{in}$ and $Q_{storage}^{out}$ described in detail below or by a microsimulation with appropriate negative diffuse irradiance and conductance to sky.

We will now describe, in detail, the calculation of $Q_{storage}^{in}$ and $Q_{storage}^{out}$.

Calculate the coefficients

$$b_o^{in}, \left(a_1^{in}, b_1^{in}\right), \left(a_2^{in}, b_2^{in}\right)$$

$$b_o^{out}, \left(a_1^{out}, b_1^{out}\right), \left(a_2^{out}, b_2^{out}\right),$$

as follows:

First choose the frequencies (besides the zero frequency) ω_1, ω_2 at which to match the V-transfer function, then calculate V at these frequencies. This calculation can be done following the standard method given in the textbook (e.g., Carslaw and Jaeger 1977). If a convection-radiation split is deemed necessary, the method given in Subbarao and Anderson (1983a) can be used. However, a convection-radiation split is rarely necessary for the inverse process because of the subsequent renormalization. Let V_1 and ϕ_1 be the magnitude and phase at frequency ω_1, and V_2, and ϕ_2 those at frequency ω_2. Then, the required coefficients are obtained by solving the set of linear equations:

$$
\begin{bmatrix}
1 & 1 & -L & 1 & -L \\
1 & \cos\omega_1\Delta & -V_1\cos(\omega_1\Delta-\phi_1) & \cos 2\omega_1\Delta & -V_1\cos(2\omega_1\Delta-\phi_1) \\
0 & -\sin\omega_1\Delta & V_1\sin(\omega_1\Delta-\phi_1) & -\sin 2\omega_1\Delta & V_1\sin(2\omega_1\Delta-\phi_1) \\
1 & \cos\omega_2\Delta & -V_2\cos(\omega_2\Delta-\phi_2) & \cos 2\omega_2\Delta & -V_2\cos(2\omega_2\Delta-\phi_2) \\
0 & -\sin\omega_2\Delta & V_2\sin(\omega_2\Delta-\phi_2) & -\sin 2\omega_2\Delta & V_2\sin(2\omega_2\Delta-\phi_2)
\end{bmatrix}
\begin{bmatrix}
b_o^{in} \\
b_1^{in} \\
a_1^{in} \\
b_2^{in} \\
a_2^{in}
\end{bmatrix}
=
\begin{bmatrix}
L \\
V_1\cos\phi_1 \\
V_1\sin\phi_1 \\
V_2\cos\phi_2 \\
V_2\sin\phi_2.
\end{bmatrix}
$$

$$(16\text{-}3)$$

(One can treat $\omega_1\Delta$ and $\omega_2\Delta$ as small angles to get a different discretization scheme.)

Compare $V(\omega)$ with

$$\frac{b_o^{in} + b_1^{in} \exp(-j\omega\Delta) + b_2^{in} \exp(-2j\omega\Delta)}{1 + a_1^{in} \exp(-j\omega\Delta) + a_2 \exp(-2j\omega\Delta)} \; ,$$

over a range of frequencies (they are guaranteed to be equal at frequencies 0, ω_1, and ω_2). If the comparison is not satisfactory, choose different or additional frequencies for matching the transfer functions. The necessary equations for matching at three or more frequencies can be obtained as a generalization of Eq. 16-3.

In what follows, we assume that a satisfactory two frequency fit has been found for V.

Determine the roots of the polynomials

$$p_{num}^{in}(a^{-1}) = b_o^{in} + b_1^{in} z^{-1} + b_2^{in} z^{-2} \; , \tag{16-4}$$

$$p_{den}^{in}(z^{-1}) = 1 + a_1^{in} z^{-1} + a_2^{in} z^{-2} \; . \tag{16-5}$$

If they are not real and lie between -1 and +1 (although it is more appropriate that the roots be between 0 and 1, we will accept negative roots if they are larger than, say, -0.5) choose a different number or values of frequencies until this constraint is satisfied. Determine α_1^{in}, β_i^{in}, α_2^{in}, and β_2^{in} by rewriting the ratio of polynomials as follows:

$$\frac{b_0^{in} + b_1^{in} z^{-1} + b_2^{in} z^{-2}}{1 + a_1^{in} z^{-1} + a_2^{in} z^{-2}} = L + (1 - z^{-1}) \sum_{i=1}^{2} \frac{\beta_i^{in}}{1 - \alpha_i^{in} z^{-1}} \; . \tag{16-6}$$

Calculate $q_i^{in}(n)$, $i=1,2$, from the recursion relation

$$q_i^{in}(n) - \alpha_i^{in} q_i^{in}(n-1) = -\beta_i^{in}(T_{in}(n) - T_{in}(n-1)$$

$$q_i^{in}(0) = 0 \; , \tag{16-7}$$

then

$$Q_{storage}^{in}(n) = \sum_{i=1}^{2} q_i^{in}(n) + q_{I,i}^{in} \alpha_i^n \; . \tag{16-8}$$

In the terminology of linear, first-order differential equations representing a simple RC circuit, the first term in Eq. 16-8 represents a discrete version of the particular solution and the second represents the solution of the homogeneous equation. The unknown initial conditions $q_{I,i}^{in}$ can be handled in one of two manners. The first method is to use values of $Q_{storage}^{in}$

only for those values of n greater than some number that ensures that the $q_i^{in}(0) \, \alpha_i^n$ term is small. Recall that α_i^n decreases as n increases. In practice, for typical buildings this might mean $n \geq 6$. The second method is to treat $q_{I,i}^{in}$ as simply additional parameters to be estimated from a linear least squares fit. For the forward process, the first method is the only relevant one. In what follows, we assume that the second method is used. A trivial extension is to combine both procedures by allowing a few hours of initialization while introducing initial heat flow parameters.

Calculate $Q_{storage}^{out}(n)$ following the same considerations as the $Q_{storage}^{in}$ term. Care is needed with the signs.

Step 6: Obtain the renormalization parameters. From a graph of all the heat flow terms as functions of time ($Q_{int}(n)$, $L(T_{in}-T_{out})$, $Q_{storage}^{in}$, $Q_{storage}^{out}$, Q_{vent}, Q_{sun} and Q_{sky}), review the categorization of heat flows into primary and secondary terms done in Step 1. Let us assume that this review confirms that p_0, p_{in}, and p_{sun} are the three renormalization parameters to be determined.

Determine p_0, p_{in}, and p_{sun} from a linear least squares fit. In the simple example given in Section 17.0, this is done in the obvious manner of fitting over the entire data set. In realistic building applications, we find it essential to use windows of data to determine the renormalization parameters in an iterative and sequential manner. First, choose a window of a few hours at the end of the coheating period when all the heat flow terms, except $L(T_{in}-T_{out})$ and of course Q_{int}, are small. From the renormalized energy balance equation (with $p_{in}^{(o)} = p_{sun}^{(o)} = 1$; the superscript denoting initial tentative values) determine p_0 from a least squares fit restricted to this period of a few hours. With p_0 fixed at this value, say, $p_0^{(1)}$ use the renormalized energy balance equation to obtain p_{in} and p_{sun}, say, $p_{in}^{(1)}$ and $p_{sun}^{(1)}$, by a linear least squares fit over the entire data range that includes cool down and sunny periods. (One can perform this fit over the entire data range with the elimination of the window of few hours used up earlier. From a practical point of view, this is inconsequential and it is easier to use the entire data range.) It is possible to introduce additional windows, for example, only the cool-down period may be used for p_{in}. This has not been necessary in numerical studies; in real buildings it may even be undesirable because p_{in} plays a role in convective charging and discharging of solar gains and better estimations are likely when such periods are included. The same argument can be used against a window for p_0 determination. However, without a window for p_0 the tradeoffs between different parameters can become intolerable. At this point we have tentative values of $p_0^{(1)}$, $p_{in}^{(1)}$, and $p_{sun}^{(1)}$. With $p_{in}^{(1)}$ and $p_{sun}^{(1)}$ in the renormalized energy balance equation, repeat the process of using the coheating window of a few hours to obtain an improved estimate $p_0^{(2)}$. With this value of $p_0^{(2)}$, use the entire period to obtain improved estimates of $p_{in}^{(2)}$ and $p_{sun}^{(2)}$. At this point, we have improved values of $p_0^{(2)}$, $p_{in}^{(2)}$, and $p_{sun}^{(2)}$. Repeat this process until satisfactory convergence.

In certain circumstances, $Q_{storage}^{in}$ and Q_{sun} may require additional parameters; such extensions are discussed in the text. Also, an analysis of the residuals

from the least squares fit may indicate a generalized least squares fit to account for autocorrelation among the residuals. If sine wave tests were done, an interpolation process is needed that takes the quantitative values of the V-admittance at the sine wave frequency and the loss coefficient, along with the qualitative information about the shapes of frequencies response functions obtained from an audit description. An example is given later. Also, if there are periods of missing data, additional parameters to reinitialize the heat flows are necessary. The necessary modifications are tedious, but direct.

Step 7: Use the renormalized energy balance equation for the intended application: long-term extrapolation, predictive load control, building-as-a-calorimeter, etc.

While the above method of directly using the renormalized equation is perfectly adequate, and can be computationally superior, we will give a more convenient formulation of simulation for long-term extrapolation. This is based on the discussion in Appendix A.

Obtain c_0^{in}, c_1^{in}, and c_2^{in} (similarly c_0^{out}, c_1^{out} and c_2^{out}) from the relation:

$$p_o L + p_{in} (1-z^{-1}) \sum_{i=1}^{2} \frac{\beta_i^{in}}{1 - \alpha_i^{in} z^{-1}} = \frac{c_0^{in} + c_1^{in} z^{-1} + c_2^{in} z^{-1}}{1 + a_1^{in} z^{-1} + a_2^{in} z^{-2}} . \quad (16\text{-}9)$$

Obtain a series of A-coefficients as follows:

$$A_o^{in} \equiv c_o^{in}$$

$$A_1^{in} \equiv c_1^{in} + c_o^{in} a_1^{out}$$

$$A_2^{in} \equiv c_2^{in} + c_1^{in} a_1^{out} + c_o^{in} a_2^{out}$$

$$A_3^{in} \equiv c_2^{in} a_1^{out} + c_1^{in} a_2^{out}$$

$$A_4^{in} \equiv c_2^{in} a_2^{out}$$

$$A_o^{out} \equiv c_o^{out}$$

$$A_1^{out} \equiv c_1^{out} + c_o^{out} a_1^{in}$$

$$A_2^{out} \equiv c_2^{out} + c_1^{out} a_1^{in} + c_0^{out} a_2^{in}$$

$$A_3^{out} \equiv c_2^{out} a_1^{in} + c_1^{out} a_2^{in}$$

$$A_4^{out} \equiv c_2^{out} a_2^{in}$$

$$A_0^{int} \equiv 1$$

$$A_1^{int} \equiv a_1^{in} + a_1^{out}$$

$$A_2^{int} \equiv a_2^{in} + a_1^{in} a_1^{out} + a_2^{out}$$

$$A_3^{int} \equiv a_1^{in} a_2^{out} + a_2^{in} a_1^{out}$$

$$A_4^{int} \equiv a_2^{in} a_2^{out} \, , \qquad\qquad (16\text{-}10)$$

$$A_0^{in} T_{in}(n) + A_1^{in} T_{in}(n-1) + \ldots + A_4^{in} T_{in}(n-4)$$

$$= A_0^{out} T_{out}(n) + \ldots + A_4^{out} T_{out}(n-4)$$

$$+ A_0^{int} Q_{sun}(n) + \ldots + A_4^{int} Q_{sun}(n-4)$$

$$+ A_0^{int} Q_{int}(n) + \ldots + A_4^{int} Q_{int}(n-4)$$

$$+ A_0^{int} Q_{aux}(n) + \ldots + A_4^{out} Q_{aux}(n-4) \, . \qquad (16\text{-}11)$$

Calculate $T_{in}(n)$ and $Q_{aux}(n)$ to satisfy any thermostatic constraints in the usual manner.

17.0 EXAMPLE

This section illustrates the PSTAR method for the forward as well as the inverse processes. This example highlights a number of essential features. Simplifications were made in the building description to keep the algebra simple. The example building is unrealistic from the point of construction practice, but illustrates some of the steps involved in applying the PSTAR method to a real building. (Real-building applications will be given in future publications.) The multizone building theory formulated earlier will not be illustrated in this example.

The example building is a one-zone building with 1000 ft^2 of exterior frame wall (nominally R-12) and 500 ft^2 of 0.3 ft storage wall with a nominal R-2.5 glazing. Table 17-1 gives the layer descriptions. The inside film conductance, which is often not known accurately, is deliberately chosen to be quite different from the American Society of Heating, Refrigerating and Air-Conditioning Engineers (ASHRAE) recommended value to explore the effect on the inverse process; many of the material properties are also chosen to be different from standard values.

Infiltration and heat flow to the ground and heat flow caused by sky temperature depression are set at zero to keep this example simple. Also, we assume that the building is electrically heated so that Q_{aux} can be absorbed into Q_{int}. Thus, only the first four terms on the right side of Eq. 16-1 survive.

The loss coefficient of the building is easy to compute. From Table 17-1, the frame wall is R-12.40 and the storage wall is R-3.338. Thus, 1000 ft^2 of the former and 500 ft^2 of the latter give a loss coefficient of 230.4 Btu/hr°F.

We can now compute the V-admittance of the building at a specific frequency, say, (12 hr)$^{-1}$. From the wall layer description of Table 17-1, the V-admittance of the frame wall (at [12 hr]$^{-1}$ per ft^2) is obtained to be $|V|$ = 0.2919 Btu/hr ft^2°F and ϕ_v = 63.07°. For 1000 ft^2 of the frame wall the V-admittance has a magnitude of 291.9 Btu/hr°F and a phase ϕ_v = 63.07°. Similarly, for 500 ft^2 of the storage wall, $|V|$ is 598.1 Btu/hr°F and ϕ_v = 28.95°. The whole building V-admittance is given by adding the two vectors:

$$291.9 \ \underline{|63.07°} + 598.1 \ \underline{|28.95°} = 855.6 \ \underline{|39.98°} \ \text{Btu/hr°F} . \qquad (17-1)$$

Figure 17-1 schematically shows this vector addition.

In this calculation we used a combined convection-radiation coefficient, strictly speaking, at a wall surface; convection to air and radiation to other surfaces must be treated separately. A convenient way to do this in the frequency-response framework is to use the interaction factor formalism (Subbarao and Anderson 1983). This is not illustrated here.

SERI ❋

Table 17-1. Audit Description of Example Building

a. **Frame Wall:**

Inside film conductance: 1.7 Btu/hr°Fft^2

Layer	Material	Thickness (ft)	Conductivity (Btu/hr·ft·°F)	Density (lbs/ft^3)	Specific Heat (Btu/lb)
1	Drywall	0.0417	0.3	50	0.24
2	Insulation	0.293	0.032	3.5	0.17
3	Sheathing	0.0417	0.035	10	0.2
4	Wood Siding	0.0833	0.08	20	0.3

Outside film conductance 3.0 Btu/hr°Fft^2

b. **Storage Wall:**

Inside film conductance: 1.46 Btu/hr°F

1	Concrete	0.3	1.0	150	0.2

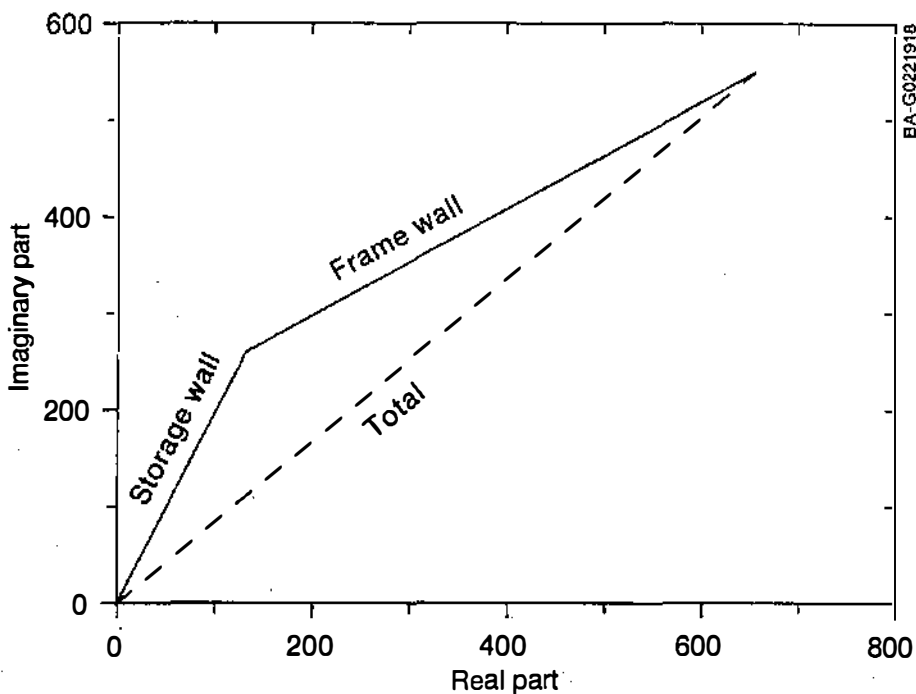Outside film conductance: 0.333 Btu/hr°F

Figure 17-1. V-factor addition for the example building

Figure 17-2 shows the polar diagram of the V-admittance of the whole building. By inspecting the figure, we should expect a good fit by matching at two or three frequencies. To keep the algebra of this example simple, we will restrict ourselves to two frequencies: $(48 \text{ hours})^{-1}$ and $(12 \text{ hours})^{-1}$. The resulting fit also is shown in Figure 17-2. Fitting at a higher frequency might have been desirable, but we will proceed anyway.

One relevant polynomial is

$$P^{in}_{den}(z^{-1}) = 1 - 0.3391 \, z^{-1} - 0.2160 \, z^{-2} \,, \qquad (17-2)$$

with roots at 0.664 and -0.325. The magnitude of these roots being less than unity, no instabilities will arise in auxiliary energy predictions. It would have been desirable if the roots were positive also, but we will proceed anyway. The other relevant polynomial is

$$P^{in}_{num}(z^{-1}) = 1384 - 1494 \, z^{-2} + 213.7 \, z^{-2} \,, \qquad (17-3)$$

with roots at 0.911 and 0.169; no instabilities will arise in inside-temperature predictions. In free-floating buildings, we are interested in predicting inside temperatures. In a thermostated building, we need to predict inside temperatures as well as auxiliary heating and cooling loads.

It is important that all the roots are inside the unit circle (for example, with magnitude < 1), if not, the number of frequencies or the values of the frequencies at which the matching is done should be modified until all roots are within the unit circle.
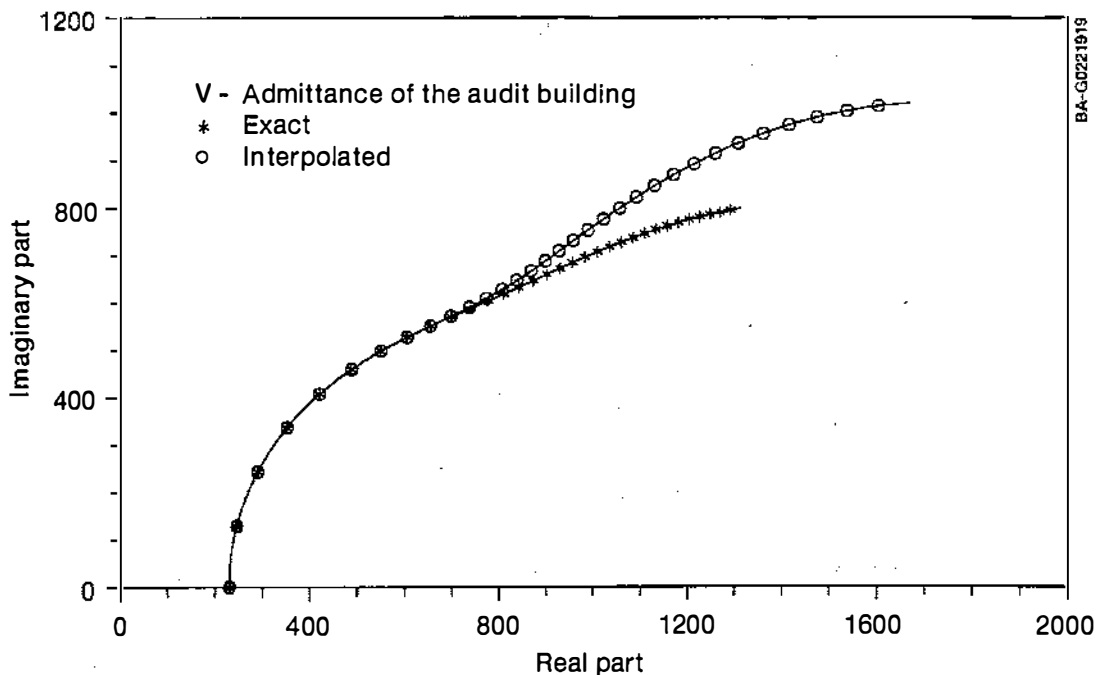

Figure 17-2. Polar diagram of the V-admittance of the audit building: exact (*) and approximate(o) based on matching at 48-hr and 12-hr cycles

With the definition given before, it can be shown that $L = 230.1$ Btu/ hr°F, $\alpha_1 = -0.325$, $\beta_1 = 645$, $\alpha_2 = 0.664$, and $\beta_2 = 509$.

Let us now consider the T_{out} driving function. The polar diagram of the W-admittance for the whole building is shown in Figure 17-3. This diagram is generated in a manner similar to that for the V-admittance. We will accept a fit based on two frequencies:

(48 hr)$^{-1}$ and (6 hr)$^{-1}$; the respective W-admittances are $221.9 \; \underline{|-15.85°}$ and $118.5 \; \underline{|-75.43°}$ Btu/hr°F.

The polynomial

$$P^{out}_{\text{den}} (z^{-1}) = 1 - 0.8719 \, z^{-1} + 0.1365 \, z^{-2} \tag{17-4}$$

has roots at 0.667 and 0.205; these being inside the unit circle, no instabilities arise in Q_{out} calculations. The polynomial

$$P^{out}_{num} (z^{-1}) = 17.25 + 92.41 \, z^{-1} - 48.68 \, z^{-2} \tag{17-5}$$

has a root outside the unit circle. It is necessary to choose a different number or values of frequencies. Because we will simplify the example later, we will not pursue this further.

The discussion of the solar driving function can proceed along two lines: (1) if shading and multiple orientations are not issues, a meteorological quantity I_{sun} on the only orientation of interest serves as the driving
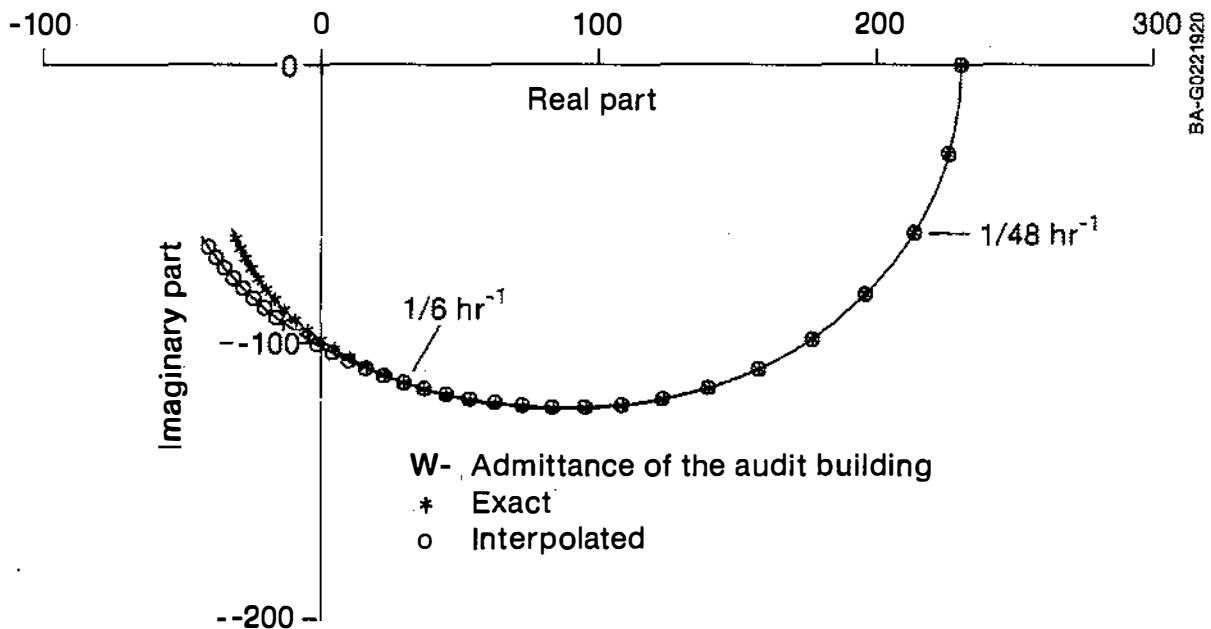

Figure 17-3. Polar diagram of the W-admittance of the audit building: exact (*) and approximate (o) based on matching at 48-hr and 6-hr cycles

function; Q_{sun}, the heat gain by the air node can be related to I_{sun} in a manner analogous to $Q_{storage}^{in}$ and $Q_{storage}^{out}$ before, or (2) if shading and multiple orientations are relevant, a single driving function does not exist and we must obtain the quantity of interest Q_{sun} directly by some other means through a separate calculation. For the example house, we assume that the storage wall is the only radiation-receiving element and (1) applies. From the properties of the storage wall listed in Table 17-1 one can show that the solar admittances are at zero frequency, 224.7 ft^2, and at (24 hr)$^{-1}$ frequency 188.0 $|-35.99°$ ft^2. For indirect gain through a storage wall some delay is desirable. With direct gain, we would choose a time delay of zero hour. How to choose the delay is an intricate question; there are discussions of such issues in time series literature such as Box and Jenkins (1979). With a one frequency (24 hr^{-1}) fit and a time delay of 1 hour we get

$$Q_{sun}(n) - 0.6946 \ Q_{sun}(n-1) = 104.9 \ I_{sun}(n-1) - 36.29 \ I_{sun}(n-2) \ . \quad (17-6)$$

The polynomials

$$P_{num}^{sun} (z^{-1}) = 104.9 \ z^{-1} - 36.29 \ z^{-2} \ , \quad (17-7)$$

$$P_{den}^{sun} (z^{-1}) = 1 - 0.6946 \ z^{-1} \ , \quad (17-8)$$

are well behaved.

Suppose we test a building with nominal description given in Table 17-1. The information in the table can be generally obtained quite easily by an audit of the building. We will therefore refer to the building corresponding to the table as the audit building. The as-built building, in general, differs from the audit building. An accurate detailed description of the as-built building is, realistically, impossible to obtain. However, we will be able to proceed by working after a certain point, not with the microparameters of Table 17-1 but with macroparameters (namely building admittances).

To keep the example simple as well as to illustrate clearly some of the important features, let us suppose we have obtained the performance data (of the as-built building, of course) under a constant outside temperature of 45°F in the absence of solar radiation. Figure 17-4 shows the performance data. (Obviously, this is computer generated; we will see how this was done later.)

In view of Eqs. 17-2 and 17-3, a simulation of the audit building can be done from the following equation:

$$Q_{int}(n) - 0.339096 \ Q_{int}(n-1) - 0.215989 \ Q_{int}(n-2)$$

$$= 1383.90 \ (T_{in}(n) - T_{out}) - 1494.43 \ (T_{in}(n-1)$$

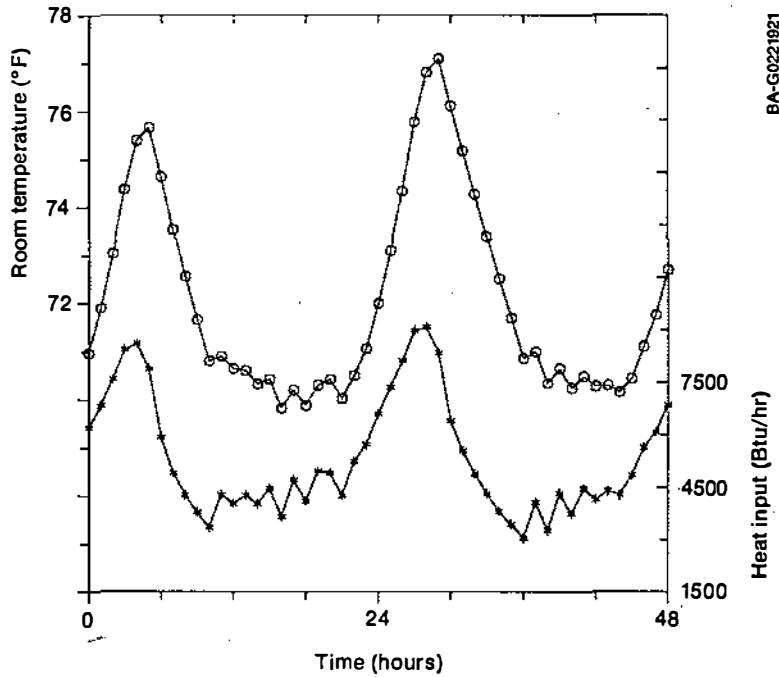$$- T_{out}) + 213.047 \ (T_{in}(n-2) - T_{out}) \ . \quad (17-9)$$

Figure 17-4. "Measured" data for the example building. T_{out} is constant at 45°F and solar radiation zero; these are not shown.

Eq. 17-9 can now be used with measured values of $Q_{int}(n)$ and T_{out} (and measured values of T_{in} for the first two hours) to predict the inside temperature. This predicted inside temperature as well as the measured values are plotted in Figure 17-5. From this figure it is clear that the audit inputs result in too high a loss coefficient; the heat storage characteristics are less clear.

Any attempt to modify Table 17-1 to obtain better agreement, for example, to calibrate a microsimulation is, we believe, haphazard and arbitrary. Instead, we proceed with the PSTAR method.

The heat balance Eq. 16-1 has reduced in this simple case to

$$Q_{int}(n) - L(T_{in}(n) - T_{out}(n)) + Q_{storage}^{in}(n) = 0 . \qquad (17-10)$$

The first term is the measured heat input, and the second is

$$230.4 (T_{in}(n) - 45),$$

where $T_{in}(n)$ represents the measured temperature.

The third term is obtained as follows:

$$Q_{storage}^{in}(n) = q_1^{in}(n) + q_2^{in}(n) + q_{I,1}^{in} \alpha_1^n + q_{I,2} \alpha_2^n , \qquad (17-11)$$
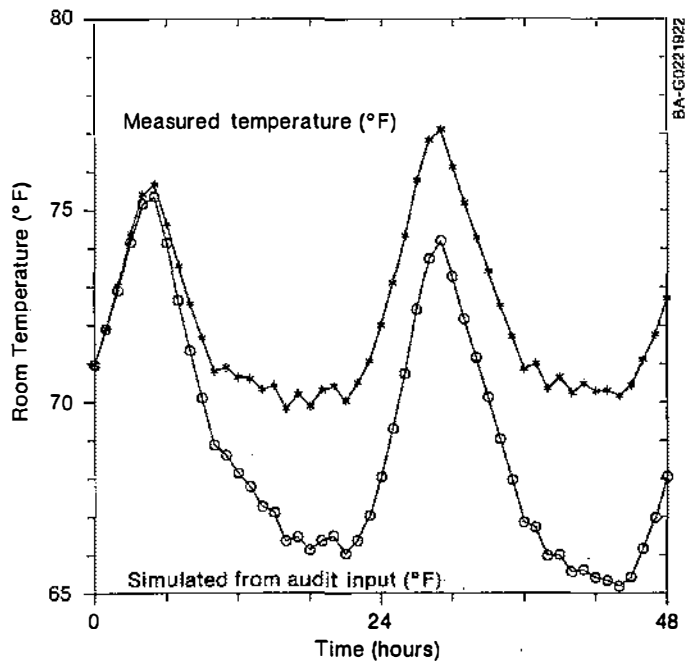
Figure 17-5. Comparison between "measured" data (*) and simulation (o) of the audit building

with

$$q_1^{in}(n) = \alpha_1 \, q_1^{in}(n-1) - \beta_1 \left[T_{in}(n) - T_{in}(n-1) \right] \,, \qquad (17-12)$$

$$q_1^{in}(o) = 0 \,, \qquad (17-13)$$

$$q_2^{in}(n) = \alpha_2 \, q_2^{in}(n-1) - \beta_2 \left[T_{in}(n) - T_{in}(n-1) \right] \,, \qquad (17-14)$$

$$q_2^{in}(o) = 0 \,. \qquad (17-15)$$

Performing a linear regression of $Q_{int}(n)$ against the four terms

$$230.4 \ (T_{in}(n) - 45),$$

$$q_1^{in}(n) + q_2^{in}(n),$$

$$\alpha_1^n,$$

and $\qquad \alpha_2^n \,,$

gives the following best fit:

$$Q_{int}(n) - 0.842 \times 230.4 \, [T_{in}(n) - 45]$$

$$+ 1.18 \, [q_1^{in}(n) + q_2^{in}(n)]$$

$$+ [519.7 \, (-0.325)^n - 965.6 \, (0.664)^n] \approx 0 \, . \qquad (17\text{-}16)$$

The last terms represents the initial heat flows, that exponentially decay to zero. Figure 17-6 shows the last three terms on the right side. The resulting fit is shown in Figure 17-7. To complete the picture, we will use Eq. 17-9 with renormalized coefficients to predict T_{in}. Figure 17-8 shows the result. Equation 17-16 tells us that the performance data are consistent with a loss coefficient of $0.842 \times 230.4 = 194$ Btu/hr°F (not 230.4) and that the mass charging and discharging is 18% higher than that predicted by the audit description. The autocorrelation of the residuals in Figure 17-7 really requires the use of generalized least squares. However, for simplicity we will not pursue this.

We will now consider signal enhancement with sinusoidal heat input. In real buildings subject to varying T_{out} and solar radiation, a 16-hr cycle was recommended. The ideas can be explained and implemented for the simple example building with the data of Figure 17-4.

From Figure 17-4 we can see that there is a dominant diurnal frequency component. So let us write

$$Q_{int} = Q_{diurnal}(n) + Q_{residual}(n) \, . \qquad (17\text{-}17)$$

Let $T_{in}^{residual}(n)$ be the temperature response to $Q_{residual}(n)$ as given by Eq. 17-16. Then $T_{in}(n) - T_{in}^{residual}(n)$ should be close to a diurnal sine wave; one can fit this to a diurnal sine wave. From the magnitudes and phases of $Q_{diurnal}(n)$ and the diurnal fit to $T_{in}(n) - T_{in}^{residual}(n)$, we can determine the admittance at the diurnal frequency. The value obtained from this signal enhancement procedure is usually very accurate. In the example building, a value of $735.2 \, \lfloor 27.6°$ was obtained.

The quantitative values of the loss coefficient and the diurnal admittance can be combined with the qualitative information of mass distributions given from an audit description to provide the response at any frequency. Figure 17-9 shows the result.

The computation was done as follows: Let us postulate that

$$V^{as\text{-}built}(\omega) = x \, V^{audit}(\omega') + y$$

$$\omega' = \omega \left[1 + (1 - a)(1 - \frac{\omega}{\omega_N}) \right]$$

$$\omega_N = \pi/\Delta \, ,$$
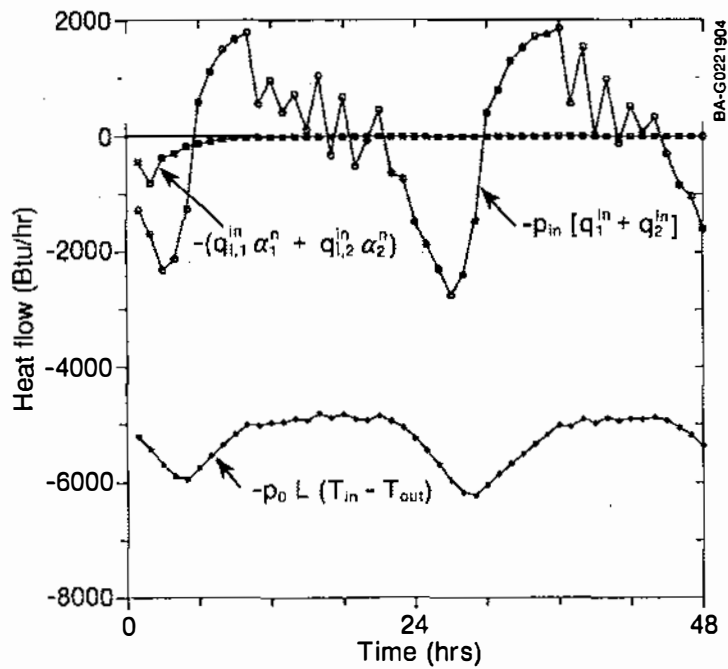
Figure 17-6. Various renormalized heat flows resulting in a linear least squares fit to $Q_{int}(n)$. Negative values represent heat loss by air node and positive values represent heat gain.

Figure 17-7. A linear least squares fit of $Q_{int}(n)$

Figure 17-8. Temperatures predicted by the parameters giving the best fit to Q_{int}

Figure 17-9. Interpolation based on a loss coefficient of 192.0, V-admittance at a 24-hr cycle of 730 \38.6° and the quantitative audit description. The exact V-admittance is also shown.

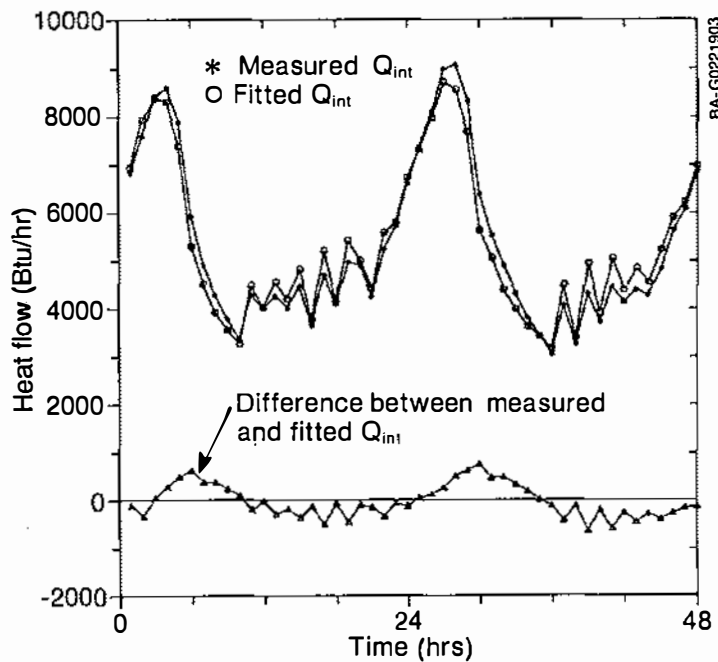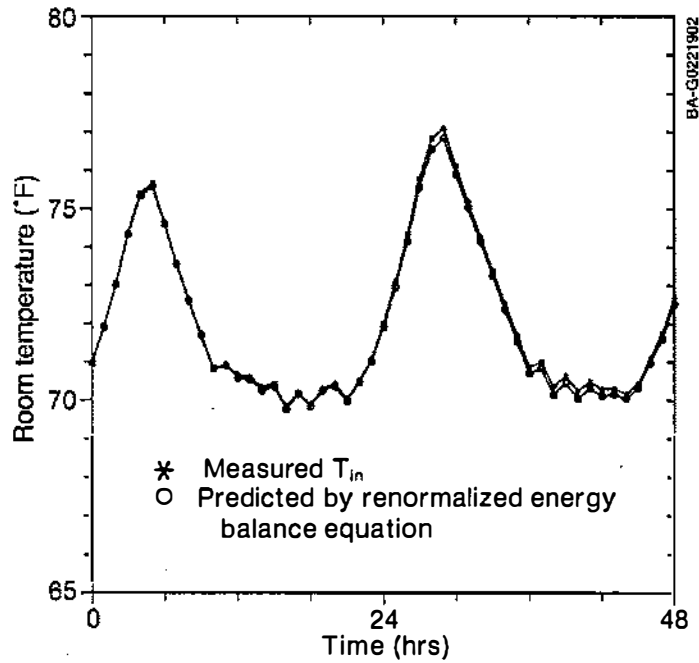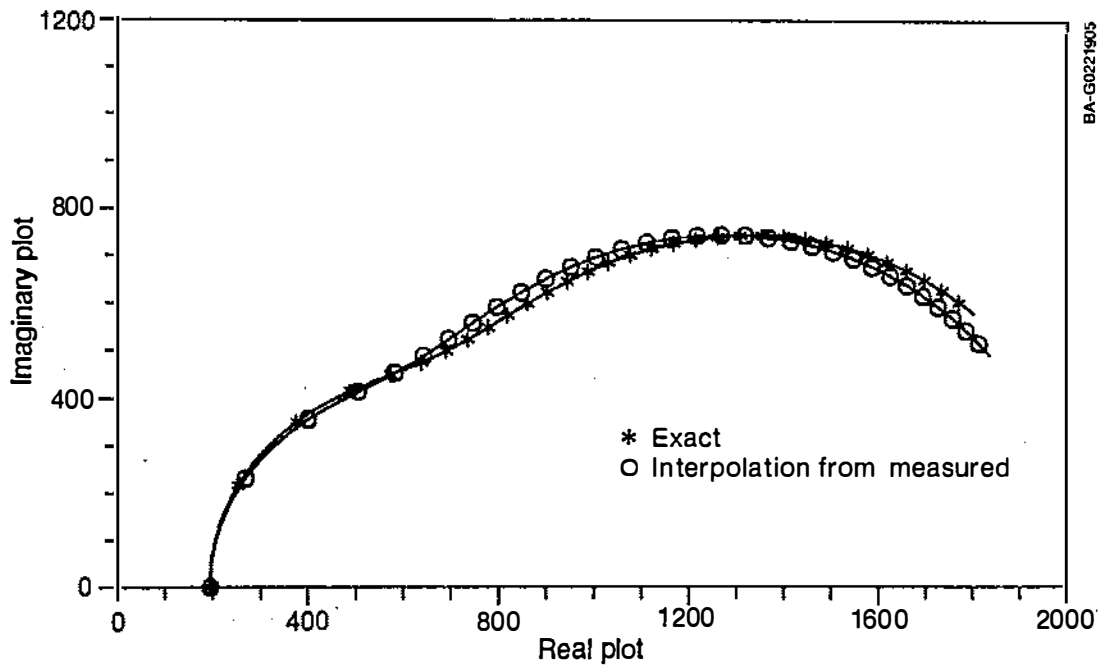where Δ = time and step = 1 hour. The above postulate ensures that ω' and ω are equal at zero frequency and at the Nyquist frequency. The term $V^{audit}(\omega')$ is calculated from an audit description. By specifying $V^{as-built}$ at zero frequency (the measured loss coefficient) and at the 24-hr cycle, the quantities x, a, and y are obtained. Now $V^{as-built}(\omega)$ can be determined at any frequency.

It can now be revealed that the measured data of Figure 17-4 was, in fact, generated from a simulation of the as-built building described in Table 4-1 (with appropriate wall areas) with a fit at 48-hr^{-1} and 12-hr^{-1} frequencies. The exact loss coefficient is 192.8 Btu/hr°F (compared with 194.0 from fitting) and the exact diurnal admittance is 728.3 $\lfloor 38.18°$ Btu/hr°F (compared with 735.2 $\lfloor 37.6°$ from signal enhancement). The exact V-admittances are also plotted in Figure 17-9.

18.0 SUMMARY AND CONCLUSIONS

This report presented a unified method of hourly simulations of a building and an analysis of performance data. The method is called Primary and Secondary Terms Analysis and Renormalization (PSTAR). PSTAR is not a new simulator competing with existing simulators; it is a way of organizing heat flows that can be obtained from existing or future simulators. (For a certain class of problems, PSTAR can provide a self-contained simulator.) The heat flow in a zone is first decomposed into a number of terms. This decomposition can be done with few restrictions. For example, for a one-zone building the instantaneous energy balance equation (using heating season terminology) is

```
  (Term 1:  Internal gains)
 -(Term 2:  Loss coefficient)×(inside outside temperature difference)
 +(Term 3:  Heat released/stored from masses coupled to inside temperature)
 +(Term 4:  Heat released/stored from masses coupled to outside
            temperature)
 +(Term 5:  Heat flow due to solar radiation, including mass effects)
 -(Term 6:  Heat loss due to sky temperature depression below ambient)
 -(Term 7:  Heat loss to ground)
 -(Term 8:  Heat loss due to ventilation/infiltration)
 +(Term 9:  Heat gain from the heating/cooling system)
+(Term 10:  Exact flow minus approximate flow given by the above
            terms) = zero.
```

The mere postulation of Term 2, 3, 4, or 5, etc., implies assumptions about constant convection and radiation coefficients. If these assumptions are deemed unsatisfactory, the error introduced (by this or any other assumptions) is picked up by Term 10. It is expected that Term 10 is small, otherwise, the above decomposition is useless. (A number of simulators such as DOE-2 and SERIRES make assumptions that amount to setting Term 10 to zero.)

Each term can be obtained from a building description and a given microdynamic simulator. (A microdynamic simulator is one that simulates each component; DOE-2 and SERIRES are examples.) For example, Term 5 can be obtained from a simulation that suppresses all terms except Term 5 and Term 9. Terms 2, 3, and 4 can be suppressed by setting inside and outside temperatures constant and equal. Other terms can be suppressed in an obvious manner. The resulting energy balance equation is Term 5 + Term 9 = 0, thereby allowing a calculation of Term 5 as the resulting cooling load.

A microdynamic simulator is not needed for every term. It is not even desirable. Just as Term 2 is obtained from a macrolevel calculation that aggregates components UAs into a building loss coefficient, Terms 3, 4, and 6 can be obtained by a macrodynamic calculation. This can be done in a number of ways; a method is developed through fitting building response at selected frequencies. Term 5 can be obtained from a macrodynamic calculation, but to account for multiple orientations, shading, and seasonal motion of the sun, etc., a microdynamic simulation is preferable.

Each term, therefore, is obtained by macrodynamic or a microdynamic calculation, or is an input to the simulation (such as Term 1).

In the forward process (for example, in predicting building performance given the building description), the above decomposition has intuitive value giving quantitative information on the role of various driving forces on the building performance. It has some computational value too; for example, Term 6 cannot be included in a simulation such as SERIRES (which does not account for sky temperature depression effects except through an external calculation).

In the inverse process (i.e., in determining building characteristics given performance data), the above decomposition plays a critical role. Suppose short-term monitoring has given dynamic data on a few channels (inside and outside temperatures, solar radiation, internal gains, and wind speed). We want to extract suitable building parameters from the data and use these parameters for long-term performance prediction (ratings), or control and diagnostics of HVAC systems. The common method is to view the building as a "black box" and fit the performance data to model parameters. This approach generally results in a dilemma. To keep the number of parameters small the model must be simple; to be realistic the model must be complex. This dilemma is resolved by treating the building not as a black box, but as a "gray box"-- starting with an audit description of the building obtained by a site visit, the various heat flow terms are calculated. Some terms, such as Term 1 are, of course, measured. Because the (known) audit description is different from the (unknown) as-built description, the energy balance equation is not satisfied by the terms obtained above.

Each term calculated (and not directly measured) above can now be classified as primary or secondary depending on its overall magnitude. Let us suppose a building is such that Terms 2, 3, and 5 are primary, Terms 4, 6, 7, and 10 are secondary, and the rest measured. A renormalization process is introduced for the primary terms:

$$\begin{aligned}
&\text{(Term 1:} &&\text{Internal gains)} \\
-p_0&\text{(Term 2:} &&\text{Loss coefficient)}\times\text{(inside outside temperature difference)} \\
-p_{in}&\text{(Term 3:} &&\text{Heat released/stored from masses coupled to inside temperature} \\
+&\text{(Term 4:} &&\text{Heat released/stored from masses coupled to outside temperature)} \\
+p_{sun}&\text{(Term 5:} &&\text{Heat flow caused by solar radiation, including mass effects)} \\
-&\text{(Term 6:} &&\text{Heat loss caused by sky temperature depression below ambient)} \\
-&\text{(Term 7:} &&\text{Heat loss to ground)} \\
-&\text{(Term 8:} &&\text{Heat loss because of ventilation/infiltration)} \\
+&\text{(Term 9:} &&\text{Heat gain from the heating/cooling system)} \\
+&\text{(Term 10:} &&\text{Exact flow--approximate flow given by the above terms)} = \text{zero.}
\end{aligned}$$

The renormalization parameters are determined so that the above renormalized energy balance equation is best satisfied in the least squares sense. This involves a simple linear regression. The renormalized energy balance equation is used for the intended application such as long-term extrapolation, control and diagnostics of HVAC systems, etc.

The need for a proper test protocol to elicit the renormalization parameters is emphasized. Coheating (introduction of electrical heat to maintain a constant indoor temperature) and cool-down tests are typically adequate. Accurate determination of admittance at a specific frequency is possible through sinusoidal heat input.

Additional parameters are introduced for special situations. The above methodology is extended to multizone buildings.

A number of caveats intrinsic to any extrapolation to long-term from short-term measurements--particularly regarding seasonal motion of the sun, ground heat flows and infiltration--were pointed out. Some areas for improvement, such as matching building response at high frequencies, were pointed out.

A number of applications are pointed out. When combined with modern data acquisition and control systems such as energy management systems in commercial buildings, power line carrier based data acquisition, etc., PSTAR is a powerful tool for a wide range of applications.

19.0 REFERENCES

ASTM, 1985. ASTM Standard Method of Test C976, "Thermal Performance of Building Assemblies by Means of a Calibrated Box." 1985 Annual Book of American Society for Testing Materials Standards. Vol. 4.06, pp. 660-683.

Balcomb, J. D., 1983. Heat Storage and Distribution Inside Passive Solar Buildings. Report No. LA-9694-MS, Los Alamos, NM: Los Alamos National Laboratory.

Balcomb, J. D., and K. Yamaguchi, 1983. "Heat Distribution by Natural Convection," Proceedings of the 8th National Passive Solar Conference. Santa Fe, NM: American Solar Energy Society, Inc., pp. 289-94.

Box, G.E.P., and G. M. Jenkins, 1976, Time Series Analysis Forecasting and Control, San Francisco, CA: Holden-Daylne.

Burch, D. M., R. M. Zarr, T. K. Faison, B. A. Licitra, and C. E. Arnold, 1987. "A Procedure for Measuring the Dynamic Thermal Performance of Wall Specimens Using a Calibrated Hot Box," American Society for Testing Materials Transactions, Vol. 93, Part II.

Burns, P., and A. Kirkpatrick, 1987. Final Report, Interzonal Heat Transfer, No. DE-AC02-83CE, Fort Collins, CO: Colorado State University.

Carslaw, H. S., and J. C. Jaeger, 1977. Conduction of Heat in Solids, 2nd Edition, Oxford, England: Oxford University Press.

DOE 2 Reference Manual. 1980. Los Alamos, NM: Los Alamos Scientific Laboratory.

Deberg, P., 1979. Use of General Models with a Small Number of Parameters, Part 2 Experimental Analysis. Preprint. Liege, Belgium.

Doebelin, E. O., 1980. System Modeling and Response, New York, NY: John Wiley and Sons.

Duffy, J. J., and D. Saunders, 1987. Low-Cost Methods for Evaluation of Space Conditioning Efficiency of Existing Homes, Final Report to National Association of Home Builders (NAHB) Research Center, 400 Prince George Center Blvd., Upper Marlboro, MD 20772: NAHB Research Foundation, Inc.

Eveleigh, V. 1972, Introduction to Control Systems Design, New York, NY: McGraw-Hill Inc.

Green, M. D., and A. Ulge, 1979. "Frequency- and Time-Domain Thermal Response of Dwellings," Building Environ., Vol. 14, pp. 107-118.

Hammersten, S. L., 1984. Estimation of Energy Balance Models for Houses, Report No. M84:18, Gavle, Sweden: Swedish Building Research Institute.

Hammsersten, S. L., D. van Hattem, H. Bloehm, and R. Colombo, 1988. "Passive Solar Component Testing using Identification Methods," Solar Energy, Vol. 41, No. 1, pp. 5.

Hittle, D. C., 1977. The Building Loads Analysis and System Thermodynamics Program, Vol. I: User's Manual, Champaign, IL: Construction Engineering Research Laboratory.

Hittle, D. C., and C. O. Pedersen, 1981. "Calculating Building Heating Loads Using the Frequency-Response of Multi-Layered Slabs," American Society of Heating, Refrigerating and Air Conditioning Engineers Transactions, Vol. 87, Part II.

IHVE, 1970. Guidebook A, Institution of Heating and Ventilating Engineers London, England: Chartered Institution of Building Services.

Jeon, H., D. C. Claridge, K. Subbarao, and J. Burch, 1988. "Thermal Dynamics from Component and Building Tests," submitted to the American Society of Mechanical Engineers Conference.

Kimura, K., 1977. Scientific Basis of Air Conditioning. London, England: Applied Science Publishers, Ltd.

Kirkpatrick A., 1987. Interzonal Heat Transfer, Final Report to the U.S. Department of Energy, Washington, DC.

Krarti, M., D. Claridge, and J. Kreider, 1985. "Interzone Temperature Profile Estimation--Below Grade Basement Heat Transfer Results" and "Interzone Temperature Profile Estimation--Slab-on-Grade Heat Transfer Results," 23rd American Society of Mechanical Engineers (ASME) Heat Transfer Conference, Denver, CO: ASME.

Kusuda, T., T. Tsuchiya, and F. J. Powell, 1971. "Prediction of Indoor Temperature by Using Equivalent Thermal Mass Response Factors." Proceedings of 5th Symposium on Temperature. Washington, DC: National Bureau of Standards.

Larson, S. C., and M. G. Van Geem, 1987. Heat Transfer Characteristics of Walls with Similar Thermal Resistance Values, Oak Ridge, TN: Oak Ridge National Laboratory.

Letherman, K. M., C. J. Palin, and P. M. Park, 1982. "The Measurement of Dynamic Thermal Responses in Room Using Pseudo-Random Binary Sequences," Building Environ. Vol. 17, No. 11.

Martin, M., and P. Burdahl, 1984. "Characteristics of Infrared Sky Radiation in the United States," Solar Energy, Vol. 33, No. 3/4, pp. 321-336.

Mitalas, G., 1983. "Calculation of Basement Heat Loss," American Society of Heating, Refrigerating and Air Conditioning Engineers Transactions. Vol. 89, pp. 420.

Muncey, R. W., 1979. Heat Transfer Calculations for Buildings. London, England: Applied Science Publishers, Ltd.

Muncey, R., J. Spencer, and C. Gupta, 1971. "Method for Thermal Calculations Using Total Building Response Factors." National Bureau of Standards Building Science Series, 39.

Nielsen, A. A., and B. K. Nielsen, 1984. "A Dynamic Method for the Thermal Performance of Small Houses: Model Set-Up, Test Design, Measurements, Parameter Estimation and Simulation," American Council for an Energy Efficient Economy (ACEEE) 1984 Summer Study on Energy Efficiency in Buildings, ACEEE, Vol. B, pp. 207-220.

Niles, P., and W. B., 1978. "A Simple Direct Gain Passive House Performance Prediction Model," Proceedings of the Second National Passive Solar Conference, Philadelphia, PA: American Solar Energy Society, pp. 534.

Norford, L. K., A. Rabl, R. H. Socolow, and A. K. Persily, 1985. "Measurement of Thermal Characteristics of Office Buildings," presented at American Society of Heating, Refrigerating and Air Conditioning Engineers/Department of Energy/Building Thermal Envelope Coordinating Committee Conference, Thermal Performance of the Exterior Envelope of Buildings III, Clearwater Beach, FL, held Dec. 2-5, 1985.

Palmiter, L., 1986. "An Introduction to Frequency Methods for Building Thermal Analysis," Proceedings of 11th National Passive Solar Conference, Boulder, CO: American Solar Energy Society.

Palmiter, L., and T. Wheeling, 1980. SERIRES 1.0, Golden, CO: Solar Energy Research Institute.

Palmiter, L., M. Toney, and J. Brown, 1988. Preliminary Evaluation of Two Short-Term Test Methods. Prepared for the Solar Energy Research Institute (SERI) under Subcontract No. HX-7-07146-1, Golden, CO: SERI.

Pryor, D. V., P. J. Burns, and C. B. Winn, 1980. "Parameter Estimation in Passive Solar Structures." Proceedings of 5th National Passive Solar Conference. Amherst, MA: American Solar Energy Society, pp. 131-35.

Rabl, A., 1988. "Parameter Estimation in Buildings: Methods for Dynamic Analysis of Measured Energy Use," Journal of Solar Energy Engineering, Vol. 110, pp. 52.

Seem, J., 1987. Modeling of Heat Transfer in Buildings, Ph.D. Thesis, Madison, WI: University of Wisconsin.

Sonderegger, R., 1978. "Diagnostic Tests Determining the Thermal Response of a House," American Society of Heating, Refrigerating and Air Conditioning Engineers Transactions, Vol. 84, Part I, pp. 691.

Sonderegger, R., P. Condon, and M. Modera, 1980. "In-Situ Measurement of Residential Energy Performance Using Electric Coheating" American Society of Heating, Refrigerating and Air Conditioning Engineers Transactions, Vol. 86, Part I, pp. 394.

Stephenson, D. G., and G. P. Mitalas, 1967. "Cooling Load Calculations by Thermal Response Factor Method." American Society of Heating, Refrigerating and Air Conditioning Engineers Transactions Vol. 73, No. 1, III.1.1.

Stephenson, D. G., and G. P. Mitalas, 1971. "Calculation of Heat Conduction Transfer Functions for Multilayer Slabs," _American Society of Heating, Refrigerating and Air Conditioning Engineers Transactions_, Vol. 77 pp. 117.

Subbarao, K., Sept. 1988. _PSTAR Primary and Secondary Terms Analysis and Renormalization: A Unified Approach to Building Energy Simulations and Short-Term Monitoring--A Summary_, SERI/TR-254-3347, Golden, CO: Solar Energy Research Institute.

Subbarao, K., 1984. _BEVA (Building Element Vector Analysis). A New Hour-by-Hour Building Energy Simulation With System Parameters as Inputs._ SERI/TR-254-2195, Golden, CO: Solar Energy Research Institute.

Subbarao, K., 1985. _Thermal Parameters for Single and Multizone Buildings and their Determination from Performance Data_, SERI/TR-253-2617, Golden, CO: Solar Energy Research Institute.

Subbarao, K., and J. V. Anderson, 1983. "A Graphical Method for Passive Building Energy Analysis," _Journal of Solar Energy Engineering_, Vol. 105, pp. 134-141.

Subbarao, K., D. Mort, and J. Burch, 1985. "Short-Term Measurements for the Determination of Envelope Retrofit Performance," _American Society of Heating, Refrigerating and Air Conditioning Engineers Transactions_, Vol. 91, Part IIB, pp. 1516.

Subbarao, K., J. Burch, and C. Christensen, 1985. "Macrodynamics: A Unified Framework for Building Energy Analysis," _Proceedings of Building Energy Simulations Conference_, Seattle, WA.

Subbarao, K., J. Burch, E. Hancock, and H. Jeon, 1985. "Measurement of Effective Thermal Capacitance in Buildings," _American Society of Heating, Refrigerating and Air Conditioning Engineers (ASHRAE)/Department of Energy/Building Thermal Envelope Coordinating Committee Conference, Thermal Performance of the Exterior Envelope of Buildings III_, held Dec. 2-5, 1985, Clearwater Beach, FL: ASHRAE, pp. 351-363.

Subbarao, K., J. Burch, and H. Jeon, 1986. Building as a Dynamic Calorimeter: Determination of Heating System Efficiency, American Council for an Energy Efficient Economy Summer Study of Energy Efficient Buildings, American Society of Heating, Refrigerating and Air Conditioning Engineers, Vol. 9, pp. 288 (1986).

Subbarao, K., J. D. Burch, C. E. Hancock, A. Lekov, and J. D. Balcomb, Sept. 1988. _Short-Term Energy Monitoring (STEM): Application of the PSTAR Method to a Residence in Fredericksburgh, Virginia_, SERI/TR-254-3356, Golden, CO: Solar Energy Research Institute.

Winn, C. B., 1982. "A Simple Method for Determining the Average Temperature Variation, and the Solar Fraction for Passive Buildings," _Proceedings of the 6th National Passive Solar Conference_, Portland, OR: American Solar Energy Society.

APPENDIX A

Z-TRANSFORMS AND TIME SERIES

This appendix presents a brief discussion of z-transforms relevant for this article. Detailed mathematical presentations are available in textbooks, for example, Eveleigh, 1972.

Consider the heat gain into the air node $\hat{q}(t)$ because of a driving function $\hat{F}(t)$; inside temperature, ambient, and solar radiation are typical driving functions we will be concerned with. For a linear system, we can write

$$\hat{q}(t) = \int_{-\infty}^{t} dt' \cdot \hat{X}(t-t') \cdot \hat{F}(t') . \qquad (A-1)$$

This convolution integral can be reduced to an algebraic equation upon taking Laplace or Fourier transforms. When we are dealing with discrete data, the analog of the Laplace transform is the z-transform and Eq. A-1 reduces to

$$q(z) = X(z) F(z) . \qquad (A-2)$$

In Eq. A-2

$$q(z) = \sum z^{-n} \cdot q_n , \qquad (A-3)$$

where q_n is the heat flow at time $n\Delta$.

A particularly simple situation arises when the transfer function $X(z)$ can be represented as a ratio of polynomials in z^{-1}. If

$$X(z) = P_{num}(z^{-1})/P_{den}(z^{-1}) , \qquad (A-4)$$

where

$$P_{num}(z^{-1}) = b_o + b_1 \cdot z^{-1} + \ldots + b_r \cdot z^{-r} , \qquad (A-5)$$

$$P_{den}(z^{-1}) = a_o + a_1 \cdot z^{-1} + \ldots + a_k \cdot z^{-k} , \qquad (A-6)$$

then one can show that

$$a_o q_n + a_1 q_{n-1} + \ldots + a_k q_{n-k} = b_o F_n + b_1 F_{n-1} + \ldots + b_r F_{n-r} . \qquad (A-7)$$

Thus, knowing the present and (a finite number of) past values of the driving function as well as (a finite number of) past values of the heat flow, the present value of the heat flow can be very simply calculated. Because the overall normalization of Eq. A-7 is arbitrary, it is often convenient to choose a_o to be equal to 1. We shall also deal primarily with the case $k=r$.

Generalization to several driving functions is straightforward. It is sufficient to demonstrate the process for two driving functions $F^{(1)}$ and $F^{(2)}$. Let the corresponding heat flows be $q^{(1)}$ and $q^{(2)}$, each of which can be represented in the form (A-1) - (A-2). Usually the total heat flow caused by the combined influence of all the driving functions is of interest. In this case, we are interested in $Q = q^{(1)} + q^{(2)}$. It follows that

$$Q(z) = [P^{(1)}_{num}(z^{-1}).P^{(2)}_{den}(z^{-1}).F^{(1)}(z)$$

$$+ P^{(2)}_{num}(z^{-1}).P^{(1)}_{den}(z^{-1}).F^{(2)}(z)]/[P^{(1)}_{den}(z^{-1}).P^{(2)}_{den}(z^{-1})] \ . \quad \text{(A-8)}$$

From this the analog of (A-7) can be easily derived. For example if

$$P^{(1)}_{num}(z^{-1}) = b^{(1)}_o + b^{(1)}_1.z^{-1} \ , \qquad\qquad\qquad \text{(A-9)}$$

$$P^{(1)}_{den}(z^{-1}) = a^{(1)}_o + a^{(1)}_1.z^{-1} \ , \qquad\qquad\qquad \text{(A-10)}$$

$$P^{(2)}_{num}(z^{-1}) = b^{(2)}_o + b^{(2)}_1.z^{-1} \ , \qquad\qquad\qquad \text{(A-11)}$$

$$P^{(2)}_{den}(z^{-1}) = a^{(2)}_o + a^{(2)}_1.z^{-1} \ , \qquad\qquad\qquad \text{(A-12)}$$

then

$$a^{(1)}_o.a^{(2)}_o.Q_n + [a^{(1)}_o.a^{(2)}_1 + a^{(2)}_1 + a^{(2)}_o.a^{(1)}_1].Q_{n-1} + a^{(1)}_1.a^{(2)}_1 Q_{n-2}$$

$$= a^{(2)}_o b^{(1)}_o F^{(1)}_n + [a^{(2)}_o b^{(1)}_1 + a^{(2)}_1 b^{(1)}_o] F^{(1)}_{n-1} + a^{(2)}_1 b^{(1)}_1 F^{(1)}_{n-2}$$

$$+ a^{(1)}_o b^{(2)}_o F^{(2)}_n + [a^{(1)}_o b^{(2)}_1 + a^{(1)}_1 b^{(2)}_o] F^{(2)}_{n-1} + a^{(1)}_1 b^{(2)}_1 F^{(2)}_{n-2} \ . \qquad \text{(A-13)}$$

In the special case $P^{(1)}_{den}(z^{-1}) = P^{(2)}_{den}(z^{-1})$, obvious simplifications occur.

APPENDIX B

FREQUENCY DOMAIN ANALYSIS AND TIME SERIES

This appendix derives the relationship between the coefficients of the poly-
nomials and frequency response. The notation is the same as that in
Appendix A. Suppose the input $F(t')$ in Eq. A-1 is of the form

$$F(t) = f_0 \exp(j\omega t) . \qquad (B-1)$$

Then the output $q(t)$ is given by

$$q(t) = X(\omega) f_0 \exp (j\omega t) , \qquad (B-2)$$

where the frequency response $X(\omega)$ is given by

$$X(\omega) = \int_{-\infty}^{t} dt\, X(t) \exp (-j\omega t) . \qquad (B-3)$$

Evaluating Eqs. B-1 and B-2 at $t = m\Delta$, we get

$$F_m = f_0 \exp(j\omega m\Delta) , \qquad (B-4)$$

and

$$q_m = X(\omega) f_0 \exp (j\omega m\Delta) . \qquad (B-5)$$

Substituting these into Eq. A-7 it follows that

$X(\omega) =$

$[b_0 + b_1 \exp(-j\omega\Delta) + \ldots + b_r \exp(-jr\omega\Delta)]/[a_0 + a_1 \exp(-j\omega\Delta) + \ldots + a_k \exp(-jk\omega\Delta)].$

$$(B-6)$$

The above equation allows us to relate the coefficients of the time series to
the frequency response. The inverse of this relationship will now be derived.
First, we assume that r=k, and that $X(\omega)$ is given at zero frequency, and r
other frequencies $\omega_1, \ldots, \omega_r$. Eq. B-6 now leads to a set of 2r+1 linear
equations for the 2r+1 unknowns $b_0, \ldots, b_r, a_1, \ldots, a_r$. (Note that $a_0=1$).
This system of linear equations can be easily written and solved by matrix
inversion.

The case of r=1 and of r=2 are of special importance. We will explicitly
write down the equations for the case of r=1.

Let $X(\omega)$ at $\omega=0$ be X_0, and $X(\omega)$ at $\omega=\omega_1$ be $X_1 e^{i\phi_1}$. Then it can easily be
shown that b_0, b_1, and a_1 are given by the linear equations

$$\begin{bmatrix} 1 & 1 & -X_0 \\ 1 & \cos \omega_1\Delta & -X_1 \cos (\omega_1\Delta-\phi_1) \\ 0 & -\sin \omega_1\Delta & X_1 \sin (\omega_1\Delta-\phi_1) \end{bmatrix} \begin{bmatrix} b_0 \\ b_1 \\ a_1 \end{bmatrix} = \begin{bmatrix} X_0 \\ X_1 \cos \phi_1 \\ X_1 \sin \phi_1 \end{bmatrix}. \qquad (B-7)$$

Another interesting way to obtain the parameters is to rewrite the relationship

$$X(\omega) = [b_o + b_1 \exp(-j\omega\Delta)]/[1 + a_1 \exp(-j\omega\Delta)] ,$$ (B-8)

in the form

$$X(\omega) = X_o + b [1 - \exp(-j\omega\Delta)]/[1 + a_1 \exp(-j\omega\Delta)] .$$ (B-9)

Then

$$a_1 = -[1 - \tan\theta \tan(\omega_1 \Delta/2)]/[1 + \tan\theta \tan(\omega_1 \Delta/2)] ,$$ (B-10)

$$b = |X(\omega_1) - X_o|/[\cos\theta (1 + \tan\theta \tan(\omega_1\Delta/2))] ,$$ (B-11)

$$\tan\theta = \operatorname{Im} X(\omega_1)/(\operatorname{Re} X(\omega_1) - X_o) .$$ (B-12)

The relationship between the transfer function and RC network will now be given. The network representation, while not central, has some intuitive value. Transfer functions and their parameterization are, of course, the central objects. An RC-network has a unique transfer function associated with it, whereas one can generally construct several networks all of which have the same transfer function. The transfer function $X(\omega)-X(\omega=0)$ can be associated with a simple single capacitor-single resistor network given in Figure 4-1- The resistor R and the capacitor C are related to a_1 and b of Eq. B-9. The precise relationship depends on the specific discretization scheme: Discrete data with sampling interval Δ implies that only driving functions and, hence, the system response at frequencies such that $\omega\Delta<<1$ are of interest. (In the extreme limit $\omega\Delta<<1$, the discretization scheme is not important.) Setting $\tan\omega\Delta/2 \approx \omega\Delta/2$ in Eqs. B-10 and B-11, it can easily be seen that the result is equivalent to central differencing with

$$R = \frac{1-a_1}{2b} \Delta, \quad c = \frac{b}{1 + a_1}$$ (B-13)

To prove Eq. B-13, note that the differential equation $d/dt(CT_m) = (T-T_m)/R$ can be rewritten as $dq/dt + q/RC = (1/R) dT/dt$ where $q = (T-T_m)/R$. Central differencing of this equation with time-step Δ leads to an equation of the form (Eq. A-7) from which (Eq. B-13) can be obtained. Modern data acquisition systems usually sample data rather fast and average them over an hour (or any desired period). The above discussion, which is based on sampling period of an hour, can be modified to deal with averaging period of an hour. Some scheme of interpolation within one hour is still needed and, for this reason, it is unclear whether it is worth the effort.

APPENDIX C

APPROXIMATIONS OF THE PSTAR APPROACH

The PSTAR process--consisting of renormalization (as appropriate) of transfer functions, renormalization (as appropriate) of certain heat flows, measurement of certain heat flows, and perturbation treatment of small heat flows--is being investigated thoroughly. Two related versions, called BEVA, were described elsewhere (Subbarao 1984, 1985) and will be briefly outlined here. These use black-box approaches, unlike the PSTAR approach that requires an audit description (a gray-box approach). We believe the PSTAR approach is superior. These black-box approaches are given only for completeness. We will present these approximations in the context of a one-zone building.

Approximation A: Instead of a renormalization of the transfer functions, we can simply view the coefficients of the polynomials (in z^{-1}) as parameters to be estimated (Subbarao 1985)]. Operationally, this means that we can start from the time series:

$$a_o^{in} T_{in}(n) + a_1^{in} T_{in}(n-1) + \ldots + a_{N_{in}}^{in} T_{in}(n-N_{in})$$

$$= a_o^{out} T_{out}(n) + a_1^{out} T_{out}(n-1) + \ldots + a_{N_{out}}^{out} T_{out}(n-N_{out})$$

$$+ a_o^{sun} Q_{sun}(n) + a_1^{sun} Q_{sun}(n-1) + \ldots + a_{N_{sun}}^{sun} Q_{sun}(n-N_{sun})$$

$$+ a_o^{int} \left(Q_{int}(n) + Q_{aux}(n)\right) + a_1^{int} \left(Q_{int}(n-1)\right) + \left(Q_{aux}(n-1)\right) + \ldots$$

$$+ a_{N_{int}} \left[Q_{int}(n-N_{int}) + Q_{aux}(N-N_{aux})\right] . \tag{C-1}$$

with the linear (in the a-coefficients) constraint

$$a_o^{in} + a_1^{in} + \ldots + a_{N_{in}}^{in} = a_o^{out} + a_1^{out} + \ldots + a_{N_{out}}^{out} . \tag{C-2}$$

One can choose $a_o^{in} = 1$ and make $T_{in}(n)$ the dependent variable in (C-1), use all measured past inside temperatures and minimize the sum of squares.

$$\sum \left[T_{in}(n) - T_{in}^{mea}(n)\right]^2 ,$$

with respect to a's. This is a linear regression problem with $N_{in} + N_{out} + N_{sun} + N_{aux} + 2$ parameters to be estimated. The physical significance of the coefficients can be obtained from the relation.

$$V(\omega) = \frac{a_o^{in} + a_1^{in} \exp(-j\omega\Delta) + \ldots + a_{N_{in}}^{in} \exp(-j N_{in} \omega\Delta)}{a_o^{int} + a_1^{int} \exp(-j\omega\Delta) + \ldots + a_{N_{int}}^{int} \exp(-j N_{int} \omega\Delta)}, \quad (C-3)$$

and similar relationships.

For simplicity additional approximations can be made, such as neglecting all small heat flows, and using the incident flux I_{sun} on a suitable orientation rather than Q_{sun} on a driving function. Also, autocorrelation among residuals can be ignored and an ordinary least squares areas method used.

There are potentially severe problems in the above approach. When the number of independent parameters $N_{in} + N_{out} + N_{sun} + N_{aux} + 2$ is large, the parameters are poorly determined and often lead to instabilities when used for long-term extrapolation. One can devise ad hoc procedures such as obtaining only zero frequency and diurnal frequency admittances from Eq. C-3 and then, for extrapolation purposes, abandoning Eq. C-1 in favor of a transfer function fitted at zero and diurnal frequencies and extrapolated for all others.

Approximation B: Instead of a renormalization of the transfer functions, fitted to calculated values at as many frequencies as necessary, we will directly parametrize the transfer functions and estimate the parameters. In the spirit of keeping the number of parameters small, we will parametrize as follows:

As seen before, this is an excellent parametrization for frame walls and, more generally, for lightweight buildings:

$$V(z) = \frac{\beta_o^{in} + \beta_1^{in} z^{-1}}{1 + a_1^{in} z^{-1}}, \quad (C-4)$$

or in frequency domain,

$$V(\omega) = \frac{\beta_o^{in} + \beta_1^{in} \exp(-j\omega\Delta)}{1 + \alpha_1^{in} \exp(-j\omega\Delta)}. \quad (C-5)$$

Similar parametrization is done of other quantities. Operationally, we start with the time series equation

$$a_o^{in} T_{in}(in) + a_1^{in} T_{in}(n-1) + a_2^{in} T_{in}(n-2) + a_3^{in} T_{in}(n-3)$$

$$= a_o^{out} T_{out}(n) + a_1^{out} T_{out}(n-1) + a_2^{out} T_{out}(n-2) + a_3^{out} T_{out}(n-3)$$

$$+ a_o^{sun} Q_{sun}(n) + a_1^{sun} Q_{sun}(n-1) + a_2^{sun} Q_{sun}(n-2) + a_3^{sun} Q_{sun}(n-3)$$

82

$$+ a_o^{int} \left(Q_{int}(n) + Q_{aux}(n)\right) + a_1^{int} \left(Q_{int}(n-1) + Q_{aux}(n-1)\right)$$

$$+ a_2^{int}\left[Q_{int}(n-2) + Q_{aux}(n-2) + a_3^{int}\left(Q_{int}(n-3)\right) + Q_{aux}(n-3)\right] , \quad (C-6)$$

with

$$a_o^{in} = \beta_o^{out} \beta_o^{sun}$$

$$a_1^{in} = \beta_o^{out} \beta_1^{sun} + \beta_o^{sun} \beta_1^{out} + \beta_o^{out} \beta_o^{sun} \alpha_1^{in}$$

$$a_2^{in} = \beta_1^{out} \beta_1^{sun} + (\beta_o^{out} \beta_1^{sun} + \beta_o^{sun} \beta_1^{out}) \alpha_1^{sun}$$

$$a_3^{in} = \alpha_1^{in} \beta_1^{out} \beta_2^{out} . \quad\quad (C-7)$$

As before, one can choose $T_{in}(n)$ as the dependent variable, and use the least squares method. The parameters to be estimated are a_1^{in}, β_o^{in}, α_1^{out}, β_o^{out}, β_1^{out}, α_1^{sun}, β_o^{sun}, and β_1^{sun}, subject to the nonlinear constraint

$$\frac{\beta_o^{in} + \beta_1^{in}}{1 - \alpha_1^{in}} = \frac{\beta_o^{out} + \beta_1^{out}}{1 + \alpha_1^{out}} . \quad\quad (C-8)$$

Regardless of whether one uses measured past temperatures or calculated past temperatures, we will have a nonlinear regression problem. Further details and applications to building data can be found in Subbarao (1984). This method can be recast in the form of thermal networks.

Document Control Page	1. SERI Report No. SERI/TR-254-3175	2. NTIS Accession No.	3. Recipient's Accession No.
4. Title and Subtitle PSTAR--Primary and Secondary Terms Analysis and Renormalization: A Unified Approach to Building Energy Simulations and Short-Term Monitoring			**5. Publication Date** September 1988
			6.
7. Author(s) K. Subbarao			**8. Performing Organization Rept. No.**
9. Performing Organization Name and Address Solar Energy Research Institute A Division of Midwest Research Institute 1617 Cole Boulevard Golden, Colorado 80401-3393			**10. Project/Task/Work Unit No.** SB811241
			11. Contract (C) or Grant (G) No. (C) (G)
12. Sponsoring Organization Name and Address			**13. Type of Report & Period Covered** Technical Report
			14.

15. Supplementary Notes

16. Abstract (Limit: 200 words)

This report presents a unified method of hourly simulations of a building and analysis of performance data. The method is called Primary and Secondary Terms Analysis and Renormalization (PSTAR). In the PSTAR method, renormalized parameters are introduced for the primary terms such that the renormalized energy balance equation is best satisfied in the least squares sense; hence, the name PSTAR. PSTAR allows extraction of building characteristics from short-term tests on a small number of data channels. These can be used for long-term performance prediction ("ratings"), diagnostics, and control of heating, ventilating, and air conditioning systems (HVAC), comparison of design versus actual performance, etc.

By combining realistic building models, simple test procedures, and analysis involving linear equations, PSTAR provides a powerful tool for analyzing building energy as well as testing and monitoring. It forms the basis for the Short-Term Energy Monitoring (STEM) project at SERI.

17. Document Analysis

a. Descriptors . Residential Buildings, Solar Architecture, Space HVAC Systems, Passive Solar Heating Systems, Mathematical Models, Thermal Analysis

b. Identifiers/Open-Ended Terms

c. UC Categories   232

18. Availability Statement National Technical Information Service U.S. Department of Commerce 5285 Port Royal Road Springfield, Virginia 22161	**19. No. of Pages** 93
	20. Price A05

Form No. 0069 (3-25-82)